

INCORPORATION OF LIGNIN COPOLYMERS
INTO POLYURETHANE MATERIALS

by

Stephen S. Kelley

Dissertation submitted to the Faculty of the
Virginia Polytechnic Institute and State University in
partial fulfillment of the requirements for the degree of

DOCTOR OF PHILOSOPHY

in

CHEMISTRY

APPROVED:

T. C. Ward, Co-Chairman

W. G. ~~Glasser~~, ~~Co-Chairman~~

G. L. Wilkes

J. E. McGrath

N. G. ~~Lewis~~

H. C. Dorn

March, 1987

Blacksburg, Virginia

INCORPORATION OF LIGNIN COPOLYMERS
INTO POLYURETHANE NETWORKS

by

Stephen S. Kelley

Committee Chairmen; W. G. Glasser, T. C. Ward

Chemistry

(ABSTRACT)

Hydroxypropyl lignins (HPLs) from several sources were reacted with propylene oxide to produce chain-extended hydroxypropyl lignin (CEHPL) copolymers with molar substitutions (MS) between 1 and 7 propylene oxide units. Isolated copolymers were characterized with respect to their chemical composition, molecular weight and thermal properties. These techniques confirmed the presence of a copolymer with between 20 and 67 % lignin. Glass transition temperatures (T_g s) of the CEHPLs followed the behavior predicted by the Gordon-Taylor equation. Properties of the CEHPLs were independent of the original lignin source.

The CEHPL copolymers were incorporated into lignin polyurethane networks (LPUs). The LPUs contained 17 to 43 % lignin and showed a single T_g . Both the T_g and the Youngs modulus (MOE) of the LPUs were strongly correlated to the lignin content and type of diisocyanate used to

prepare the network. Swelling studies indicated that the LPUs prepared from CEHPLs with a high MS (5 - 7) were not highly crosslinked networks. The LPU properties also appeared to be independent of the lignin source.

In another set of experiments a HPL was separated into five fractions (F-HPLs) with molecular weights (MWs) between 1.5 and 10×10^3 daltons. The T_g of the F-HPLs was correlated to molecular weight by the Fox-Flory equation. The fractionated HPLs were incorporated into polyurethane networks. The T_g s of these networks were related to the MW of the F-HPL. Swelling studies indicated that low molecular weight monofunctional fragments limited network formation.

The LPUs were also used as one component in LPU/polymethyl methacrylate (PMMA) interpenetrating polymer networks (IPNs). These IPNs varied in their LPU/PMMA composition and the presence of crosslinking. Dynamic mechanical and thermal analysis showed two phases in all of the IPNs. Mechanical properties were dependent on the IPN composition and phase crosslinking. For IPNs with a crosslinked LPU phase, the MOE values indicated the presence of dual phase continuity.

A second series of IPNs was prepared to investigate the effects of lignin content on IPN properties. Phase separation appeared to be related to the lignin content. Mechanical properties were related to lignin content and not the phase behavior.

ACKNOWLEDGMENTS

Special tribute goes to Drs. W. G. Glasser and T. C. Ward for their professional and personal guidance and support. They both recognize the relationships between academic freedom, learning and enjoying one's work. I thank them for the many examples they set, both in science and tennis.

I would also like to thank all my "pals." You may not have helped me get through any faster but you made it possible for me even to finish. Members of my committee, Drs. Wilkes, McGrath, Lewis and Dorn, deserve recognition for the examples they set and their help, direct and indirect, on this dissertation.

Finally, to and my "family;" now it's your turn.

TABLE OF CONTENTS

ACKNOWLEDGEMENTS.....	iv
TABLE OF CONTENTS.....	v
LIST OF TABLES.....	vii
LIST OF FIGURES.....	ix
CHAPTER 1.	
Introduction.....	1
Goals and Approach.....	13
CHAPTER 2. Preparation of Chain-Extended Hydroxypropyl Lignin.	
Introduction.....	21
Experimental.....	26
Results and Discussion.....	29
Conclusions.....	34
CHAPTER 3. Characterization of Chain-Extended Hydroxypropyl Lignins.	
Introduction.....	41
Experimental.....	44
Results and Discussion.....	46
Conclusions.....	57
CHAPTER 4. Structure-Property Relationships of Polyurethane Networks Prepared from Chain-Extended Hydroxypropyl Lignins.	
Introduction.....	74
Experimental.....	77
Results and Discussion.....	82
Conclusions.....	100

CHAPTER 5. Effects of Hydroxypropyl Lignin Molecular Weight on Prepolymer and Network Properties.	
Introduction.....	124
Experimental.....	127
Results and Discussion.....	129
Conclusions.....	145
CHAPTER 6. Polymer Composites from Lignin-Based Polyurethanes and Polymethyl Methacrylate	
Introduction.....	164
Experimental.....	169
Results and Discussion.....	172
Conclusions.....	185
CHAPTER 7. Effects of Lignin Content on the Properties of Interpenetrating Polymer Networks.	
Introduction.....	204
Experimental.....	207
Results and Discussion.....	208
Conclusions.....	214
CHAPTER 8.	
Conclusions.....	223
VITA.....	228

LIST OF TABLES

	PAGE
Table 1-1. Frequency of interunit linkages in lignins containing 100 phenylpropane units.....	18
Table 2-1. Estimates of loss of propylene oxide during reaction and amount of chain-extended hydroxypropyl lignin (CEHPL) copolymer produced.....	37
Table 3-1. Chemical analysis of chain-extended hydroxypropyl lignins (CEHPLs).....	64
Table 3-2. Composition of CEHPLs.....	65
Table 3-3. Molecular weight and thermal properties of CEHPLs.....	66
Table 4-1. Dynamic mechanical properties of lignin-based polyurethanes (LPUs).....	105
Table 4-2. Effect of lignin content and diisocyanate type on the activation energy of the LPU's T_g	107
Table 4-3. Mechanical properties of LPUs.....	108
Table 4-4. Network properties of LPUs as determined from swelling experiments.....	110
Table 4-5. Contribution to the change in T_g with network formation predicted from the model of Chan <i>et. al.</i> and the Fox equation....	112
Table 5-1. Molecular, thermal, and chemical characteristics of the original Kraft HPL and five fractions of varying molecular weight.	151
Table 5-2. Thermal properties of LPUs prepared with the original and fractionated HPLs.....	153
Table 5-3. Network properties of LPUs prepared with the original and fractionated HPLs.....	154

Table 5-4. Determination of copolymer effect, cT_g , and crosslinking effect, T_g , in the T_g of LPU's prepared from the original and fractionated HPLs.....	155
Table 5-5. Mechanical properties of LPU's prepared from the original and fractionated HPLs...	156
Table 6-1. Sources of various chemicals used in preparation of LPU/PMMA composites.....	190
Table 6-2. Nomenclature and composition of LPU/PMMA composites.....	191
Table 6-3. Dynamic mechanical and thermal properties of LPU/PMMA composites.....	193
Table 6-4. Effect of S-1 composition on the activation energy (E_a) of the glass transition (T_g).....	195
Table 6-5. Effect of composition on the mechanical properties of IPNs, S-1s, and S-2s.....	196
Table 7-1. Composition of LPU/PMMA IPNs prepared from lignin polyols of varying hydroxypropyl chain lengths.....	217
Table 7-2. Effect of lignin content on the thermal properties of IPNs prepared with different CEHPLs.....	218
Table 7-3. Effect of lignin content on the mechanical properties of IPNs prepared with different CEHPLs.....	219

LIST OF FIGURES

	PAGE
Figure 1-1. The three basic building blocks which may be polymerized to form lignin in wood.....	19
Figure 2-1. GPC chromatograms of the reaction products of guaiacol and propylene oxide with CsOH as a catalyst. Peak A is the guaiacol starting material, peak B is hydroxypropyl guaiacol, and peaks C and D are the chain extended materials with molar substitutions of 2 and 3, respectively.....	38
Figure 2-2. GPC chromatograms of the products of the reaction of propylene oxide with hydroxypropyl lignin, using KOH and 18-crown-6 as catalyst. Chromatogram I is the crude reaction product, II is the acetonitrile soluble fraction, III is the water soluble fraction and IV is the purified chain extended hydroxypropyl lignin. A refractive index (—) detector and an UV (— —) detector (254 nm) were used in series.....	39
Figure 3-1. ¹ H-NMR spectra of a lignin, hydroxypropyl lignin (HPL) and chain-extended hydroxypropyl lignin (CEHPL). The ranges were adopted from reference 26..	67
Figure 3-2. Relationship between the intensity of the ¹ H-NMR aromatic signal, range 2&3 (O), the UV absorptivity at 280 nm., (X), and the lignin content of the CEHPLs.....	68
Figure 3-3. Total hydroxyl content as measured by ¹ H-NMR (filled symbols) and titration (open symbols) of CEHPLs; OS (○), KL (□) and FK (△). The line represents the OH content of a theoretical heximer with a DS of 1.5.....	69

Figure 3-4.	High pressure gel permeation chromatograms of the organosolv series of chain-extended hydroxypropyl lignins OS-HPL (—), OS-A (· · · · ·), OS-B (— · —) OS-C (x x x x), and OS-D (— — —).....	70
Figure 3-5.	Changes in the molecular weight (M _n) of CEHPLS, as measured from GPC, with increasing molar substitution, measured by ¹ H-NMR; OS (O), KL (X) and FK (+). The solid line represents the predicted M _n for a sample with 1.7 reactive sites on each lignin repeat unit (DS=1.7).....	71
Figure 3-6.	Changes in the normalized T _g with changes in the CEHPL copolymer composition. The solid line represents the T _g predicted from the Gordon-Taylor relationship (equation 3 in text) with k=.24. The normalization involves insertion of the T _g from either experiment or the Gordon-Taylor equation into the following equation: $\text{Normalized } T_g = \frac{T_g - T_{g1}}{T_{g2} - T_{g1}}$ where T _{g1} is between 32 and 63 C for the three respective HPLs and T _{g2} is -75 C for polypropylene oxide homopolymer.....	72
Figure 4-1.	Dynamic mechanical properties of FK chain-extended hydroxypropyl lignins crosslinked with TDI: FK-A (—) FK-B (— —), and FK-C (· · · · ·).....	114
Figure 4-2.	Differential scanning calorimetry thermograms of the OS chain-extended hydroxypropyl lignin series crosslinked with TDI: OS-B (· · · · ·), OS-C (— —) and OS-D (—).....	115
Figure 4-3.	Effect of lignin content and diisocyanate type on the T _g of LPUs prepared from chain-extended hydroxypropyl lignins crosslinked with HDI (O) and TDI (X). Two points (+) were taken from reference 23.....	116

Figure 4-4.	Glass transition temperatures of LPUs normalized for the aromatic content (wt %) of both the lignin and diisocyanate. The LPUs were crosslinked with HDI (O) and TDI (X). Two points (+) were taken from reference 23.....	117
Figure 4-5.	Effect of lignin content and diisocyanate type on the T _g range for LPUs crosslinked with HDI (O) and TDI (X). Networks formed from the original hydroxypropyl lignins and crosslinked with HDI are shown separately (+).....	118
Figure 4-6.	Load-elongation response of OS polyols crosslinked with HDI and TDI. The first letter represents the type of diisocyanate, HDI (H) or TDI (T) and the second letter represents the polyol, ie. OS-A is a CEHPL organosolv lignin with a lignin of 58% (reference 17). Response 1 is that of a HDI crosslinked LPU prepared from a mixture of a HPL and PEG (reference 15). Response 2a and 2b are polyurethanes prepared with a molecular weight between crosslinks (M _c) which is similar to the LPUs (reference 29).....	119
Figure 4-7.	Effect of lignin content and diisocyanate type on the Youngs modulus (MOE) of LPUs crosslinked with HDI (O) and TDI (X). Also included are the MOE values for LPUs prepared from blends of HPLs and PEG and crosslinked with HDI (+) and TDI (-) (reference 15).....	120
Figure 4-8.	MOE of LPUs normalized for the aromatic content (wt. %) of both the lignin and diisocyanate. The LPUs were crosslinked with HDI (O) and TDI (X) Also included are the MOE values for LPUs prepared from blends of HPLs and PEG and crosslinked with HDI (+) and TDI (-) (reference 15).....	121
Figure 4-9.	Relationship between the T _g (T _g film - T _g polyol) and the molecular weight	

<p>between crosslinks (M_c) for LPU's cross-linked with HDI (O) and TDI (X). The plots provide values for the model of Chan <i>et. al.</i> (reference 36 and equation 9 in text).....</p>	122
<p>Figure 5-1. High pressure gel permeation chromatograms of the original (—) and fractionated HPLs: fraction 1 (—•••) fraction 2(x x x), fraction 3 (—•—) fraction 4(••••), and fraction 5(— —).</p>	157
<p>Figure 5-2. Plot of the Fox-Flory relationship (equation 1 in text) for the fractionated (O) and original (+) HPLs.....</p>	158
<p>Figure 5-3. Relationship between intensity of aromatic $^1\text{H-NMR}$ signal (Range 2&3) and UV absorptivity (280 nm) for the original (+) and fractionated (O) HPLs.</p>	159
<p>Figure 5-4. $\text{Tan } \delta$ and $\log E'$ response for LPU's prepared from the fractionated HPLs: fraction 5 (—), fraction 4 (x x x) fraction 3 (— —), fraction 2 (—•••) and fraction 1 (••••).....</p>	160
<p>Figure 5-5. Plot of the Fox equation (equation 3 in text) used to determine cT_g (O) for the equation of Chan <i>et. al.</i>. The T_gs of the fractionated HPLs were determined from DSC while the T_g of the polymeric HDI and very high molecular weight HPL were determined from group contribution theory (reference 28) and the Fox-Flory relationship (equation 1), respectively.....</p>	161
<p>Figure 5-6. Effect of the molecular weight between crosslinks (M_c) on ΔT_g of LPU's prepared from fractionated HPLs (O) and the original HPL (+), from equation 9 in Chapter 4.....</p>	162
<p>Figure 6-1. Dynamic mechanical properties of S-1s with varying LPU/PMMA compositions: S-1 (.75) (••••), S-1 (.6) (—•••), S-1 (.5) (— —), S-1 (.4) (x x x) and</p>	

	S-1 (.25) (—). The T _g of the LPU was -37 C and the T _g of the PMMA was 116 C.....	198
Figure 6-2.	Dynamic mechanical properties of IPNs with varying LPU/PMMA compositions: IPN (.75) (••••), IPN (.5) (— —), IPN (.25) (—). The T _g of the LPU was -37 C and the T _g of the PMMA was 126 C.....	199
Figure 6-3.	Dynamic mechanical properties of S-2s with varying LPU/PMMA compositions: S-2 (.75) (••••), S-2 (.6) (—•••), S-2 (.5) (— —), S-2 (.4) (×××) and S-2 (.25) (—). The T _g of the LPU ca. was -52 C and the T _g of the PMMA was 126 C.....	200
Figure 6-4.	Dynamic mechanical properties of blends with varying LPU/PMMA compositions: B (.75) (••••), B (.5) (— —), B (.25) (—). The T _g of the LPU ca. was -52 C and the T _g of the PMMA was 116 C.....	201
Figure 6-5.	Effect of composition and IPN type on the Youngs modulus (MOE): IPNs (◊) S-1s (◻) and S-2s (○). The lines represent equations 1-3 in the text. These equations are the logarithmic rule of mixtures (eq. 1, ref. 12), the equation of Davies with n=1/5 (eq. 2, ref. 12) and the equation of Budiansky (eq. 3, ref. 13).....	202
Figure 7-1.	Effect of lignin content on the dynamic mechanical properties of IPNs: IPN-28 (••••), IPN-21 (— —), IPN-17 (—•—), and IPN-13 (—).....	220
Figure 7-2.	Effect of lignin content on the T _g of IPNs: T _g of the PMMA (X), T _g of the LPU (O), and T _g of IPN-25 and IPN-28 where only one T _g was observed (+).....	221
Figure 7-3.	Effect of lignin content on the mechanical properties of IPNs: MOE (O) strength (+) and strain (X).....	222

CHAPTER 1

INTRODUCTION

Lignin Chemistry

Lignin is a complex biopolymer comprised of phenylpropane repeat units (1,2). In wood, lignin accounts for 25 - 30% of the weight of the dry plant material and is found to be closely associated with the carbohydrates (3-5). Together these two classes of polymers comprise between 90 and 99% of the wood substrate. Thus lignin may be considered as one of the most abundant natural polymers. The study of lignin as a material has lagged behind that of many other natural polymers. The extremely complex and intractable nature of the polymer has been a major limitation to complete characterization. While the exact structure of lignin remains an enigma, major advances in understanding have been made in several areas. Lignin chemistry is the subject of several reviews (6-9).

Advances in lignin chemistry have been made in conjunction with advances in instrumentation and improved understanding of fundamental concepts in other fields including polymer chemistry and biochemistry (10-16).

Today, progress in lignin chemistry is being made with the advent of new spectroscopic techniques (12,13,14) and with the application of concepts from statistics (15) and physical chemistry (10,11,16) . However, many important questions in lignin chemistry remain unresolved. Several of these unresolved questions which are important to the current study will be discussed.

The complex and heterogeneous nature of lignin is now well recognized (1,2,6-9). The complex nature of lignin revolves around the initial coupling of radical isomers and secondary condensation reactions(7). The process is quite complex under the most controlled conditions but in nature one must add factors such as isogenetic variation within species, weather and atmospheric pollutants, site and growth factors and other natural perturbations, all of which may affect the plant's biosynthetic pathways and thus lignin structure (17,18). In spite of these convoluting effects, there are several generally accepted reaction sequences which combine to yield lignin. Lignin is formed from a combination of three basic phenylpropane monomers: coumaryl, coniferyl and sinapyl alcohols (Figure 1-1). These monomers differ only in the presence of methoxyl groups ortho to the phenolic hydroxyl.

The initial coupling of the monomeric units is due to combination of two of the five major free radical isomers. The number of radical isomers which may couple depends on which of the phenyl propane starting materials is considered. Following the initial radical combination, there is also the potential for nucleophilic additions to the propane side chain. There is evidence that nucleophilic additions or exchange reactions continue for several years (19). The combination of radical and nucleophilic reactions produce the 15 different linkages between phenyl propane units which have been identified. Several of these linkages may involve covalent bonds formed between lignin and adjacent carbohydrates (20). The product of these reactions is a three dimensional, crosslinked structure. However, from this multitude of potential structures, a few prominent bonds apparently account for a majority of lignin interunit linkages. A brief summary of these lignin linkages is shown in Table 1-1.

Additional complications for the characterization of lignin result during the isolation of lignin from the tree. All isolation processes used for lignin structural analysis are a balance of two mutually exclusive goals: high yield and representative chemical structure. Since lignin in wood is an insoluble material, a removal of quantities

greater than 1 or 2 weight percent requires degradation or derivatization of the in situ lignin. Thus the properties of native lignin must be deduced from the modified isolated components (10-14) or must be studied in situ (14,21). Both of these approaches have been attempted with some success, though each approach has limitations.

For example, work on isolated lignin has shown the potential for significant secondary interactions (10,16). In isolated samples these interactions complicate molecular weight measurements (10) and may limit the number of conformations that the lignin sample may adopt (15). In solid wood these interactions may affect the orientation (21) of the lignin polymer and influence the mechanical properties of the wood (16). However, the precise relationships between the secondary interactions known to be present in isolated lignins and the importance of these interactions in situ have not been established.

Efforts to study lignin in situ are limited by the insoluble nature of the material and the presence of carbohydrates. Developments in spectral techniques such as solid state nuclear magnetic resonance, infrared, and Raman spectroscopy allow one to study solid materials (17,21). However, interference from the other wood

components complicates detailed studies of lignin structure.

Lignin Derivatives: Chemical and molecular structure of isolated lignins will be influenced by the conditions used in the isolation process such as reaction time, temperature, pH, solvent ratios and catalyst (6-9). Once lignin has been isolated, precise characterization of the chemical structure is still difficult. An incomplete knowledge of the exact chemical structure of lignins has hampered attempts to utilize this material. For example, if one hopes to react lignin with formaldehyde and use the product as an active component in a phenol-formaldehyde resin, the number of unsubstituted sites ortho to a free phenolic hydroxyl group is critical. To a lesser extent, substituents on the α and β carbons will affect the potential for side reactions. Thus, lignin has been frequently considered as an inert filler rather than an active component of the material (6).

To overcome the insoluble nature of isolated lignin in wood, utilization generally requires the preparation of a lignin derivative. The most common industrial derivative is a liginosulfonate, which is a water soluble by-product of wood pulping. Liginosulfonates have a number of

applications as surfactants. A number of other lignin derivatives have been prepared for use in other applications. Among these derivatives are hydroxyalkyl lignins (22-24). These copolymers are the product of the reaction of lignin with a 1,2-epoxy. Propylene oxide is a common 1,2-epoxy used in lignin modification reactions. Preparation of hydroxypropyl lignins (HPLs) imparts several beneficial properties to the copolymers. The HPLs are soluble in most polar or protic organic solvents, they contain a single type of reactive functional group (secondary hydroxyls) and they possess a lower glass transition temperature (T_g) than the parent lignin (23). Due to improved solubility, the preparation of HPLs also allows an accurate characterization of the copolymer. The present work takes advantage of the benefits offered by hydroxypropylation.

For this work the crucial HPL copolymer parameters were the copolymer composition, molecular weight and molecular weight distribution. These factors will affect copolymer solubility and the ability to form a complete, crosslinked network. The copolymer composition may influence the thermal and mechanical properties of the polyurethane. Networks based on HPL copolymers may be formed by

crosslinking the polyols with diisocyanates to form polyurethanes.

Polyurethanes

Polyurethanes constitute a most versatile polymer system (25-29). Polyurethanes are the product of a condensation reaction between a hydroxyl-containing molecule (polyol) and a multifunctional isocyanate. By varying the chemical composition and functionality of either the polyol or the isocyanate, a wide range of materials may be prepared. These materials range between homogeneous or heterogeneous flexible elastomers to high modulus, semi-crystalline materials. Depending on the desired level of material reliability and performance, the types of the two polyurethane components varies widely.

Moderate- to high-molecular weight (10^3 - 10^4 daltons) polyols are commonly polyesters or polyethers, though polyethylene and polybutadiene polyols are also used (26). The polyol backbones may contain a variety of polar or aromatic substituents (30). These polyols may be linear or branched. Each of these materials will provide different properties to the system but they are generally flexible materials and are generically termed the "soft segments."

Low molecular weight (<100 daltons) polyols can be combined with an excess of diisocyanate to form a regular repeating unit which is capable of forming an aggregated "hard segment". This hard segment prepolymer may then be combined with a high molecular weight diol, soft segment, to form a phase separated material with unique properties.

Much of the versatility of polyurethanes may be attributed to effective control over the extent and type of interactions between the soft and hard segments (27,31). Phase separation of the hard and soft segments allows for the formation of macromolecular structures which act as network junctions. The material properties may then be influenced by varying the concentration or distribution of the hard segments. Interaction between the soft segments and hard segments may be achieved by variation in the composition of the soft segments. Inclusion of rigid or polar groups in the soft segment may influence the extent of phase separation. In the case of HPLs, the copolymer composition will influence the ratio of rigid to flexible groups.

In the case of lignin-based polyurethanes (LPU), the aromatic lignin molecules may be viewed as the high modulus rigid segments while the propylene oxide chains are

comparable to the flexible soft segments. The presence of observable phase separation will depend on the length of the hydroxypropyl chains. Covalent bonding between the two polyol components could limit the potential for extensive phase separation, which has been observed in many polyurethanes.

Formation of Lignin Networks

As discussed above, the complex nature of lignin, both in situ and isolated, causes problems for lignin utilization. Formation of a hydroxypropyl derivative alleviated several problems by improving solubility, lowering T_g , and creating a single type of hydroxyl group (23). However, there were two other considerations which must be addressed. The first was the broad molecular weight distribution which complicated the formation of a homogeneous network. The second consideration was a distribution of hydroxyls among molecules with similar molecular weights. The average functionality of the particular lignin derivative will be dependent on both of these distributions.

The formation of a polymer network depends on the average functionality of the systems. A broad molecular

weight distribution may allow for a large number of chain ends or tightly crosslinked centers depending on the functionality of the system. Both free chain ends and crosslink points would influence the properties of the network.

Flory (32) and others have developed models for the gelation of a network. These models predict that the molecular weight of the system will rise as the reaction proceeds to the gel point. Above the gel point two components, the gel and the sol, may be identified in the system. The gel is considered as an infinite network while the sol is made up of low molecular weight materials which may continue to be incorporated into the gel. The relationship between the gel point and the extent of reaction is determined by the functionality of the original components. If a difunctional isocyanate is used, the lignin derivative must have an average functionality of greater than two to allow for formation of a network if the stoichiometry is correct. An individual molecule with high functionality is more likely to be incorporated into the gel than a molecule with low functionality. Molecules with low functionality are likely to remain entrapped as sol molecules which do not contribute significantly to the

strength properties of the networks. The sol molecules will influence the mechanical properties of the networks.

The formation of a network and the distribution of the sol and gel components has a significant influence on the properties of a material. From a practical standpoint, a highly cured network most efficiently uses the original components to provide mechanical strength and will provide the greatest long-term stability. A small sol component may impart beneficial properties to the material by providing low T_g or enhancing elongation properties. However, a large proportion of molecules with low functionality does not usually bode well for the formation of a complete, homogeneous network.

The structure of networks may be studied with numerous techniques. Combination of information from a wide variety of experimental techniques may result in a good understanding of a material (33,34). Due to practical limitations of time and availability, a limited number of techniques was selected to study the LPU networks or LPUs as one component in a polymer composite. Dynamic mechanical and thermal analysis allow one to determine the number and type of phases present in a material. Interactions between components may also be estimated with

these two techniques. Mechanical properties which may not be sensitive to subtle changes in chemistry provide important practical information about a material's behavior. A measure of network properties may be obtained with swelling experiments. A combination of these techniques allows one to develop a coherent understanding of the relationships between variations in chemistry and the resulting changes in the material properties.

Goals and Approach

The long-term goal of this work was to demonstrate an ability to modify and utilize lignin as a major component of polymeric systems. It is envisioned that the lignin would be covalently incorporated into the polymer systems and provide benefits over and above those of a low-cost filler. To realistically accomplish these broad goals, one must develop an understanding of lignin which allows it to be viewed as any other polymer material, albeit a complex one. Thus lignin can not be viewed as a mystical material which is unique in polymer science. Instead lignin must be viewed as a complex material, whether completely understood or not, whose behavior obeys the rules established for all other polymers.

The approach undertaken to meet these goals involved a five point study:

- 1) Study the reactions of lignin models with propylene oxide in various solvent-catalyst combinations. Develop a system to prepare chain-extended propylene oxide model products.

2) Prepare and characterize three series of chain-extended hydroxypropyl lignin copolymers (CEHPLs). These CEHPLs differ in the methods used to isolate the original lignin. Study the effects of the lignin's origin on the copolymer properties.

3) Incorporate these CEHPL copolymer polyols into polyurethane networks. Study the dynamic mechanical, thermal, engineering and network properties of these LPUs, in particular the effects of the copolymer composition, diisocyanate type and lignin origin.

4) Fractionate hydroxypropyl lignin into discrete polyols with varying molecular weights. Incorporate and characterize the LPUs prepared from these fractions. Relate the characteristics of these LPUs to the molecular weight and functionality of the fractionated polyols.

5) In a separate study, prepare a series of LPU-PMMA composites, including interpenetrating polymer networks. Explain the properties of these composites in relation to their network structures. Compare the properties of the LPU-PMMA composites to the properties of similar polyurethane/PMMA composites prepared by other workers.

REFERENCES: CHAPTER 1.

1. T. Higuchi, Advan. Enzymol., 34,207 (1971).
2. A. B. Wardrop, J. Appl. Polym. Sci. (Appl. Polym. Symp.), 28,1041 (1976).
3. R. M. Rowell, The Chemistry of Solid Wood, Advances in Chemistry Series No. 207, American Chemical Society, Washington, D.C., 1984.
4. E. Sjostrom, Wood Chemistry Fundamentals and Applications, Academic Press, New York, 1981.
5. D. Fengel and G. Wegener, Wood: Chemistry. Ultrastructure Reactions, Walter de Gruyter, New York, 1984.
6. K. V. Sarkanen and C. H. Ludwig, eds., Lignins: Occurrence, Formation, Structure and Reactions, Wiley-Interscience, New York, 1971.
7. W. G. Glasser, Ch. 2 in Pulp and Paper Chemistry and Chemical Technology, 3rd ed., Vol. 1, J. P. Casey, ed., Wiley- Interscience, 1980.
8. E. Adler, Wood Sci. Technol., 11,169 (1971).
9. K. Freudenberg and A. C. Neish, Constitution and Biosynthesis of Lignin, Springer-Verlag, New York, 1968.
10. S. Sarkanen, D. C. Teller, E. Abramowski, and J. L. McCarthy, Macromol., 15,1098 (1982).
11. W. G. Glasser, H. R. Glasser, and N. Morohoshi, Macromol., 14,253 (1981).
12. H. H. Nimz, D. Robert, O. Faix, and M. Nemr, Holzforschung., 35,16 (1981).
13. T. P. Schultz, M. C. Templeton, and G. D. McGinnis, Anal. Chem., 57,2867 (1985).

14. A. Janosi, J. Schurz, and N. Matin, Cell. Chem. Tech. 19, 487 (1985)
15. M. Remko, Z Phys. Chem. 138(2), 223 (1985)
16. S. S. Kelley, T. C. Rials, and W. G. Glasser, J. Mater. Sci., in press.
17. D. F. Barron, R.L. Frost, L. Doimo, and M.J. Kennedy, J. Macromol. Sci., Chem. Ed., A22(3) 303(1985).
18. A. B. Wardrop, in Aspects of Xylem Cell Development J. R. Barnett, ed. Castle House Publications, London 1981
19. G. J. Leary, Wood Sci. Technol., 16,16 (1982).
20. O. Eriksson and B. O. Lindgren, Svensk Papperstidn., 80(2), 59 (1977).
21. R. H. Atalla, Science, 227, 39, Jan 4 (1985).
22. W. G. Glasser, O. H-H. Hsu, D. L. Reed, R. C. Forte, and C.-F. Wu, in Urethane Chemistry and Applications, K. Edwards, ed., ACS Symposium Series No. 172, American Chemical Society, Washington, D.C., 1981, p. 311.
23. W. G. Glasser, C. A. Barnett, T. G. Rials, and V. P. Saraf, J. Appl. Polym. Sci., 29,1815 (1984).
24. W. G. Glasser, L. C-F. Wu, and J-F. Selin, Wood and Agricultural Residues: Research on Use for Feed, Fuels, and Chemicals., E. J. Soltes, ed., Academic Press, 1983, p. 149
25. P. J. Manno, in Urethane Chemistry and Applications, K. Edwards, ed., ACS Symposium Series No. 172. American Chemical Society, Washington, D.C., 1981, p. 9.
26. I. S. Lin, J. Biranowski, and D. H. Lorenz, Chemistry and Applications, K. Edwards, ed., ACS Symposium Series No. 172, American Chemical Society, Washington, D.C., 1981, p. 523 and references therein.

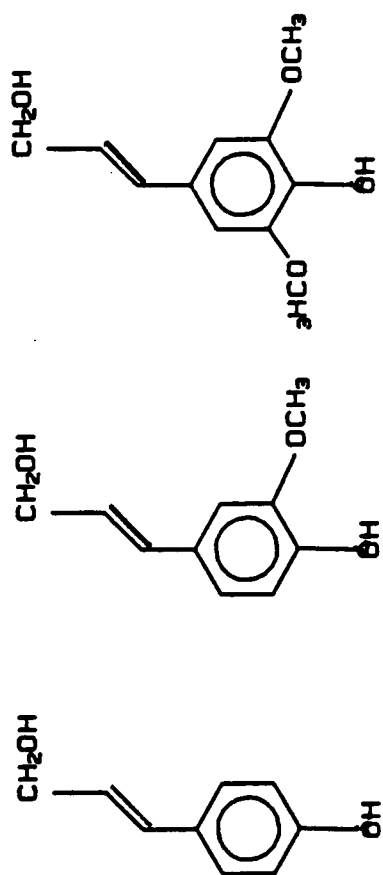
27. C. Hepburn and R. J. W. Reynolds, Chap. 7 in Molecular Behavior and the Development of Polymeric Materials, A. Ledwith and A. M. North, eds., Chapman and Hall, London, 1975.
28. B. Kanner and B. Prokai, Advances in Urethane Science and Technology, Vol. 2, Technomic Publishing Co., Westport, 1973.
29. C. S. Paik Sung, in Polymer Alloys II, D. Klempner and K. L. Frisch, eds., Plenum Press, New York, 1979.
30. D. Klempner and K. C. Frisch, in Urethane Chemistry and Applications, K. Edwards, ed., ACS Symposium Series No. 172, American Chemical Society, Washington, D.C., 1981, p. 533.
31. R. J. Lookwood and L. M. Alberino, in Urethane Chemistry and Applications, K. Edwards, ed., ACS Symposium Series No. 172, American Chemical Society, Washington, D.C., 1981, p. 363 and references therein.
32. P. J. Flory, Principles of Polymer Chemistry, Cornell University Press, Ithaca, 1953.
33. C. D. Craver, Polymer Characterization: Spectroscopic, Chromatographic and Physical Instrumental Methods, Advances in Chemistry Series No. 203, American Chemical Society, Washington, D.C., 1983.
34. C. A. May, Chemorheology of Thermosetting Polymers, ACS Symposium Series No. 227, American Chemical Society, Washington, D.C., 1983.

TABLE 1-1

Frequency of Interunit Linkages in Lignins
Containing 100 Phenylpropane Units (ref. 7)

<u>Linkage Type</u>	<u>Frequency</u>
β -0-4	41
α -0-4	5
β -5	14
β -1	11
β - β -all ex. THF ^a	11
Dibenzyl-THF ^a	-
5-5	16
4-0-5	12
α - β	-
β -6	4
1-5,6-5,1-0-4	5
Miscellaneous	-
Total	<u>119</u>

^a THF stands for tetrahydrofuran structures



P-HYDROXYPHENYL GUAIACOL SYRINGYL

FIGURE 1-1. The three basic building blocks which may be polymerized to form lignin in wood.

Chapter 2

PREPARATION OF CHAIN-EXTENDED HYDROXYPROPYL LIGNIN

Synopsis

Hydroxyl containing lignin model compounds could be reacted with propylene oxide using several different alkaline-earth cations as catalyst. The reaction was affected by the type of catalyst, with Cs being the most effective single catalyst. Hydroxypropyl lignin could be reacted with propylene oxide at 70 C using KOH and 18-crown-6 ether as catalysts. By varying the amount of propylene oxide the molar substitution (the number of hydroxypropyl groups in a chain) of the hydroxypropyl lignin could be increased. This chain-extended hydroxypropyl lignin could be isolated by a series of liquid/liquid extractions.

Introduction

Ring opening polymerization of 1,2-epoxies has been extensively studied for almost 60 years (1). Since that time the preparation of low and high molecular weight polyalkylene oxides has been the subject of much work and several reviews (2-7). Much of the initial work centered around relatively simple acidic and basic catalysts (2), although the product of these reactions were generally low- to moderate-molecular weight species. Preparation of high molecular weight polyalkylene oxides was made possible by the development of metal alkoxide catalysts (8). Since then a number of effective phase transfer and coordination catalysts (9,10) have allowed for the preparation of high molecular weight stereoregular or optically active polyalkylene oxides (5,6). In spite of extensive studies over many years, the mechanism of the ring opening for some of the simplest cases has not been resolved (7).

Two of the simplest, though not the most efficient, ring openings are the acid (2) and base (2,11) catalyzed reactions. Despite the strained nature of the 1,2-epoxide ring, the entropy contribution of the ring opening reaction does not dominate in all cases (2). Simple acid catalysts have generally been found to be more effective than simple

bases due in part to the basic nature of the epoxide ring. The ring opening under acidic conditions is viewed as a reaction with the epoxide oxygen acting as the nucleophile. The direction of the ring opening will vary depending on the substituents but generally, formation of the primary hydroxyl is favored. For substituents with strong inductive effects, a S_N1 mechanism has also been proposed (13).

The base catalyzed reaction has also received considerable attention but is still not completely understood (7,14,15). In the simplest case the reaction appears to be S_N2 in character with steric considerations influencing the formation of the secondary hydroxyl. The less substituted carbon may also more easily accommodate the partial negative charge. The simple case may be complicated by the presence of ion-pairs (2,14) or hydrogen bonding (11) between the initiator and epoxide oxygen.

Some of the early studies of the anionic polymerization of 1,2-epoxies focused on alkaline earth catalysts. These initial studies (15) concluded that LiOH and NaOH were ineffective catalysts while KOH, RbOH and CsOH were effective. Typically these studies were conducted under bulk, anhydrous conditions. These early results appeared to

conflict with later studies which showed a series of Na alkoxides to be effective catalysts in the presence of various solvents and initiators (16,17). In solution with a polar or protic solvent, the rate of ring opening was related to the basicity of the alkoxide. The more basic catalyst produced the highest reactivity.

In the case of protic solvents or non-protic solvents with initiators, the ring opening becomes more complex. Under these conditions the activated species appears to be a termolecular complex (2,18). A protic solvent or initiator may hydrogen bond with the epoxide oxygen and reduce the electron density on the terminal carbon. This makes the terminal carbon susceptible to attack by the catalyst or nucleophilic species. The presence of hydrogen bonding between a protic species, phenol, and the epoxy oxygen has been observed spectroscopically (19) although the exact nature of the transition state is still not completely resolved. While solvent effects or an initiator may increase the susceptibility of the epoxide to attack, a stronger nucleophile will also increase the rate of the ring opening reaction. This approach has also been utilized in several studies where solvation of the alkoxide cation was investigated (20). The large alkaline earth metal cations, K and Cs, were solvated in DMSO while the

small cations, Li and Na, were found as ion pairs. Addition of alcohol allowed for solvation of all the cations and was related to previously observed differences in the rates of base catalyzed reactions.

While the addition of a protic solvent allows for solvation and an increase in catalyst activity, it is inappropriate for some ring opening polymerizations. In the polymerization of 1,2-epoxies the protic initiator may also promote side reactions which reduce the efficiency of the polymerization (2,14). Thus a second approach for solvation of the cation has been considered.

Crown ethers are known to solvate cations to various degrees depending on the size of the cation and the size of the ring. In the case of the K cation, 18-crown-6 ether is known to provide an effective solvation sphere (21). The use of crown ethers to promote the formation of high molecular weight epoxies has been discussed in both the scientific (11,21-23) and patent literature (24). The purpose of the crown ether is to solvate the cation which produces a more nucleophilic anion for both electronic and steric reasons. Even with the addition of the crown ether, the reactivity of the system was increased by the presence of an initiator. Thus the addition of 18-crown-6, a

potassium catalyst, and a polar solvent has been used for the preparation of moderate to high molecular weight polypropylene oxide polymers or copolymers (23) .

Lignin Model Compounds

The reactivity of various lignin model compounds with 1,2-epoxies has previously been investigated (18,25). A series of studies investigated the reaction of lignin model compounds with propylene oxide using Na guaiacolate as a catalyst and DMF and glycerol as solvents. The rate of the reactions was related to the acidity of the functional group on the lignin model, with the more acidic groups being more reactive. Guaiacol and vanillic alcohol were exceptions to this trend, with their reactivity decreasing with an increase in acidity. The activation energies were fairly constant between 14.2 and 15.2 kcal/mol.

Other studies were carried out at high temperature (180 C) with KOH as a catalyst (26). These studies showed that the rate of copolymer formation was related to the amount of KOH and the acidity of the functional group. The reactivity followed the trend of Aliphatic $O^- > OH^- >$ Aromatic $O^- > RCOO^-$ from most reactive to least reactive. The trend follows nucleophilicity which provides that the

strongest nucleophile is the most reactive species. The order of reactivity conflicts with an earlier study (18). The apparent conflict may be due to the presence of a base which would ionize the active hydroxyl and change the strength of the nucleophile. Neither of the studies with lignin model compounds investigated the effects of an initiator or variation of solvent polarity to allow for charge separation. It was also noted that the model compound reaction products contained a single propoxyl group on each reactive site (26). Under the conditions used for the original reaction, chain extension was not observed.

The goal of this initial study was to determine a set of reaction conditions which would allow the preparation of chain-extended hydroxypropyl lignins (CEHPLs). Initially a lignin model compound (guaiacol) was used to allow for accurate characterization. Then several series of CEHPLs were prepared and purified.

Experimental

Preparation of Chain-extended hydroxypropyl guaiacol: A typical formulation consisted of 1.0×10^{-3} mol guaiacol, 5.0×10^{-5} mol catalyst, 2.0×10^{-2} mol propylene oxide,

and 6.0×10^{-2} mol solvent. In some experiments 1.0×10^{-5} mol 18-crown-6 ether was also added. The reaction mixtures were heated in sealed stainless steel reactors at 75 C for varying lengths of time, up to 100 hrs in some cases.

Preparation of Lignin Derivatives: Typically (26) 30 g of lignin, 1 g KOH, 40 ml propylene oxide and 120 ml of toluene were combined in a 600 ml stainless steel mechanically stirred (Parr, Inc.) reactor. The reactor was sealed and heated to 180 C. while the mixture was vigorously stirred. The HPL was isolated by evaporation followed by liquid/liquid extraction with hexane/ acetonitrile. The HPL product was used as the starting material for subsequent chain extension and preparation of the fractionated kraft HPL.

The CEHPLs were prepared using the same general procedure, but with the addition of a crown ether and a trace of acetone. Thus a typical reaction mixture consisted of 11.0 g of HPL (0.04 moles), 0.58 g of KOH (0.01 moles), 1.3 g of 18-crown-6 (0.005 moles), 70 ml of toluene (0.76 moles), and 3.0 ml of acetone (0.05 moles). This mixture was sealed in a 600 ml stainless steel Parr reactor and heated to 75 C. Propylene oxide was added at a rate of 1.5 ml/hr to achieve the desired level of chain-extension.

The reaction product was isolated by evaporation of solvent and dissolution in acetonitrile (27). Liquid/liquid extraction with hexane/acetonitrile for one week was used to remove polypropylene oxide (PPO) homopolymer. The acetonitrile-soluble fraction was isolated by evaporation and redissolved in chloroform for a subsequent water/chloroform liquid/liquid extraction for an additional week. The chloroform-soluble fraction was isolated by evaporation and stored over P₂O₅ for subsequent analysis. The CEHPL products were all brown in color and varied in consistency between a tacky solid and low viscosity liquid.

Methods

The gel permeation chromatography (GPC) analysis was performed on an LDC system with ultraviolet (UV) (280 nm) and refractive index (RI) detectors. An Altex polystyrene-divinyl benzene resin of gel size of 50 nm was used with THF as a solvent and a flow rate of 1 ml/min was used for analysis of the model compounds. Analysis of the lignin reaction products was carried out under the same conditions but used a set of three Altex columns with nominal pore sizes of 10², 10³, and 10⁴ nm. The columns were calibrated

with monodisperse polystyrene and lignin model compounds with molecular weights up to 784 gm/mol (28) .

Results and Discussion

Several constraints were placed on the selection of reaction conditions. Selection of solvents was limited by the desire to use the same reaction conditions with both lignin model compounds and lignin. The ideal reaction system would allow for the initial reaction at high temperature and pressure and then a decrease in temperature and continuing reaction to the desired copolymer composition. It was also desirable that the entire reaction be carried out in one vessel with a minimum of purification between steps. A high copolymer yield was also desirable although both copolymer and homopolymer could be used together in certain processes.

Model Compounds

Solvent Effects: Solvents which were tested included toluene, chloroform, acetonitrile and hexane. Protic solvents (i.e. MeOH) were not used as they might reduce the extent of copolymerization by promoting side reactions. Other solvents (i.e. DMSO, DMF) posed difficulties in

solvent removal after the reaction was complete. Oxygenated solvents (dioxane, tetrahydrofuran) have the potential to homopolymerize and thus were not suitable.

No chain extension was observed in any of the four selected solvents by GPC analysis. Potassium hydroxide was used as the catalyst in all of these experiments. A review of the literature had revealed several reports of cation effects for alkaline earth catalyst systems. A series of experiments was performed using different catalysts, with toluene as the solvent.

Catalyst Effects: A series of alkaline earth catalysts was investigated. These catalysts were NaOH, KOH, CsOH, potassium guaiacolate and cesium guaiacolate. It was anticipated that the cesium cation systems could allow for chain extension due to better solvation of Cs^+ than K^+ . The GPC analysis showed that none of these catalyst systems allowed for substantial chain extension. With extended reaction times (>100 hrs) the cesium guaiacolate system showed the presence of some hydroxypropyl guaiacol with a molar substitution of 1-3, Figure 2-1. It was calculated that only 5 percent of the propylene oxide was incorporated into the guaiacol product. This low efficiency was not considered acceptable so a third approach was attempted the

hydroxypropyl lignins. This approach involved the addition of 18-crown-6 which can chelate K^+ ions (21).

Reactions of Hydroxypropyl Lignins

Addition of crown ether: Crown ethers have the ability to solvate alkaline earth metals in many organic solvents. Multiple interactions between the oxygens of the crown ether and the cation allows for solvation. Solvation of the cation increases the reactivity of the nucleophile through electronic and steric effects. Thus the addition of 18-crown-6, which has been shown to be effective at solvating K^+ (21-23), should increase the reactivity of the secondary hydroxyl (23).

Efficiency of Polymerization: The effectiveness of the chain extension reaction was measured with two different mass balances. The first mass balance estimated the total amount of reaction product. This estimate accounted for propylene oxide which did not react or was lost due to leakage. The second mass balance determined the amount of chain-extended hydroxypropyl lignin (CEHPL) copolymer isolated from the mixture of homopolymer and copolymer reaction products. These values are shown in Table 2-1.

It was apparent from the loss of 9 - 38% of the propylene oxide that the system used for the chain extension reaction was not completely sealed. Most likely, the syringe-line used for continuous addition allowed for a loss of propylene oxide. The amount of copolymer produced was generally between 69 and 86% of the non-volatile material removed from the reaction. One exception was KL-E (Table 2-1.) which provided only 60% of the reaction product as isolatable copolymer. The balance of the reaction products were propylene oxide homopolymer, which was soluble in hot hexane, or propylene glycol oligomers which were soluble in hot water. The water soluble material was quite dark in color and probably contained some low molecular weight lignin.

It should be emphasized that both the isolated CEHPL copolymer and the extracted propylene oxide homopolymer and oligomers were suitable for inclusion in a polyurethane polyol. However, since the ultimate goal of this study was to investigate the effects of lignin variables on network properties, the PPO homopolymer was removed to simplify the subsequent interpretation.

Purification of CEHPL: The majority of the homopolymer and a small amount of copolymer were removed by the initial

hexane/ acetonitrile extraction. It should be noted that these lignin derivatives had already been subjected to a hexane/acetonitrile extraction after the initial propoxylation reaction. This previous extraction may have also removed some low molecular weight HPL copolymer. The results, which showed about 5% (by wt.) water soluble material, suggested that for isolation of the CEHPL copolymer, a water/chloroform extraction or possibly dialysis was desirable. This second treatment was in addition to the hexane/acetonitrile extraction and allowed for the isolation of a pure copolymer.

After isolation of the CEHPL copolymer, high pressure gel permeation chromatography (GPC) was used to characterize the molecular weights of the different fractions. A similar characterization was done with low pressure Sephadex columns (27). Tetrahydrofuran was used as a solvent to insure complete solubility of both the isolated homopolymer and the copolymer. The GPC results are shown in Figure 2-2. The UV detector has been shown to be sensitive primarily to the lignin copolymer while the RI detector is sensitive to both the lignin copolymer and the polypropylene oxide homopolymer (27). As seen in Figure 2-2, the reaction product before extraction contains low molecular weight material which exhibits a strong RI

response and a very small UV response. The material isolated in the hexane and water fractions show a low molecular weight RI response. The RI and UV responses exhibit similar behavior for the final copolymer. This observation was used as confirmation that a clean copolymer was isolated following the two extractions.

Conclusions

The ring opening reaction of 1,2-epoxies with alkaline earth metals may be affected by solvent, cation type and the presence of an initiator. In the complex lignin system the reactivity was affected by the catalyst concentration which allowed for ionization of a limited number of functional groups. Under conditions of low temperature and adequate solvation both K and Cs showed catalytic activity for the ring opening reactions. The addition of 18-crown-6 ether provided for solvation of the K cation and thus allowed for preparation of chain-extended hydroxypropyl lignins (CEHPLs). The reaction generally produced between 68% and 86% CEHPL with the balance made up of propylene oxide homopolymer or oligomers. The CEHPL copolymer could be separated from the propylene oxide homopolymer/oligomer mixture by liquid/liquid extractions in acetonitrile/hexane and chloroform/water.

REFERENCES: CHAPTER 2

1. H. Staudinger and H. Lehmann, Ann., 505,41 (1933).
2. Y. Ishii and S. Sakai, in Ring Opening Polymers, K. C. Frisch, ed., Marcel Dekker, New York, 1969, p. 14.
3. J. E. McGrath, ed., Ring Opening Polymerization: Kinetics, Mechanisms and Synthesis, ACS Symposium Series No. 286, American Chemical Society, Washington, D.C., 1984
4. J. E. McGrath, ed., Anionic Polymerization: Kinetics, Mechanisms and Synthesis, ACS Symposium Series No. 166, American Chemical Society, Washington, D.C., 1980.
5. P. Sigwalt, Pure Appl. Chem., 48,257 (1976).
6. T. Tsuruta, Pure Appl. Chem., 53,1745 (1981).
7. N. S. Enikolopiyan, Pure Appl. Chem., 48,317 (1976).
8. C. C. Price and M. Osgon, J. Am. Chem. Soc., 78(690), 4787 (1956).
9. T. Aida, R. Mizuta, Y. Yoshida, and S. Inoue, Makromol. Chem., 182,1073 (1981).
10. T. Aida and S. Inoue, Makromol., 14,1166 (1981).
11. H. Koinuma, K. Naito, and H. Hirai, Makromol. Chem., 183, 1383 (1982).
12. G. Gee, W. C. H. Higginson, P. Levesley, and K. J. Taylor, J. Chem. Soc., 18,1338 (1959).
13. R. E. Parker and N. S. Isaacs, Chem. Rev., 59,737 (1959).
14. E. C. Steiner, R. R. Pelletier, and R. O. Trucks, J. Amer. Chem. Soc., 86,4678 (1964).
15. D. N. Kirk, Chem. Ind., 3,109 (1972).

16. S. G. Yeates, H. H. Teo, R. M. Mobbs, and C. Booth, Makromol. Chem., **185**,1559 (1984).
17. H. H. Teo, R. H. Mobbs, and C. Booth, Eur. Polym. J. **18**,541 (1982).
18. L. N. Mozheiko, M. F. Gromova, L. A. Bakalo, and V. N. Sergeeva, Poly. Sci. USSR, **23**(1),141 (1981).
19. J. Itakura and F. Patal, Makromol. Chem., **68**,158 (1963).
20. J. H. Exner and E. C. Steiner, J. Amer. Chem. Soc., **96**,1782 (1974).
21. S. Slomkowski and S. Penczek, Macromol., **13**,229 (1980).
22. G. N. Arkhipovich, Y. A. Ugolkova, and K. S. Kazanskii, Polym. Bull., **12**,181 (1984).
23. H. Becker and G. Wagner, Acta. Polym., **35**(1),28 (1984).
24. J. H. Exner, D. P. Sheets, and E. C. Steiner, U. S. Patent No. 3,760,005 (1973).
25. V. N. Sergeeva, M. F. Gromova, L. N. Mokheiko and J. Spiss, Tezisy Dokl. - Vses Konf. Khim. Ispol'z Lignina 6th, (CA 87;70002X).
26. L. C-F. Wu and W. G. Glasser, J. Appl Polym. Sci., **29**,1111 (1984).
27. W. G. Glasser, L. C-F. Wu, and J.-F. Selin, in Wood and Agricultural Residues: Research on Use for Feed, Fuels and Chemicals, E. J. Soltes, ed., Academic Press, New York, 1983, p. 149.
28. J. A. Hyatt, submitted to Holzforschung, (1987)

TABLE 2-1

ESTIMATES OF THE LOSS OF PROPYLENE OXIDE DURING REACTION AND THE AMOUNT OF CHAIN EXTENDED HYDROXYPROPYL LIGNIN (CEHPL) COPOLYMER PRODUCED.

CEHPL TYPE	PROPYLENE OXIDE LOSS (wt. %) ¹	CEHPL PRODUCED (wt. %) ²
OS-A	9	82
OS-B	30	82
OS-C	-	-
OS-D	22	75
KL-A	39	77
KL-B	24	79
KL-C	-	-
KL-D	17	80
KL-E	30	60
KL-F	38	73
FK-A	12	86
FK-B	13	79
FK-C	22	69

¹ Loss due to leakage in pressure line.

² CEHPL copolymer isolated from reaction product after liquid/liquid extractions.

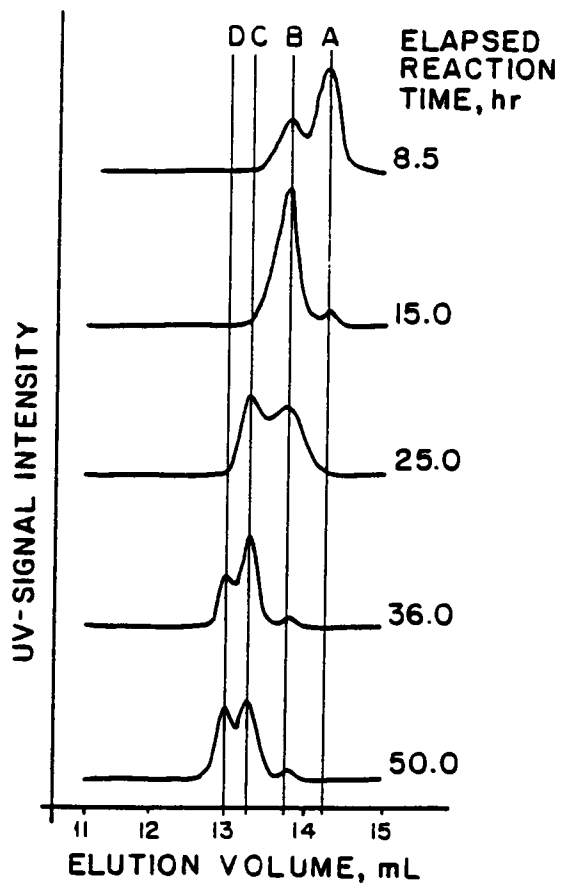


FIGURE 2-1. GPC chromatograms of the reaction products of guaiacol and propylene oxide with CsOH as a catalyst. Peak A is the guaiacol starting material, peak B is hydroxypropyl guaiacol, and peaks C and D are the chain extended materials with molar substitutions of 2 and 3 respectively.

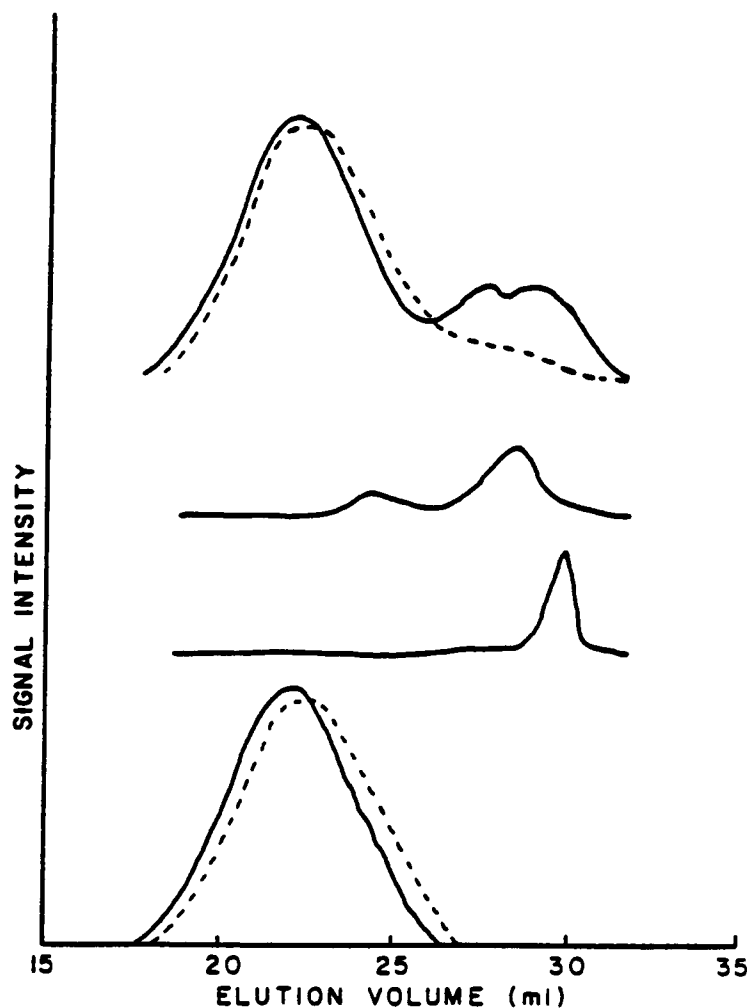


FIGURE 2-2. GPC chromatograms of the products of the reaction of propylene oxide with hydroxypropyl lignin using KOH and 18-crown-6 as catalyst. Chromatogram I is the crude reaction product, II is the acetonitrile soluble fraction, III is the water soluble fraction and IV is the purified chain extended hydroxypropyl lignin. A refractive index (—) detector and an UV (— —) detector (254 nm.) were used in series.

CHAPTER 3

CHARACTERIZATION OF CHAIN-EXTENDED HYDROXYPROPYL LIGNINS

SYNOPSIS

A series of chain-extended hydroxypropyl lignins (CEHPLs) was prepared from three different lignin sources. Chemical, molecular weight and thermal analysis showed that the molar substitution (MS) of propylene oxide varied and affected copolymer properties. The MS was defined as the number of hydroxypropyl repeat units which comprise the chain attached to a single reactive site on lignin. As the MS increased from 1 to 7.2, the number average molecular weight increased while the glass transition temperature (T_g) decreased from 63 C to -65 C. The change in T_g with increasing MS followed the Gordon-Taylor relationship. Differences in the chemical composition of the original lignin (organosolv or Kraft) were not obvious as the lignin content of the copolymer decreased below 50%.

INTRODUCTION

For centuries, natural polymers served mankind's needs for clothing and shelter. These natural polymers include leather, cotton, silk, wool, wood and wood components. Over the past 80 years, these natural polymers have been replaced with synthetic materials which possess either superior properties or comparable qualities at a reduced cost. However with the realization of limitations on some natural resources and with efforts of developing economies to utilize local resources, there has recently been renewed interest in integrating natural polymers into the commercial mainstream. Many research efforts have focused on improvements of properties through chemical modification of the natural polymer (1-7). These modifications frequently include grafting a second polymer onto the natural polymer to improve strength, durability, resistance to degradation, dimensional stability, solubility or processability. A number of these chemical modifications have been applied to wood and wood components in an attempt to achieve improved properties.

Whole wood has been modified through grafting of both low and high molecular weight additives (6-10). The wood components, cellulose and lignin, have also been modified

by chemical reactions. The major commercial products are based on cellulose derivatives which include ethers, esters and a number of other products (11,12). Lignin derivatives have also received recent attention due to the abundance of this underutilized material. Uses include industrial surfactants and other water soluble copolymers (13-16).

Lignin has been modified by a variety of techniques. These modifications include the traditional sulfonation reactions (17) and more recently, preparation of water-soluble graft copolymers (14,15). These materials show promise as viscosity control agents in several areas of application. Other approaches to lignin utilization focused on structural applications (18-22). Some of the earliest work on lignin modification were attempts to incorporate lignin into phenol-formaldehyde resin (23). Much of this work continues with new innovations and better analytical schemes.

Lignin has been reacted with a series of alkylene oxides to yield star-like polyols which can then be crosslinked by a variety of materials. While the idea is mentioned in several sources (24-29), much work has been done by Glasser et al. (21,26-29). In this work lignin has been reacted with propylene oxide in an effort to improve

solubility and thermal properties (26). The resulting hydroxypropyl lignins (HPL) may then be crosslinked with diisocyanates to produce high strength polyurethane films, coatings and foams (21,26). While these lignin-based polyurethanes showed high moduli and strengths they were fairly brittle and had poor elongation properties (21). In an effort to overcome these limitations, a series of chain-extended polyurethanes were prepared with HPL and polyethylene glycols (PEG) (27) or polybutadiene glycols (PBD) (29). While these flexible extenders improved the elongation of the subsequent polyurethanes they were limited by either the PEG content or phase separation (PBD). Thus it was considered desirable to prepare homogeneous, lignin-based polyurethanes with a large percentage of the flexible component. One way of achieving this goal was to synthesize chain-extended hydroxypropyl lignins (CEHPLs). Thus, while the degree of substitution would remain constant, the molar substitution (MS) would be greater than one.

There are a variety of methods used to polymerize alkylene oxides. The polymerization can be carried out with acidic or alkaline catalysts in a number of solvents (30-34). The reaction of HPLs with addition of propylene oxide with 18-crown-6 ether and KOH as catalyst allowed for

the formation of CEHPLs (34). These CEHPLs could be separated from the propylene oxide homopolymer by a series of liquid/liquid extractions.

The goal of this study was to relate the CEHPL composition to the chemical, molecular and thermal properties of the copolymer. To obtain this goal several analytical steps were required. First, it was anticipated that the CEHPL composition could be determined by several spectral techniques. Then the effects of CEHPL composition on thermal and mechanical properties would be investigated. Applicability of the Gordon-Taylor copolymer equation to the thermal properties of the CEHPLs was tested. Finally, differences in the chemistry of the parent lignins were also examined to determine if these differences influenced CEHPL properties.

EXPERIMENTAL

Three different HPLs were used as starting materials for the preparation of CEHPLs. The three HPLs were based on lignins isolated by the organosolv and kraft processes. The kraft lignins were of two types, one of which had been fractionated to remove the low and high molecular weight materials and the second of which had not been modified.

The properties of these and other HPLs have been described in detail elsewhere (33). The preparation and isolation of the HPLs and CEHPLs have been detailed previously (34).

Analysis

Gel permeation chromatography (GPC) analyses were done on a set of 3 μ -spherogel columns (Altex) using non-stabilized THF. The columns with gel sizes of 1,000, 10,000, and 100,000 Å were calibrated with monodisperse polystyrene and lignin model compounds with molecular weights up to 784 gm/mol. An LDC system with a UV detector (280 nm) and a flow rate of 1 ml/min were used.

The $^1\text{H-NMR}$ spectra were obtained for acetylated CEHPL derivatives on a Bruker 270 MHz instrument using deuteriochloroform as solvent and TMS as internal standard. The quantitative analysis of the spectra using integration and subdividing the spectra into ranges is described elsewhere (26).

Glass transition temperatures (T_g s) were determined using a Perkin-Elmer Differential Scanning Calorimeter Model 4, equipped with a Thermal Analysis Data Station. About 20 mg of sample was heated to 120 C, cooled to -80 C,

and scanned at 20 C/min with dry helium as a purge gas. The T_g was defined as one-half the change in heat capacity occurring over the transition.

The ultraviolet (UV) adsorbances were determined on a Varian-Cary 219 spectrophotometer at 280 nm (36). The total hydroxyl content was determined by back titration of acetic acid after acetylation of the CEHPLs (37).

RESULTS AND DISCUSSION

A series of chemical techniques was used to determine the composition of the CEHPL copolymer. The effects of copolymer composition on chemical, molecular weight, and thermal properties were determined. Each of these techniques, to a greater or lesser extent, is sensitive to the purity of the copolymer. Purity of the copolymer was of concern since the method used in this work to prepare chain-extended hydroxypropyl lignins (CEHPL) produced a mixture of polypropylene oxide (PPO) homopolymer and CEHPL copolymer. To investigate the chemical and thermal properties of the CEHPL copolymer and to study the effects of various CEHPL formulations on the properties of resulting polyurethanes, the CEHPL copolymer had to be separated from PPO homopolymer.

It should be emphasized that the material separated from the CEHPL copolymer was primarily PPO homopolymer which could be a useful component in a polyurethane network. However, since the final goal of this work was to investigate the effects of CEHPL copolymer variables on network properties, the PPO homopolymer was removed to simplify the subsequent interpretation.

Chemical Analysis of CEHPLs

The composition of the CEHPL copolymer was investigated with three independent techniques. $^1\text{H-NMR}$ provided a separable response for both the lignin and the propylene oxide components of the copolymers. Ultraviolet absorption (UV) at a single wavelength (280 nm) proved to be sensitive to only the lignin component of the CEHPL (36). Total hydroxyl content provided an indirect measure of composition through a measure of end groups (37). Thus each of these techniques provided for a measure of CEHPL structure which may be used to explain molecular and thermal properties.

$^1\text{H-NMR}$ Analysis: The purified CEHPLs were acetylated and subjected to $^1\text{H-NMR}$ analysis in accordance with earlier

work (26). Differences between lignin, HPL, and CEHPL became apparent (Figure 3-1). The $^1\text{H-NMR}$ results were quantified by dividing the spectrum into ranges as discussed previously (26) and the results are shown in Table 3-1. $^1\text{H-NMR}$ results reflected an increase in hydroxypropyl character as the amount of PO added to the reaction increases. In particular, the signal intensity in ranges 4 + 5 and 8 increases while the signal in ranges 2 + 3 decreases as more PO is added. These signals are due, in part, to the methylene (range 5), methine (range 4) and methyl protons (range 8) on PO, and the aromatic protons (ranges 2 + 3) on lignin, respectively.

The MS can be calculated from $^1\text{H-NMR}$ data in two ways, both of which are illustrated in Table 3-1. The first method (Method A) was adopted from earlier work (26), and it was based on the ratio of the $^1\text{H-NMR}$ signals representing the methyl group of the propyl substituent (range 8) and that of the acetyl group (ranges 6 and 7). Essentially this ratio was a measure of the fraction of PO repeat units (methyl protons) per hydroxyl group (O-acetyl).

The second method (Method B) of calculating MS was based on a distinction between CH_3 signals in relation to the type of bonding, and this was only applicable to the

more highly substituted CEHPLs. For these spectra one could distinguish two doublets in range 8 (representing the CH₃ group). The downfield doublet was assigned to the protons of the methyl group of the propylene oxide unit connected to the aromatic oxygen, while the upfield doublet was assigned to the methyl protons of subsequent (PO-PO linked) propylene oxide units. This assignment was based on the downfield shift induced by the high electron density surrounding the aromatic ring (38). By ratioing these doublets it was again possible to estimate the MS of a CEHPL. Table 3-1 illustrates that fair agreement is reached between the two methods.

The weight fraction HPL or lignin in the CEHPL could be computed with a knowledge of both the degree of substitution (DS) and the MS of the copolymers (Table 3-2). (The DS for these HPLs has been determined previously (26).) The data in Table 3-2 shows that the HPL or lignin content of the CEHPL decreases steadily through the three different series. This reduction was confirmed by a reduction in the intensity of the signal in ranges 2 + 3 (Table 3-1). The signal in these ranges was assigned to the aromatic protons on lignin (26) and the decrease in signal intensity corresponds to the decrease in lignin content deduced from the increase in the length of the propylene

oxide chains (Figure 3-2). However, since both of these variables were derived from $^1\text{H-NMR}$ and despite the strong correlation, independent confirmation to the lignin content was desirable.

UV Analysis: The decrease in the signal intensity of the Range 2 and 3 protons in the $^1\text{H-NMR}$ data corresponded to a decrease in the extinction coefficient of the CEHPL (Figure 3-2). The UV absorption response of the CEHPL, at 280 nm, is specific for the basic repeat unit of lignin (36). As the lignin content in the CEHPL decreases, the UV absorbance declines in a similar fashion (Figure 3-2). A strong, linear relationship, provided further evidence that the CEHPL composition was varied in a consistent manner. Neither $^1\text{H-NMR}$ nor UV absorptivity showed any significant differences between the chain-extended OS or KL. These lignins differ in their chemical structures but the differences were overwhelmed by the effects of chain extension.

Total OH Analysis: The percent hydroxyl was also determined by titration (37). The percent hydroxyl previously has been calculated from the $^1\text{H-NMR}$ data (26). The DS for these lignins was determined previously to be between 1.5. and 2.0. Results for OH contents by these two

methods are shown in Table 3-2. The $^1\text{H-NMR}$ values are consistently higher than those obtained from titration. This difference could be due to several factors, but due to their consistent nature they were attributed to problems with the measured values for the degree of substitution (DS). The DS calculation assumed that the number of protons on the HPLs and CEHPLs remained the same as that of the original lignin. If side reactions occurred during propoxylation, the number of protons on the lignin C-9 unit may change and cause a systematic error.

Hydroxyl contents determined by both titration and $^1\text{H-NMR}$ are shown in Figure 3-3 along with the theoretical hydroxyl content of a lignin hexamer. The theoretical curve was calculated assuming a DS of 1.5 and a monomer molecular weight of 180. Both of the measured hydroxyl contents follow the shape of the predicted curve. This systematic decrease in the hydroxyl content was consistent with an increase in the MS of the CEHPL. The hydroxyl contents measured by titration which were a direct measure of the CEHPL were taken as the correct value for all subsequent calculations.

Analysis by several techniques allowed for the determination of differences in the chemical composition of

the CEHPLs. Estimates of the CEHPL composition were based on the DS measured by $^1\text{H-NMR}$ which may contain systematic errors. However, the consistent change in the CEHPL composition as MS increased was considered to be reliable.

Molecular Weight Characteristics

As the MS of the CEHPLs increased, the molecular weight of the copolymer should also increase. The magnitude of this increase should be related to the length of the propylene oxide arms radiating from the lignin center.

Gel Permeation Chromatography: High performance gel permeation chromatography was used to characterize the CEHPLs in regard to their molecular structure. The results are shown in Figure 3-4. The number average and weight average molecular weights, M_n and M_w , respectively, as well as the dispersity ratio (DR) and first moment of M_n (S_n) are shown in Table 3-3. From Figure 3-4 it is apparent that as the MS of the CEHPL increased, the elution volume decreased. This decrease in elution volume can be related to an increase in molecular weight. The DR and S_n also increased as the MS of the CEHPL increased (Table 3-3). While an increase in molecular weight was predictable as

the chain length increased, the apparent magnitude of the increase was surprising.

Considerable attention has recently surrounded the use of GPC for the determination of M_n and M_w for various lignins. The major controversy has revolved around association phenomena (39) and the reliability of molecular weight standards for calibrating the GPC columns (40). With the elimination of carboxyl and phenolic OH groups and addition of a bulky propylene oxide chain onto the aromatic ring, association was not considered to be significant. However, the use of linear polystyrene as standards for star-like lignin derivatives was not without problems. Thus, while the absolute values of the average molecular weights might be questioned, the trends and relative differences were considered to be reliable.

The predicted changes in M_n at a DS of 2.0, along with the actual M_n values, are shown in Figure 3-5. While an actual increase in M_n was expected, the experimental M_n of all CEHPLs was consistently larger than the predicted M_n . This observation can be rationalized by several possible phenomena. As the MS increases, the composition and hence the solubility of the CEHPL changes. In a good solvent (THF) the propylene oxide arms are likely to adopt an

expanded conformation compared to the lignin center. Thus, the hydrodynamic volume of the CEHPL star will increase due to both a real change in molecular weight as well as a change in chemical composition.

A second explanation for the differences between the theoretical and experimental molecular weights could be secondary condensation of the lignin. Lignin possesses a small number of vinyl groups. During propoxylation, these groups could react to raise the molecular weight of the CEHPLs.

Thermal Properties

The T_g and T_g range for the CEHPLs were determined (Table 3-3). A wide range (63 C. to -65 C.) of T_g values was found. The T_g range varied between 48 C. and 16 C. depending on the copolymer composition. The wide range in T_g s was reflected in the physical appearance of the CEHPL which varied between a tacky solid and a low-viscosity liquid.

The T_g range may be viewed as an indication of the heterogeneity of the system. (41). With only three types of covalent bonds in the backbone, PPO would be viewed as

having a limited number of energy absorbing responses. However, lignin, with its structural complexity, would be visualized as possessing a large number of conformations which would have different rotational energies. Thus as the composition of the CEHPL was varied, the relative contribution of the different components to energy dissipation would also vary. As the PPO content increased, the relatively few dissipative mechanisms in this component would dominate, providing for a reduction in the T_g range.

Application of the Gordon-Taylor Equation: There are a variety of equations for correlating a copolymer's composition with its glass transition. These vary from a simple linear average to complex equations that include free volume effects and secondary chemical interactions (42). One simple but useful copolymer equation is the Gordon-Taylor equation (43) (Eq. 3):

$$T_g = \frac{T_{g1} + (kT_{g2} - T_{g1}) C_2}{1 - (1 - k)C_2} \quad (\text{Eq. 2})$$

where

T_g = glass transition temperature of the CEHPL
copolymer

T_{g1} and T_{g2} = glass transition temperatures of HPL and
PPO, respectively

C_2 = weight fraction of PPO

k = constant for the copolymer system

The constant (k) for the copolymer system was determined from the experimental data with a procedure which was described elsewhere (44). The determined value of 0.25 was very close to that found by a least squares fit of k values to the experimental data (0.24).

Equation 3 predicts that the T_g of the CEHPL decreases, in a non-linear fashion, as the weight fraction of the low T_g PPO increased. Normalized T_g values versus HPL content are plotted in Figure 3-6, along with the normalized line predicted from equation 3. The normalization was used to alleviate differences in the T_g of the three HPL starting materials. Thus the effect of changes in composition (i.e. MS) could be shown for all of the CEHPLs.

Lignin was not considered as the homopolymer since the

hydroxypropylation reaction converts phenolic hydroxyls and carboxyls to secondary hydroxyls. The more acidic phenolic hydroxyls have a profound effect on T_g due to hydrogen bonding. Conversion of lignin to an HPL introduces two modifications, a change in chemical composition and a change in the type of functional groups present. Defining the HPL, rather than the original lignin, as the homopolymer produced agreement between the data and the Gordon Taylor equation. The agreement between the data and the Gordon Taylor equation, a general copolymer equation, is another example of how lignin may be chemically modified in a controlled and predictable fashion.

CONCLUSIONS

Three hydroxypropyl lignins (HPLs) could be used as starting materials in the preparation of chain-extended hydroxypropyl lignins (CEHPL). The purified CEHPL copolymer could be characterized with regard to its chemical, molecular and thermal properties. Quantitative analysis by $^1\text{H-NMR}$ allowed for the determination of CEHPL composition. The $^1\text{H-NMR}$ spectra showed a continuous decrease in the lignin signals (aromatic protons) and an increase in the intensity of methyl and methylene protons associated with propylene oxide. A similar decrease in the UV absorbance

confirmed the decrease in lignin content as the MS of the CEHPL increased. The hydroxyl content of the copolymer also decreased as the MS increased. Total hydroxyl content of the CEHPLs could be determined by titration. These hydroxyl values were less than those found by the $^1\text{H-NMR}$ technique used previously but were considered to be more reliable.

The GPC analysis allowed for characterization of the molecular weight distribution of the purified copolymer. As the MS of the CEHPL increased, so did the molecular weight. The increase in molecular weight was found to be unexpectedly large, which was attributed to changes in copolymer solubility or condensation reactions. The GPC analysis again highlighted the problem of finding appropriate standards for the calibration of lignin chromatograms.

The glass transitions (T_g s) of the CEHPLs were found to be closely related to the copolymer composition. As the percentage of the low T_g polyether component increased, the T_g of the copolymer decreased. This relationship could be modeled through the Gordon-Taylor equation. Thus, it was found to be possible to determine the lignin content of CEHPL derivatives that varied in physical appearance

between a glassy solid and a low viscosity liquid. The T_g and molecular weight of a CEHPL could be controlled in a predictable manner depending on the MS of the system. These CEHPL show potential for incorporation into polyurethane networks which should possess a wide range of physical and mechanical properties.

REFERENCES: CHAPTER 3

1. E. A. MacGregor and C. T. Greenwood, Polymers in Nature, Wiley, New York, 1980.
2. C. E. Carraher and L. H. Sperling, eds., Polymer Applications of Renewable Resource Materials, Plenum, New York, 1983.
3. E. F. Jordan, Jr., and S. H. Fearheller, J. Appl. Polym. Sci., **25**, 2755 (1983).
4. P. L. Nayak, J. Macromolec. Sci. Rev.: Macromolec. Chem., **C14**(2), 193 (1976).
5. D. K. Setua, in Proceedings of the ACS Division of Polymeric Materials: Science and Engineering, Vol. 52, American Chemical Society, Washington, D.C., 1985.
6. T. Nakagami and T. Yokota, Mokuzai Gakkaishi, **29**(3), 240 (1983).
7. S. V. Lonikar, N. Shiraishi, T. Yokota, M. Tanahashi, and T. Higuchi, J. Wood Chem. Tech., **5**(1), 111 (1985).
8. R. M. Rowell in The Chemistry of Solid Wood, R. M. Rowell, ed., Advances in Chemistry Series No. 207, American Chemical Society, Washington, D.C., p. 175 (1983).
9. V. Hornof, B. V. Kokta, and J. L. Valade, J. Appl. Polym. Sci., **20**, 1543 (1976)
10. A. J. Stamm, in Wood Technology: Chemical Aspects, ACS Symposium Series No. 43, I. S. Goldstein, ed., American Chemical Society, Washington, D.C., 1977.
11. R. M. Rowell and R. A. Young, eds., Modified Cellulosics, Academic Press, New York, 1978.
12. A. F. Turbak, ed., Cellulose Technology Research, ACS Symposium Series No. 10, American Chemical Society, Washington, D.C., 1975.

13. K. V. Sarkanen and C. H. Ludwig, eds., Lignins: Occurrence, Formation, Structure, and Reactions, Wiley-Interscience, New York, 1971.
14. J. J. Meister, D. R. Patll, and H. Channell, Ind. Eng. Chem. Prod. Res. Dev., 24,306 (1985).
15. A. H. A. Tinnemans, H. F. Martens, G. J. van Veldhuizen and P. J. Greidanus, in International Symposium on Wood and Pulping Chemistry, 1985, p. 105.
16. J. A. Hyatt, R. H. S. Wang, and R. A. Rowell, in International Symposium on Wood and Pulping Chemistry, 1985, p. 221.
17. D. W. Glennie, in Lignins: Occurrence, Formation, Structure, and Reactions, K. V. Sarkanen and C. H. Ludwig, eds., Wiley-Interscience, New York, 1971.
18. D. A. I. Goring, in Lignins: Occurrence, Formation, Structure, and Reactions, K. V. Sarkanen and C. H. Ludwig, eds., Wiley-Interscience, New York, 1971, p. 695.
19. R. F. Nichols, U. S. Patent No. 2,854,422 (1958).
20. A. L. Lambuth, U. S. Patent No. 4,279,788 (1981).
21. V. P. Saraf and W. G. Glasser, J. Appl. Polym. Sci., 29,1831 (1984).
22. L. N. Mozheiko, M. F. Gromova, L. A. Bakalo, and V. N. Sergeeva, Polym. Sci. USSR, 23C1,141 (1981).
23. P. C. Muller, S. S. Kelley, and W. G. Glasser, J. Adhesion, 17,185 (1984).
24. D. T. Christian, M. Look, A. Nobell, and T. S. Armstrong, U. S. Patent No. 3,546,199 (1970).
25. W. G. Glasser, O. H-H. Hsu, D. L. Reed, R. C. Forte, and L. C-F. Wu, in Urethane Chemistry and Applications, K. Edwards, ed., ACS Symposium Series No. 172, American Chemical Society, Washington, D.C., 1981, p. 311.

26. W. G. Glasser, C. A. Barnett, T. G. Rials, and V. P. Saraf, J. Appl. Polym. Sci., **29**,1815 (1984).
27. V. P. Saraf, W. G. Glasser, G. L. Wilkes, and J. E. McGrath, J. Appl. Polym. Sci., **30**,2207 (1985).
28. T. G. Rials and W. G. Glasser, Holzforschung, **38**(4), 191 (1984).
29. V. P. Saraf, W. G. Glasser, and G. L. Wilkes, J. Appl. Polym. Sci., **30**,3809 (1985).
30. H. Koinuma, K. Naito, and H. Hirai, Makromol. Chem. **183**,1383 (1982).
31. J. H. Exner, D. P. Sheetz, and E. C. Steiner, U. S. Patent No. 3,760,005
32. L. C-F. Wu and W. G. Glasser, J. Appl. Polym. Sci., **29**,1111, (1984).
33. W. G. Glasser, L. C-F. Wu, and J.-F. Selin, Wood and Agricultural Residues: Research on Use for Feed, Fuels, and Chemicals, E. J. Soltes, ed., Academic Press, 1983, p. 149.
34. S. S. Kelley, Chapter 2 of this work (1987).
35. J. A. Hyatt, submitted to Holzforschung (1986).
36. D. B. Johnson, W. E. Moore, and L. C. Zank, Tappi, **44**(11),793 (1961).
37. N. Morohosi, Bull. Exp. Forest. Tokyo Univ. Agr. Tech. No. 10, 183 (1973).
38. R. M. Silverstein, G. C. Bassler, and T. C. Morrill, Spectrometric Identification of Organic Compounds, 4th ed., John Wiley & Sons, New York, 1981.
39. S. Sarkanen, D. C. Teller, E. Abramowski, and J. L. McCarthy, Macromol., **15**,1098 (1982).
40. M. E. Himmel, K. K. Oh, D. W. Sopher, and H. L. Chum, J. Chromatogr., **267**,249 (1984).

41. S. Lau, J. Pathak, and B. Wunderlich, Macromol., 15,1278 (1982).
42. T. K. Kwei, J. Polym. Sci.: Polym. Lett., 22,307 (1984).
43. M. Gordon and J. S. Taylor, J. Appl. Chem., 2,493 (1952).
44. L. A. Wood, J. Polym. Sci., 28,319 (1958).

TABLE 3-1
 CHEMICAL ANALYSIS OF CHAIN-EXTENDED HYDROXYPROPYL LIGNINS (CEHPLs)

CEHPL Type	¹ H-NMR Signal in Range (% total)			Molar Substitution (MS) Method ¹		Ave.
	2&3	4&5	6&7	8	B	
OS-HPL	11.1	38.0	23.7	27.1	1.0	1.0
OS-A	9.9	38.8	20.7	30.6	1.5	1.5
OS-B	6.4	43.1	13.2	36.8	2.8	3.0
OS-C	2.1	45.1	10.5	42.3	4.1	4.5
OS-D	1.6	45.2	7.0	46.2	6.6	7.2
KL-HPL	10.4	38.6	23.8	27.2	1.0	1.0
KL-A	8.7	40.5	16.3	34.6	2.1	2.2
KL-B	6.0	41.2	12.9	39.9	3.1	3.2
KL-C	4.9	44.4	11.7	39.0	3.3	3.6
KL-D	4.5	45.4	10.1	40.4	4.0	4.2
KL-E	4.5	43.2	9.5	42.8	4.5	4.6
KL-F	2.4	46.3	7.0	44.3	6.3	6.8
FK-HPL	12.2	36.7	24.9	26.2	1.0	1.0
FK-A	6.5	36.0	21.2	36.3	1.7	1.9
FK-B	4.0	42.5	15.4	38.1	2.5	2.9
FK-C	2.9	44.4	8.4	44.3	5.3	5.7

¹ Defined in text.

TABLE 3-2.
COMPOSITION OF CEHPL' s.

CEHPL Type 1	Ave. MS	Lignin Content of CEHPL (%) 2	HPL Content of CEHPL (%) 3	OH Content of CEHPL (%) ¹ H-NMR Titration
OS-HPL	1.0	67	100	9.8
OS-A	1.5	58	86	8.4
OS-B	3.0	41	61	6.3
OS-C	4.5	32	47	4.9
OS-D	7.2	22	33	3.5
KL-HPL	1.0	65	100	11.4
KL-A	2.2	45	70	7.5
KL-B	3.2	36	56	5.6
KL-C	3.6	34	52	5.0
KL-D	4.2	30	47	4.9
KL-E	4.6	28	44	4.6
KL-F	6.8	21	33	3.6
FK-HPL	1.0	63	100	10.4
FK-A	1.9	48	75	7.2
FK-B	2.9	37	59	5.4
FK-C	5.7	23	37	4.0

1 The Degree of Substitution (DS) were determined for these lignins in ref.26 and multiplied by 0.8. Thus the DS of OS-HPL=1.5, KL-HPL=1.7 and FK-HPL=1.8

2 Determined from:
$$\frac{(58 * DS) + 180}{[(MS * 58) * DS] + 180} * 100$$

3 Determined from:
$$\frac{[(MS * 58) * DS] + 180}{[(MS * 58) * DS] + 180} * 100$$

TABLE 3-3
MOLECULAR WEIGHT AND THERMAL PROPERTIES OF CEHPL's.

CEHPL Type	Lignin Content of CEHPL (%)	Mn (*10 ⁻³)	Mw (*10 ⁻³)	DR ¹	Sn (*10 ⁻³)	Tg (C)	Tg Range (C)
OS-HPL	67	0.6	1.2	1.9	0.8	32	46
OS-A	58	1.3	2.4	1.9	1.6	5	48
OS-B	41	1.4	3.5	2.4	2.7	-14	40
OS-C	32	4.7	21.9	4.7	19.4	-50	21
OS-D	22	8.0	104.6	13.1	100.5	-54	8
KL-HPL	65	0.7	1.4	2.0	1.0	58	47
KL-A	45	1.2	2.3	2.0	1.6	3	33
KL-B	36	2.1	4.7	2.2	3.5	-20	26
KL-C	34	6.8	18.0	2.7	14.2	-30	28
KL-D	30	4.7	34.8	7.4	32.4	-36	21
KL-E	28	8.5	77.0	9.1	72.6	-56	18
KL-F	21	11.8	110.2	9.4	104.1	-65	16
FK-HPL	63	1.0	1.7	1.7	1.1	63	40
FK-A	48	1.2	2.7	2.2	2.0	25	32
FK-B	37	1.9	6.3	3.3	1.9	-24	22
FK-C	23	6.6	57.4	8.8	54.0	-53	18

¹ The ratio of Mw/Mn.

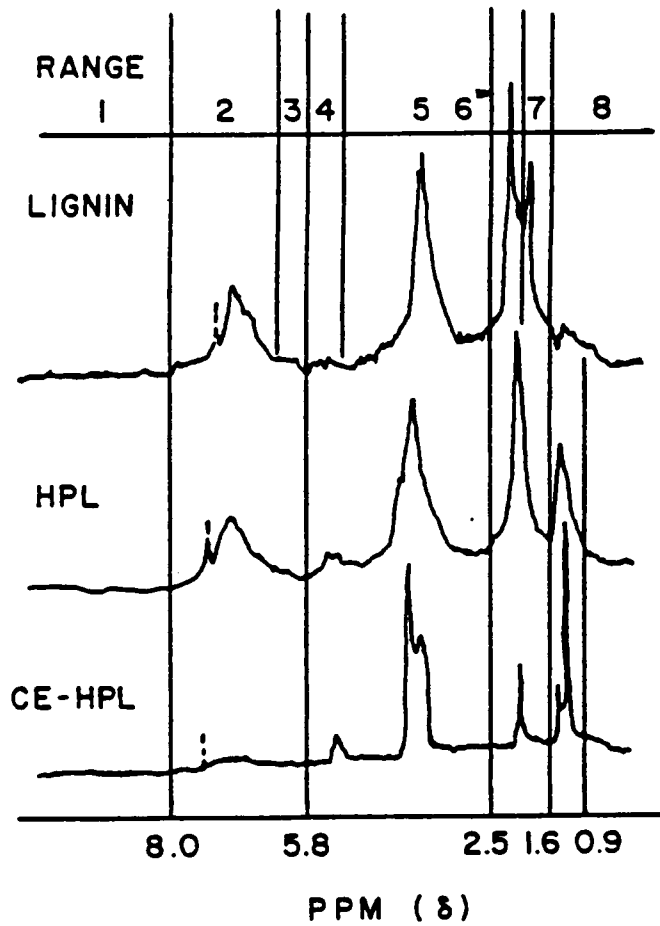


FIGURE 3-1. $^1\text{H-NMR}$ spectra of a lignin, hydroxypropyl lignin (HPL) and chain-extended hydroxypropyl lignin (CEHPL). The ranges were adopted from Reference 26.

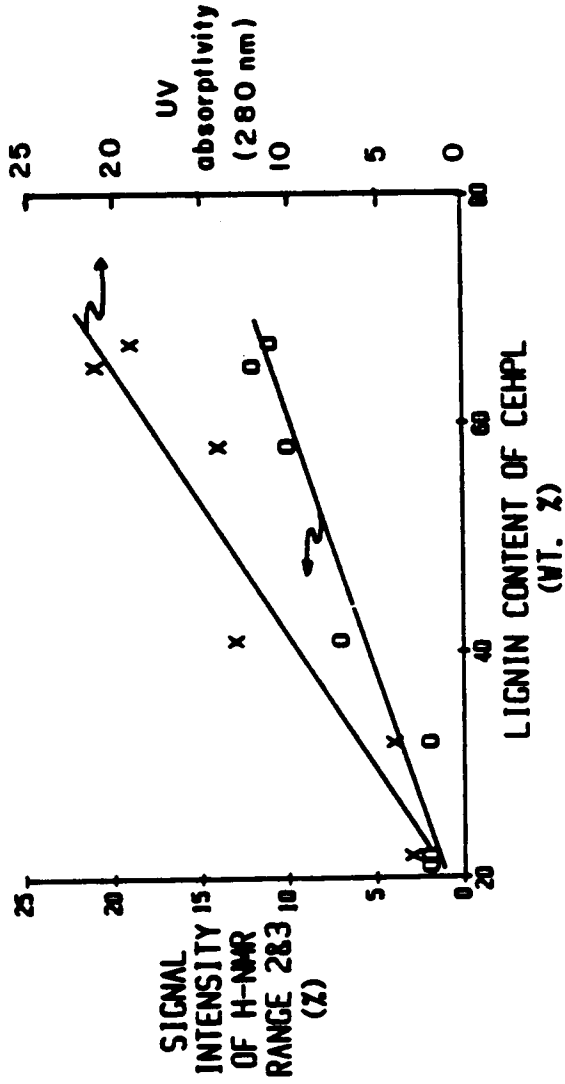


FIGURE 3-2. Relationship between the intensity of the $^1\text{H-NMR}$ aromatic signal, range 2&3, (O), the UV absorptivity at 280 nm. (X) and the lignin content of the CEHPLs.

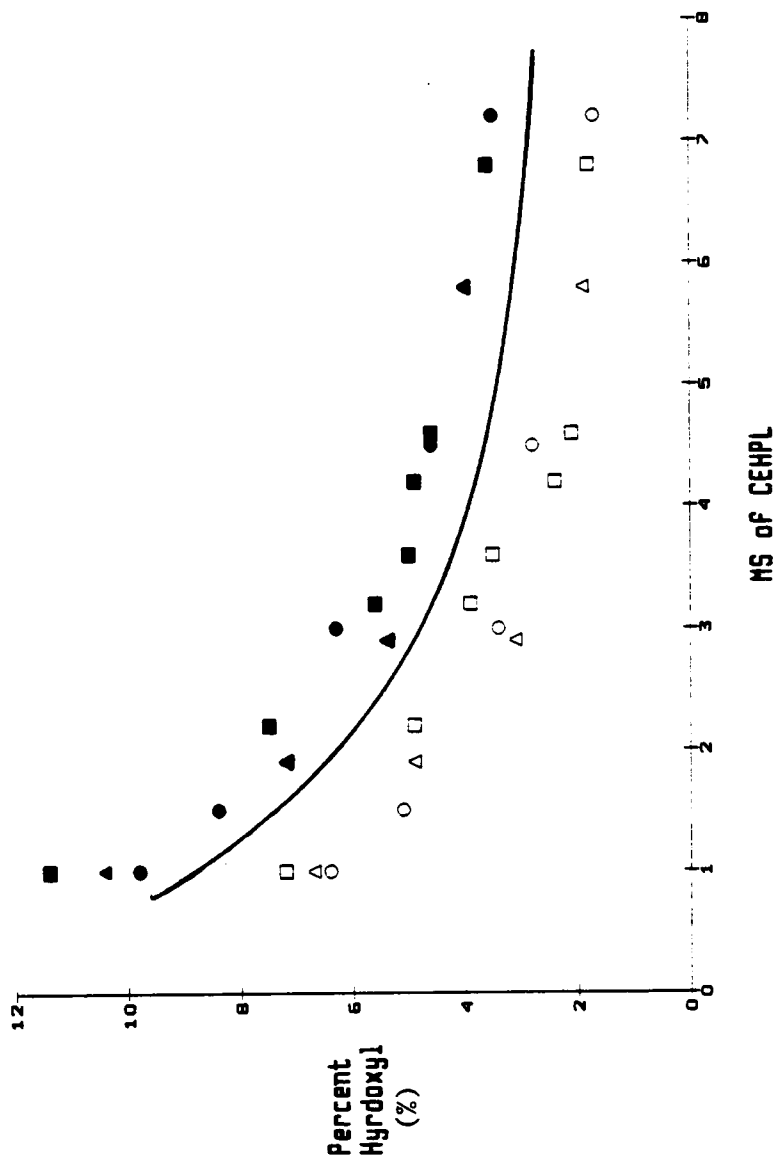


FIGURE 3-3. Total hydroxyl content as measured by $^1\text{H-NMR}$ (filled symbols) and titration (open symbols) of CEPHLs; OS (O), KL (□) and FK (Δ). The line represents the OH content of a theoretical heximer with a DS of 1.5

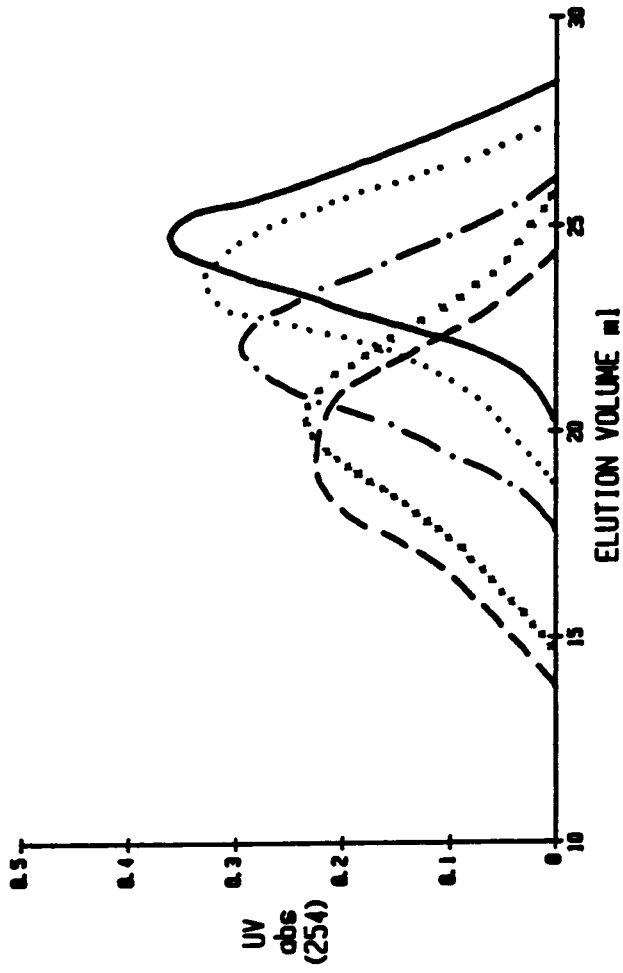


FIGURE 3-4. High pressure gel-permeation chromatograms of the organosolv series of chain-extended hydroxypropyl lignins: OS-HPL (—), OS-A (.....), OS-B (---), OS-C (x x), and OS-D (---).

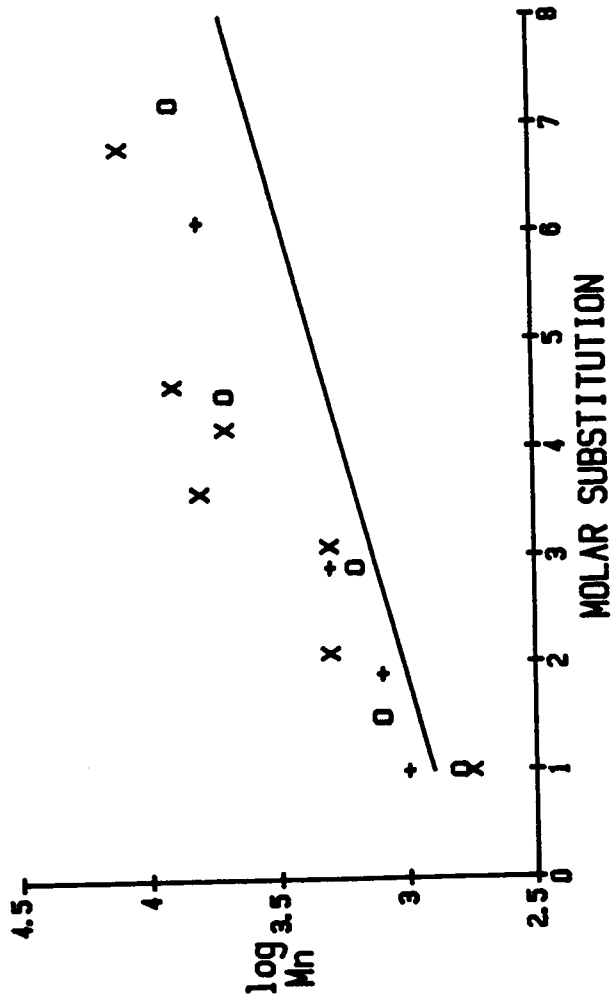


FIGURE 3-5. Changes in the molecular weight (M_n) of CEHPLs, as measured from GPC, with increasing MS, measured by $^1\text{H-NMR}$; OS (O), KL (X) and FK (+). The solid line represents the predicted M_n for a sample with 1.7 reactive sites on each lignin repeat unit.

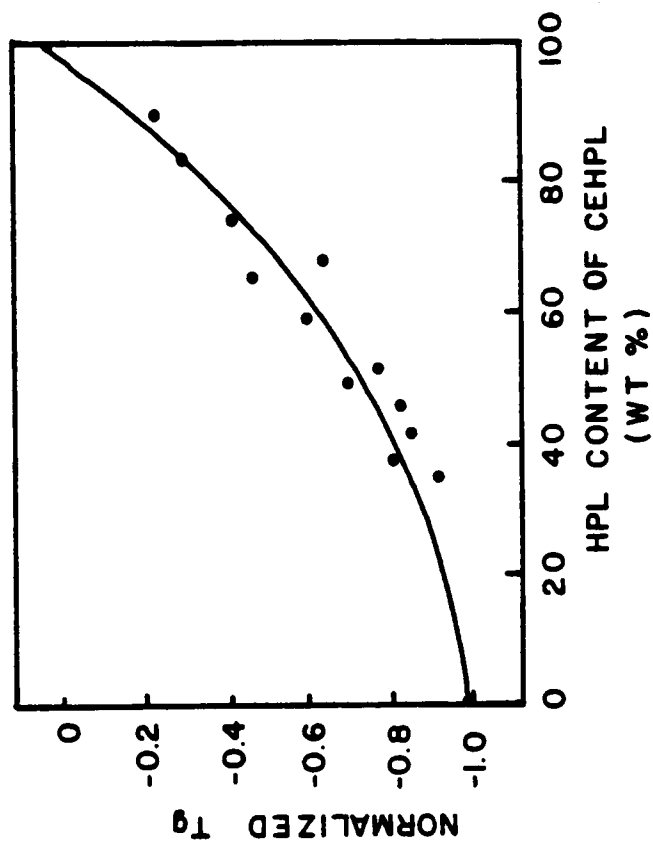


FIGURE 3-6. Changes in the normalized T_g with changes in the CEHPL copolymer composition. The solid line represents the T_g predicted from the Gordon-Taylor relationship (equation 3 in text) with $k=0.24$. The normalization involves insertion of the T_g from either experiment or the Gordon-Taylor equation into the following equation. Normalized $T_g = (T_g - T_{g1}) / (T_{g2} - T_{g1})$; where T_{g1} is between 32 and 63 C for the three respective HPLs, and T_{g2} is -75 C for polypropylene oxide homopolymer.

Chapter 4

STRUCTURE-PROPERTY RELATIONSHIPS OF POLYURETHANE NETWORKS PREPARED FROM CHAIN-EXTENDED HYDROXYPROPYL LIGNINS

SYNOPSIS

A series of lignin-based polyurethane (LPU) films was prepared from chain-extended hydroxypropyl lignins (CEHPL). In appearance, these films ranged from brittle and dark brown to rubbery and bronze. The thermal, mechanical and network properties of these LPUs were investigated. Both DMTA and DSC analysis showed a single T_g which varied between -53 C and 101 C depending on the lignin content of the LPU. From swelling experiments, molecular weight between crosslinks (M_c) was determined and found to vary over two and one-half orders of magnitude. The molecular weight between crosslinks (M_c) could be related to the change in T_g that accompanied network formation. Stress-strain experiments showed a variation in Young's modulus between 7 and 1300 MPa. Most of the variation in material properties could be related to the lignin content and to a lesser extent to the type of diisocyanate, hexamethylene diisocyanate or toluene diisocyanate. The source of the CEHPL had no effect on the observed

properties. From these results it was concluded that the properties of LPUs could be controlled and engineered for a wide variety of practical uses.

INTRODUCTION

Polyurethanes are among the most versatile crosslinked polymer systems in wide use today. Current applications span the range from high modulus binders and fibers to elastomers and flexible foams (1,2). Part of this versatility is due to the range of available diisocyanates and the variety of polyols. Polyol backbones can be aliphatic, or contain ether or ester linkages (3). A number of naturally occurring polyols have been reported but few have achieved general acceptance.

Lignin has been mentioned as a component of polyurethanes in a number of reports in both the patent and scientific literature (4-8). The advantages of lignin are related to both its renewable nature and its abundance as a low value, underutilized, polymeric by-product of the pulp and paper industry (9). Utilization of lignin in polyurethanes has been hindered by poor solubility, a variety of different functionality and insufficient

molecular characterization (10). These factors have combined to limit lignin to the role of a low-cost, inert filler. While some formulations have described chemical modifications of lignin (4), most have used lignin in combination with an excess of polyethers or polyalkylene glycols (8,9). To overcome the limitations of poor solubility and a variety of reactive hydroxyls, several workers (11-13) have suggested reacting lignin with alkylene oxides to produce hydroxyalkyl lignin copolymers.

These hydroxyalkyl lignin copolymers, primarily hydroxypropyl lignin (HPL), have been used both in mixtures of the polypropylene oxide oligomeric coproduct (12,13) and as an isolated copolymer (10). The use of a variety of lignin sources and diisocyanates allowed preparation of polyurethane films with glass transition temperatures (T_g) between 63 C and 198 C and Young's moduli between 1280 and 2390 MPa (14). These studies concluded that the polyaromatic nature of the HPL allowed preparation of homogeneous, rigid networks. The major limitation of these materials was poor elongation properties, usually below 10%. In an effort to overcome this limitation and provide for a wider range of thermal and mechanical properties a series of polyethylene glycol (PEG) (15) or polybutadiene glycol (PBD) (16) extended lignin-based polyurethanes was

prepared by mixing the two polyol components prior to crosslinking.

With the addition of a second flexible, soft segment component, lignin-based polyurethanes (LPUs) were found with a wide range of T_g s (38 C - 158 C), Young's moduli (380 - 1670 MPa) and ultimate strain (6 - 43%) (15). Addition of PEG was limited to 17.8% of the polyol and no phase separation was observed (15). The molecular weight of the PEG also affected the properties of the polyurethanes. These polyurethanes contained between 35 and 45% lignin. The PBD extended films (16) were phase separated even at low levels of PBD addition. The elongation properties of the PBD films were poor until the HPL content dropped below 20% (ca. 12% lignin). The poor mechanical properties were attributed to macrophase separation of the PBD and HPL.

With a realization of the limitations for synthesis of homogeneous polyurethanes with addition of a second component, work was undertaken to modify material properties through changes in the HPL (17). To limit or eliminate phase separation a polyether soft segment was attached directly to the lignin derivative. This, in effect, yields a star-like copolymer with a rigid aromatic center and radiating flexible polyether arms. With an

increase in the content of the soft-segment component, it was anticipated that the toughness and elongation properties would improve. Thus it was expected that a wide variety of engineering properties could be achieved in a predictable manner with lignin-based polyurethanes. The chemical and thermal characteristics of the chain-extended hydroxypropyl lignin prepolymers are described elsewhere (17).

The current investigated the effects of polyol composition on the thermal, mechanical and network properties of polyurethanes. In addition to the effects of soft segment content, differences in source of the original lignin were also investigated.

EXPERIMENTAL

Materials

Polyols. Preparation and characterization of the hydroxypropyl lignin (HPL) (18,19) and chain-extended hydroxypropyl lignin (CEHPL) (17) polyols is described elsewhere.

Diisocyanates. 1,6-Hexamethylene diisocyanate (HDI) and 2,4-Toluene diisocyanate (TDI), practical grade, Eastman Kodak Co., Rochester, NY, were used as purchased.

Methods

Film preparation. One gram of the CEHPL was dissolved in 1.5 ml of MEK with sodium sulfate added as a desiccant, and the solution was kept under nitrogen. The proper amount of diisocyanate was added to give an NCO/OH ratio of 1.8 (based on a percent hydroxyl determined by titration). Three percent (total solids) dibutyl tin dilaureate (T-9 Catalyst, Union Carbide Corp.) was added and the mixture (ca. 50% solids) was rapidly stirred for one minute. The resin was poured through a glass wool plug onto a glass plate covered with a thin layer of silicone oil (L-520, Union Carbide Corp.). The plate was covered, to minimize evaporation of diisocyanate, and the resin was allowed to cure for 20 hours. The cover was removed and the films were post-cured in an air-circulation oven at 120 C. for two hours. The films were stored in a desiccator over P₂O₅. All films were prepared in duplicate.

Differential Scanning Calorimetry (DSC). A Perkin-Elmer DSC 4 equipped with a Thermal Analysis Data

Station was used. The data was collected on the second scan of samples (ca. 20 mg) heated at 20 C./min under a helium atmosphere. The glass transition temperature (T_g) was defined as one-half the change in heat capacity over the transition. The T_g was determined for two samples from each of the two films.

Dynamic Mechanical Thermal Analysis (DMTA). A Polymer Laboratories DMTA was used to determine the viscoelastic properties of the polyurethane films. The test geometry was dual cantilever bending and was used with a heating rate of 5 C/min, a strain of 1% and a frequency of 1 Hz. Care was taken to maintain sample dimensions of 0.1 mm thickness, 8 mm width and 2 mm free length. The DMTA measurements were made on duplicate samples from each of the two films. The sample chamber was purged with nitrogen. Activation energy (E_a) for the T_g was calculated using equation 1:

$$\log f = \log f_0 - E_a/RT \quad (\text{eq. 1})$$

where

- f = frequency of vibration
- f₀ = pre-exponential factor
- R = universal gas constant
- T = tan δ peak temperature

For these studies the geometry remained the same but the heating rate was 1 C/min and five frequencies between 0.1 and 30 Hz were used.

Stress-Strain Testing. Uniaxial stress-strain and ultimate property measurements were made using a standard Instron testing machine (Model 1122) employing a crosshead speed of 1 mm/min. Samples were cut with a die in a dog-bone shape. Tensile characteristics were calculated on the basis of initial dimensions (gage length 10 mm and width 2.8 mm).

Swelling studies. The polyurethane films were swollen in DMF to allow determination of sol fraction and the molecular weight between crosslinks (M_c). Each swelling experiment was run in triplicate on ca. 0.2 g of film swollen in 15 ml of DMF. The films were swollen for three days at room temperature, separated from the solvent and

dried at 120 C to a constant weight. Film densities were determined in duplicate with a 25 ml pycnometer. The M_c was found using the Flory-Rehner method (20), equation 2.

$$M_c = \frac{-V_s \rho_p (C^{0.33} - C/2)}{\ln(1 - C) + C + XC^2} \quad (\text{eq. 2})$$

where

M_c = molecular weight between crosslinks

V_s = molar volume of solvent (76.87 cc/mole for DMF)

ρ_p = density of polymer

X = Flory-Huggins constant

C = relative concentration = $W_D / \rho_p V$

W_D = dry weight of extracted film

V_{∞} = final swollen volume = $W_D / \rho_p + (W_{\infty} - W_D) / \rho_s$

W_{∞} = weight of swollen polymer

ρ_s = density of solvent (0.94 g/cc for DMF)

The percent sol fraction was calculated as shown below (equation 3).

$$\text{Sol fraction (\%)} = \frac{W_o - W_D}{W_o} \quad (\text{eq. 3})$$

with

W_0 = initial weight of polymer

W_D = dry weight of extracted polymer

Percent swell was calculated with equation 4.

$$\text{Percent swell (\%)} = \frac{W_{\infty} - W_D}{W_D} \quad (\text{eq. 4})$$

with W_{∞} and W_D defined above.

RESULTS AND DISCUSSION

Considerable experience has been gained in the synthesis of HPL based polyurethane (LPU) films (14,21). An excess of diisocyanate has been found to be necessary to form a complete network. The volatile nature of the diisocyanates necessitated covering the curing resin to allow for reasonably consistent stoichiometry. Limits on solvent evaporation also allowed for gellation of the polyurethane in a swollen condition. Thus the solids content was found to have a minor effect on the observed T_g but this variable was not studied in depth. The procedure used for film preparation was not optimized.

The use of a slight excess of diisocyanate also allows the occurrence of side reactions (22). Isocyanates are capable of reacting with urethane and urea linkages to form trifunctional allophanate and biuret linkages, respectively. However, the presence of biuret linkages is likely to be insignificant due to a low relative reaction rate and the absence of urea linkages. Allophanate linkages are capable of affecting the network structure of these polyurethanes.

The films ranged in appearance between dark brown and light bronze. The physical properties varied between extremely brittle to very flexible and tacky. All the films appeared to be homogeneous to the unaided eye.

Dynamic Mechanical and Thermal Behavior

A considerable quantity of information was gathered from a DMTA study of the LPU films. A selected series of DMTA scans are shown in Figure 4-1. The only difference between these films was the MS of the propylene oxide chains attached to lignin, and therefore the lignin content of the chain-extended hydroxypropyl lignin (CEHPL) polyol. As the MS of the hydroxypropyl chains increased, resulting in a decrease in the lignin content of the LPU, the $\tan \delta$

peak temperature and the breadth of the $\tan \delta$ peak decreased, while the $\log E'$ drop increased.

Thermal analysis provided a second method for characterizing materials. The DSC thermograms for a second series of polyurethanes which differed only in the MS of the CEHPL are shown in Figure 4-2. Again the T_g s of the polyurethanes decreased as the MS increased (lignin content in the CEHPL decreased). It is important to note that only one T_g was observed by both DSC and DMTA in all the films over a wide temperature range (-75 C to 150 C).

The results for all of the LPU's are summarized in Table 4-1. Six types of LPU's were prepared from three polyols which were crosslinked by two diisocyanates. The three polyols differed in the chemical structure of the original lignin (OS and KL) and the isolation method used to obtain the starting HPL (KL vs. FK). The diisocyanates contained either a rigid aromatic ring (TDI) or flexible aliphatic chain (HDI) as the backbone.

The observed $\tan \delta$ peak temperature can be related to the glass transition temperature (T_g) of the material. The \tan peak width was used as an indication of the number and intensity of energy dissipative mechanisms in the material

(23). Finally, the decrease in the $\log E'$ on heating was considered a reflection of network structure, particularly the molecular weight between crosslinks (M_c).

The T_g range (DSC) and the $\tan \delta$ one-half peak height (DMTA) are also shown in Table 4-1. Both of these parameters can be used as an indication of energy dissipative mechanisms for a system (23). The differences between the DSC T_g and the DMTA $\tan \delta$ peak temperature are due to frequency effects and differences in the heating rates.

The effects of the lignin content in the CEHPL and diisocyanate type on the film T_g (DSC) are shown in Figure 4-3. It is obvious that the film T_g decreases rapidly as lignin content in the LPU decreases. It should also be noted that the T_g of two underivatized lignin films prepared for a separate study follow the same relationship (23). While a decrease in the percent lignin reduced the T_g of the films for both the TDI and HDI series, there are also some apparent differences in T_g due to the diisocyanate type. Films prepared from the same polyol and crosslinked with TDI or HDI exhibited consistent differences at a lignin content above 25%. The TDI crosslinked films have a consistently higher T_g than those

crosslinked with HDI until the lignin content of the LPU's decreased to about 25%. This difference can be rationalized by the nature of the diisocyanate. With HDI the reactive groups are connected by a flexible aliphatic chain while in TDI a rigid aromatic ring connects the isocyanate groups. This difference in T_g for HDI and TDI crosslinked LPU's has been observed earlier (14).

Previous work has noted a relationship between rigid structures in the polymer's backbone (25) or even the aromatic content of a network (26) and physical properties. When the T_g 's for the CEHPL-based networks are plotted against aromatic content (based on a C_6H_6 unit and weight percent), (Figure 4-4), a relationship between aromaticity and T_g is noted. In addition, at a constant aromatic content the HDI crosslinked films have a higher T_g than the TDI crosslinked films.

There are several possible explanations for these differences between the HDI and TDI crosslinked networks. As will be shown below, the TDI films had a higher molecular weight between crosslinks (M_c) than those prepared with HDI, and this could explain the low T_g for the TDI networks. A high M_c for the TDI-based films compared to the HDI crosslinked films can be explained by

two effects. First, the rigid aromatic ring might limit the conformations available for the second isocyanate group after the first group had reacted (27). Thus, the network forming reactions of the second isocyanate group could be limited for steric reasons. The second possible effect is related to the reactivity of the second isocyanate group in TDI. After the first isocyanate group reacts, the high electron density across the aromatic ring allows for a decrease in the reactivity of the second group (28). Although it should be noted that no free isocyanate groups were observed by infrared spectroscopy. This decrease in the reactivity of the second group was not a factor with HDI. Thus it was apparent that the T_g s of these polyurethanes were related to both the content of the aromatic component in the film and the chemical nature of the diisocyanate used as a crosslinker. The type of diisocyanate could in turn influence the network T_g through differences in M_c .

F-LPUs E_a : A second measure of material properties is the activation energy (E_a) of the T_g . To further investigate the relationship between thermal properties and lignin content seen in the T_g data, the E_a of the T_g was determined by DMTA for one polyurethane film series. These results are shown in Table 4-2. As the T_g of the network

decreased, with a decreasing lignin content, the E_a of the transition also declined. The decrease in E_a with a decrease in the lignin content may be due to the nature of the two polyol components. For a material in the glassy state, as the temperature increased, the flexible PPO contributes to small-scale local molecular motions more easily than the aromatic lignin. On this local scale, the PPO facilitated an increase in free volume with heating, which would precede the observed T_g . The magnitude of this effect would become more prominent as the PPO content increased. At high PPO contents, the increase in free volume would be sufficient to allow relatively unhindered motions of the rigid lignin. Thus the E_a of the entire system was reduced as the PPO content increased.

For polyols with a similar lignin content (FK-A and FK-B) the TDI films had a higher T_g and a higher E_a than the corresponding HDI films. The differences in E_a between the TDI and HDI films, as with the differences in T_g , were due to the flexibility of the crosslinker and possibly to differences in the network M_c . The more rigid TDI crosslinker required more energy to initiate the transition, producing a higher E_a .

Range of LPU Glass Transitions: Besides the T_g s and

$\tan \delta$ peak temperatures, Table 4-1 also shows the range over which the T_g occurs and the $\tan \delta$ peak width, which is typically measured at one-half of the peak height. Both of these measurements of network properties reflect the complexity and magnitude of molecular motions present in the system (24). As the lignin content in the CEHPL declined, so did the T_g range and the $\tan \delta$ one-half peak width. This trend is shown in Figure 4-5 for the T_g range. There was one exception to this trend: the T_g range and one-half peak width increased for the LPU's prepared from the slightly chain-extended material compared to LPU's prepared from the parent HPL. The decrease in lignin content in this range corresponds to an increase in the MS of the polyol from 1.0 to approximately 2.0 (18). With an MS of 2.0 there are two distinct types of ether linkages present in the CEHPL. The original arylalkyl linkages between lignin and the first PO unit would have different rotational energy barriers than the dialkyl linkages between subsequent PO units. Thus the T_g for LPU's prepared from CEHPL's with an MS of 2.0 could be expected to be broadened.

The T_g range could also be affected by both the distribution of molecular weights between crosslinks (M_c) and the sol content of the networks. However, the T_g range

appeared to be strongly related to the lignin content. As the content of the chemically diverse lignin in the LPU increased so did the range of the T_g response.

The modulus in the rubbery region may be used to determine M_c (24). However, due to the design of the DMTA instrument, in this study the absolute value of the $\log E'$ was not considered to be reliable and thus the M_c values were determined by the swelling experiments presented in the final section of this chapter.

Mechanical Properties

Preparation of LPUs allowed control of the T_g over a wide range of temperatures. At room temperature the mechanical properties of the LPUs varied dramatically. Figure 4-6 shows the load vs. elongation behavior of a series of LPUs. These differences appeared to be related to both MS and diisocyanate type. In addition, Figure 4-6 shows the mechanical properties of several polypropylene glycol (PPG)-based polyurethanes (curves 2a and 2b) (29). Also included in Figure 4-6 is the load vs. elongation behavior of a PEG-extended HPL film (curve 1) (15). As noted before, the PEG extended HPL films were limited to low levels of flexible extender addition.

Mechanical properties for all the LPU's are shown in Table 4-3. The mechanical properties of the LPU's varied with a maximum breaking strength of 66.5 MPa (H-OS-HPL) and an elongation at break of 95% (T-OS-C). The mechanical properties of the LPU's could be related to the lignin content and diisocyanate type as shown in Figure 4-7. The modulus of elasticity (MOE) decreased dramatically as the lignin content of the films decreased. The MOE can be related to the stiffness of the polymer backbone (25). Thus as the lignin content decreased, there was a corresponding decrease in the MOE of the network. From Figure 4-7 it is apparent that the MOE can be controlled in two ways. MOE could be varied by almost three orders of magnitude with percent lignin rising from 23 to 43%. At a constant lignin content the MOE could be varied an order of magnitude through the selection of diisocyanate.

A second MOE value (response 1) is also shown in Figure 4-7. This LPU was prepared from a blend of a HPL and PEG (15). While the range of lignin contents for LPU's prepared from the blends was not as large as that of the CEHPL copolymers, there was a significant trend. Networks prepared from the CEHPL copolyols allowed for much greater

control over MOE. Attachment of the soft-segment to lignin provided a wide variety of homogeneous LPUs.

As the lignin content of the LPUs increased, MOE and breaking strength increased while elongation at break decreased (Table 4-3). However, this material property data contained much more scatter than the MOE results, while the TDI and HDI network data could not be distinguished. An inverse relationship between strength and strain is typical of many polymer networks (30). This inverse relationship reflects the limited chain mobility of these systems. Chain mobility can be limited by both the chemical nature of the polymer backbone (aromatic vs. polyether content) and the crosslink density of the network (31).

Network Stiffness: When the MOE is plotted against the aromatic content of the network (based on a weight percent of C₆H₆) the HDI and TDI networks were not substantially different as seen in Figure 4-8. This parallels the trend for the T_g data. The minor differences between the MOE of HDI and TDI networks (Figure 4-8) could be due to differences in the M_c of the LPUs seen earlier. A low M_c could limit chain mobility and lead to a high MOE (31). The possible effect of M_c on the thermal properties of the LPUs was shown to be substantial. A decreased M_c would result

in restricted molecular motion which may be translated into increased chain stiffness and a high MOE.

While the LPU mechanical properties depended on the chemical nature of the network, the source of the lignin (OS vs. KL) did not influence MOE. In previous work, networks prepared from OS and KL HPLs were found to be similar and in the current study small differences in lignin chemistry were dominated by the effects of chain extension. The origin of the lignin did not influence the breaking strength and elongation at break. Chain stiffness and M_c influenced molecular motion as reflected by the T_g and MOE data, while ultimate properties were typically more sensitive to defects than to differences in network density.

Swelling Studies

Swelling experiments can be used to characterize networks (32), and have been applied to other LPUs (21). These experiments allow one to distinguish components which are covalently bonded into the network from entrapped sol molecules. The M_c of a network can also be estimated from swelling experiments if the Flory-Huggins chi parameter (χ) is known. If the CEHPL polyols are viewed as multi-

functional stars then as the MS increases, so does the average length of the radial arms. These radial arms are reactive at their terminus, so that as the MS increases, so does the distance between the lignin centers. Thus the tightness of the network decreases and its ability to swell increases. If equilibrium swelling is assumed, the density of a network can be quantified through use of equation 2 and knowledge of X and percent swell.

To calculate X, the solubility parameter of the polymer must be determined. If one knows the volume fraction of each component and its respective solubility parameter, then the solubility parameter of the network may be found (Equation 5) (33). The solubility parameter of each component, PPO (34), lignin (35), and HDI (34) or TDI (34), was known or calculated from group contribution theory:

$$\delta = \rho_p \sum V_i \delta_i \quad (\text{eq. 5})$$

where

ρ_p = density of the network

V_i = volume fraction of component i

δ_i = solubility parameter of component i

With an estimate of δ_p , X may be found through equation 6:
(33)

$$X = \frac{V_s (\delta_s - \delta_p)^{1/2}}{RT} \quad (\text{eq. 6})$$

where

- X = Flory-Huggins constant
- V_s = molar volume of solvent (DMF)
- R = universal gas constant
- T = absolute temperature
- δ_s = solubility parameter of solvent
- δ_p = solubility parameter of the network

The sol fraction and percent swell were determined and are shown in Table 4-4. As the lignin content decreased the sol fraction and percent swell increased. The X parameter and M_c values for the LPU's were also calculated and are shown in Table 4-4. Since X is related to the network composition through δ_p , there is a constant increase in X as the lignin content decreases.

The M_c values calculated in Table 4-4 from equation 2 were related to both the X parameter and percent swell and there was a consistent increase in M_c as the lignin content

decreased. While the M_c would be expected to increase as the length of the polyether arms increased (lignin content decreased) the magnitude of the change was surprising. The large M_c values were consistent with the high sol fractions. Both of these observations indicate that an incomplete network was formed from the highly chain-extended polyols. Incomplete networks may be the result of cyclization reactions or small amounts of hydroxyl containing impurities present in the high molecular weight CEHPLs.

The M_c values were typically lower for the polyols crosslinked with HDI compared to TDI. As mentioned previously this can be attributed to steric and chemical differences between the isocyanate groups. Observed differences in M_c helped explain the differences in the thermal and mechanical properties of the HDI and TDI LPUs after they were normalized for differences in aromaticity, Figures 4-4 and 4-8 respectively. Interactions between a network's composition and M_c can be quantified by several models, one of which is that of Chan *et al.* (36).

Application of a Network Model

Two other studies of LPUs have applied the model developed by Chan et al (36) . This model was based on work with epoxy networks and was used to explain the change in T_g with network formation. Two separate effects were explicitly considered in the model; a change in T_g due to crosslinking and a change in T_g due to the creation of a copolymer (equation 7):

$$\Delta T_g = \Delta_c T_g + \Delta \rho T_g \quad (\text{eq. 7})$$

where

$$\Delta T_g = (T_g \text{ LPU network}) - (T_g \text{ CEHPL polyol})$$

$$\Delta_c T_g = \text{copolymer effect, i.e. } T_g \text{ of a comparable linear copolymer}$$

$$\Delta \rho T_g = \text{crosslinking effect, i.e. change in } T_g \text{ due to addition of crosslinks}$$

The crosslinking effect, $\Delta \rho T_g$, has been related to the average molecular weight between crosslinks, M_c , by equation 8:

$$\Delta \rho T_g = k(1/M_c) \quad (\text{eq. 8})$$

Substitution of equation 8 into equation 7 yields equation 9:

$$\Delta T_g = \Delta_c T_g + k(1/M_c) \quad (\text{eq. 9})$$

For the LPU, both ΔT_g and M_c were known, which allowed the determination of $\Delta_c T_g$ and k graphically (Figure 4-9). For the HDI crosslinked networks, the slope of the line, k , is 3.1×10^3 with an intercept of $\Delta_c T_g$ of -7°C . For the TDI crosslinked networks, the slope k is 25.1×10^3 with an intercept of $\Delta_c T_g$ of 10°C . The intercept ($M_c^{-1} = 0$) represents a linear copolymer without crosslinks. Again the rigid nature of the TDI was reflected by the high $\Delta_c T_g$ and k . For similar $1/M_c$ levels, a high k may be interpreted as an indication of a large increase of T_g due to crosslinking.

It should be noted that there were differences between the system examined in the current study and the other LPU systems (23,37) and the epoxy system used by Chan *et al.* (36). The major difference between these networks was that the composition of the networks used in the current study varied while the composition of the networks in the previous studies (23,36,37) remained relatively constant. Viewed another way, in the current study M_c was varied by extending the length of the hydroxypropyl arms on the lignin which lead to variations in ΔT_g required for equation 9. In the other studies, M_c was varied by changing

the functionality of the system.

Values of $\Delta_c T_g$ can be determined independently of equation 9 with the Fox relationship (38), equation 10.

$$\frac{1}{T_g} = \frac{w_1 + w_2}{T_{g1} + T_{g2}} \quad (\text{eq. 10})$$

where w_1 and w_2 are the weight percent of the two components, polyol and diisocyanate, and T_g , T_{g1} , and T_{g2} are the T_g s of the copolymer, polyol, and diisocyanate, respectively. The T_g in equation 10 should then be equivalent to $\Delta_c T_g$ in equation 9. Both of these values are shown for the LPU's in Table 4-5.

From the results in Table 4-5 it was apparent that the two sets of $\Delta_c T_g$ s were not equivalent. Results from the model of Chan et al. predict that the mixing of the polyol with the lower T_g diisocyanates would result in an increase in the T_g of the polymer. The Fox relationship, equation 10, predicts an intermediate T_g for the idealized homopolymer from the mixing of the polyol with the low T_g diisocyanate.

From the strong correlation between ΔT_g and M_c

shown in Figure 4-9 it was apparent that the extent of crosslinking affected the change in T_g with network formation. However, the discrepancy between the ΔT_g values calculated from equations 9 and 10 led to the conclusion that the model of Chan et al. could not be accurately applied to this system.

CONCLUSIONS

A series of homogeneous LPU films with a wide variety of properties could be prepared from CEHPLs. The T_g and T_g range of the LPUs, which could be measured with both DMTA and DSC, was related to both the lignin content and diisocyanate type. At a constant NCO/OH ratio the LPU networks crosslinked with TDI possessed a higher T_g and T_g range than those crosslinked with HDI. But if the T_g was expressed as a function of the aromatic content of the network, the HDI crosslinked networks yielded a higher T_g than TDI networks. This was seen as an indication that HDI networks were more highly crosslinked than the TDI networks. The mechanical properties of LPU films varied widely. The MOE and ultimate strength decreased while the ultimate strain increased as the lignin content decreased. The LPU networks prepared from CEHPL polyols were more sensitive to the lignin content than networks which used

polyethylene glycol as a soft segment. The MOE was also found to vary depending on the type of diisocyanate used, with TDI providing a higher MOE than HDI at a similar lignin content.

The CEHPL networks could be characterized by swelling experiments. The sol fractions of the networks prepared from CEHPLs with a low lignin content were as high as 54%. This observation, coupled with a large M_c value, indicated that the LPUs were not completely crosslinked. The incomplete crosslinking could be due to both a problem with measuring the total OH and the low reactivity of TDI after the first isocyanate group has reacted.

This study showed that the source of the lignin (OS vs. KL) did not affect LPU properties. The LPU properties were dominated by the lignin content and diisocyanate type. With a knowledge of these two parameters, LPUs could be prepared in a controlled manner.

REFERENCES: CHAPTER 4

1. P. J. Manno, in Urethane Chemistry and Applications, K. Edwards, ed. ACS Symposium Series No. 172, American Chemical Society, Washington, D.C., 1981, p.9.
2. I. S. Lin, J. Biranowski, and D. H. Lorenz, in Urethane Chemistry and Applications, K. Edwards, ed. ACS Symposium Series No. 172, American Chemical Society, Washington, D.C., 1981, p. 523, and references therein.
3. E. N. Doyle, The Development and Use of Polyurethane Products, McGraw-Hill, New York, 1971.
4. W. G. Glasser and O. H-H. Hsu, U. S. Patent No. 4,017,474 (1977).
5. K. Kratzl, K. Buchtela, J. Gratzl, J. Zauner, and O. Ettinghausen, Tappi, 45(2),113 (1962).
6. A. L. Lambuth, U. S. Patent No. 4,279,788 (1981).
7. R. F. Nichols, U. S. Patent No. 2,854,422 (1958).
8. T. R. Santelli and R. T. Wallace, U. S. Patent No. 3,577,358 (1971).
9. W. G. Glasser, O. H-H. Hsu, D. L. Reed, R. C. Forte, and L. C-F. Wu, Urethane Chemistry and Applications, K. Edwards, ed. ACS Symposium Series No. 172, American Chemical Society, Washington, D.C., 1981, p. 311.
10. W. G. Glasser, C. A. Barnett, T. G. Rials, and V. P. Saraf, J. Appl. Polym. Sci., 29,1815 (1984).
11. D. T. Christian, M. Look, A. Nobell, and T. S. Armstrong, U.S. Patent No. 3,546,199 (1970).
12. L. N. Mozheiko, M. F. Gromova, L. A. Bakalo, and V. N. Sergeeva, Polym. Sci. USSR 23C1,141 (1981).

13. O. H-H. Hsu and W. G. Glasser, Wood Sci., 9(2),97 (1976).
14. V. P. Saraf and W. G. Glasser, J. Appl. Polym. Sci., 29,1831 (1984).
15. V. P. Saraf, W. G. Glasser, G. L. Wilkes, and J. E. McGrath, J. Appl. Polym. Sci., 30,2207 (1985).
16. V. P. Saraf, W. G. Glasser, and G. G. Wilkes, J. Appl. Polym. Sci., 30,2207 (1985).
17. S. S. Kelley, Chapter 4 of this work (1987)
18. W. G. Glasser, C. A. Barnett, P. C. Muller, and K. V. Sarkanen, J. Agric. Food Chem., 31(5),921 (1983).
19. L. C-F. Wu and W. G. Glasser, J. Appl. Polym. Sci., 29,1111 (1984).
20. E. A. Collins, J. Bares, and F. W. Billmeyer, Experiments in Polymer Science, Wiley-Interscience, New York, 1973, p. 481.
21. T. G. Rials and W. G. Glasser, Holzforschung, 38(4),191 (1984).
22. K. Shibiyama and M. Kodama, J. Polym. Sci.: Part A-1, 4,83 (1966).
23. T. G. Rials and W. G. Glasser, Holzforschung in press (1986)
24. L. E. Nielsen, Mechanical Properties of Polymers, Reinhold, New York, 1962.
25. J. A. Brydson, Chapter 3 in Polymer Science: A Materials Science Handbook, Vol. 1., A. D. Jenkins ed. American Elsevier Publishing, New York, 1972, p. 193
26. M. E. M. Helene, L. W. Reeves, and C. Robinson, in Liquid Crystals and Ordered Fluids, Vol. 4. A. C. Griffin and J. F. Johnson, eds. Plenum Press, New York, 1982, p. 451.
27. W. Gzerwinski and G. Ciemniak, Ange. Makromole. Chemie, 134,23 (1985).

28. W. Cooper, R. W. Pearson, and S. Darke. Ind. Chem., 36 121 (1960).
29. D. J. Hourston and J. A. McCluskey, J. Appl. Polym. Sci., 30,2157 (1985).
30. H. G. Elias, Macromolecules: Structure and Properties 2nd. ed., Plenum Press, New York, 1983
31. I. M. Ward, Mechanical Properties of Solid Polymers. 2nd ed., Wiley-Interscience, New York, 1983.
32. M. Rutkowska and A. Kwiatkowski, J. Polym. Sci.: Symp. No. 53, 141 (1975).
33. A. Rudin, The Elements of Polymer Science and Engineering., Academic Press, 1982, Chapter 12.
34. C. M. Hansen, J. Paint Technol., 39,505, 104 (1967).
35. D. Smith and W. G. Glasser, Final Report to the Westvaco Corp., 1978.
36. L. C. Chan, H. N. Nae, and J. K. Gillham, J. Appl. Polym. Sci., 29,3307 (1984).
37. S. S. Kelley, Chapter 6 of this work (1987)
38. T. G. Fox, Bull. Am. Phys. Soc., 2(1), 123 (1956).
39. D. J. Hourston and J. A. McCluskey, J. Appl. Polym. Sci., 302157 (1985).

TABLE 4-1

**DYNAMIC MECHANICAL AND THERMAL PROPERTIES
OF LIGNIN-BASED POLYURETHANES (LPUs)**

LPU Type	Lignin Content of LPU (%) ¹	Tan δ Peak Temp (°C)	DMTA		DSC	
			Peak 1/2 Peak Width (°C)	Tg (°C)	Tg Range (°C)	
<u>HDI Series</u>						
OS-HPL	40	90	38	72	40	105
OS-A	37	55	54	36	63	
OS-B	30	14	38	-1	22	
KL-HPL	43	90	32	80	36	
KL-A	31	38	55	18	41	
KL-B	27	-1	34	-14	29	
KL-C	25	-20	31	-28	24	
KL-D	23	-24	27	-38	20	
FK-HPL	37	85	34	74	38	
FK-A	32	46	49	32	58	
FK-B	29	-10	27	-24	25	

TABLE 4-1 continued

LPU Type	Lignin Content of LPU (%) ¹	DMTA		DSC	
		Tan δ Peak Temp (°C)	1/2 Peak Width (°C)	T _g (°C)	T _g Range(°C)
<u>TDI Series</u>					
OS-B	30	84	49	61	62
OS-C	25	-20	35	-35	48
OS-D	20	-28	26	-42	40
KL-A	31	79	69	56	64
KL-B	27	46	68	25	58
KL-C	25	32	63	1	50
KL-D	23	22	52	-5	41
KL-E	21	-33	30	-45	36
KL-F	17	-36	26	-53	33
FK-A	30	127	56	101	49
FK-B	27	30	42	12	36
FK-C	19	-23	28	-47	26

¹ Based on the average MS as determined in Chapter 3. Lignin contents of the films vary due to molecular weight differences between HDI and TDI.

TABLE 4-2
EFFECT OF LIGNIN CONTENT AND DIISOCYANATE TYPE
ON THE ACTIVATION ENERGY OF THE LPU'S T_g

<u>LPU Type</u>	<u>Lignin Content of LPU (%)¹</u>	<u>LPU T_g (°C)</u>	<u>E_a of T_g (kJ/mol)</u>
<u>HDI Series</u>			
FK-HPL	37	85	212
FK-A	32	46	156
FK-B	29	-10	107
<u>TDI Series</u>			
FK-A	30	127	352
FK-B	27	30	315
FK-C	19	-23	271

¹ Based on the average MS as determined in Chapter 3. Lignin contents of the films may vary due to molecular weight differences between HDI and TDI.

TABLE 4-3
MECHANICAL PROPERTIES OF LPUs

<u>LPU Type</u>	<u>Lignin Content in LPU (%)¹</u>	<u>Youngs Modulus (MPa)</u>	<u>Ultimate Strength (MPa)</u>	<u>Ultimate Strain (%)</u>
HDI Series				
OS-HPL	40	1,300	66.5	6.6
OS-A	37	171	28.1	21.1
OS-B	30	97	14.7	55.0
KL-HPL	43	1,270	53.9	7.9
KL-A	31	146	16.1	12.1
KL-B	27	10	10.3	43.0
KL-C	25	6	2.9	39.6
KL-D	23	8	2.7	36.2
FK-HPL	37	1,410	65.0	8.1
FK-A	32	126	19.2	40.0
FK-B	29	25	3.4	59.0

TABLE 4-3 continued

LPU Type	Lignin Content in LPU (%) ¹	Youngs Modulus (MPa)	Ultimate Strength (MPa)	Ultimate Strain (%)
<u>TDI Series</u>				
OS-B	30	451	46.9	8.4
OS-C	25	85	15.0	95.0
OS-D	20	7	7.4	56.8
KL-A	31	950	52.7	6.8
KL-B	27	221	21.8	21.5
KL-C	25	140	15.5	68.0
KL-D	23	79	12.2	63.0
KL-E	21	13	2.4	47.4
KL-F	17	13	2.3	44.6
FK-A	30	975	34.0	5.1
FK-B	27	127	17.3	99.0
FK-C	19	15	3.6	55.7

¹ Based of the average MS as determined in Chapter 3. Lignin contents of the films vary due to molecular weight differences between HDI and TDI.

TABLE 4-4
NETWORK PROPERTIES OF LPUs AS DETERMINED FROM SWELLING EXPERIMENTS.

LPu Type	Sol Fraction (%)	Swell (%)	X_1	M_c 2
<u>HDI Series</u>				
OS-HPL	2.6	69	.01	250
OS-A	6.9	57	.06	180
OS-B	3.6	42	.14	320
KL-HPL	10.6	154	.01	420
KL-A	7.0	51	.10	400
KL-B	8.5	73	.18	800
KL-C	38.9	69	.26	710
KL-D	22.0	125	.27	1,070
FK-HPL	20.4	100	.04	560
FK-A	11.9	81	.19	450
FK-B	20.2	70	.40	620

TABLE 4-4 continued

LPU Type	Sol Fraction (%)	Swell (%)	\bar{X}_1	\bar{M}_c^2
<u>TDI Series</u>				
OS-B	8.6	98	.02	410
OS-C	34.8	279	.18	3,400
OS-D	50.9	390	.47	25,600
KL-A	12.5	92	.03	510
KL-B	12.8	152	.12	730
KL-C	9.0	147	.20	960
KL-D	14.2	177	.24	1,320
KL-E	53.6	372	.48	27,900
KL-F	38.4	396	.49	30,500
FK-A	11.3	137	.01	670
FK-B	30.8	264	.14	2,320
FK-C	40.6	376	.43	19,480

1 Calculated from group contribution theory using equations 5 and 6 in text.

2 Calculated using equation 2 in text.

TABLE 4-5

CONTRIBUTION TO THE CHANGE IN T_g WITH NETWORK FORMATION PREDICTED
FROM THE MODEL OF CHAN *et. al.* AND THE FOX EQUATION

LPU Type	$\frac{\Delta T_g^1}{(C)}$	$\frac{\Delta T_g^2}{(C)}$	$\frac{\Delta T_g^3}{(C)}$	$\frac{\Delta T_g^4}{(C)}$
<u>HDI Series</u>				
OS-HPL	40	12	28	-19
OS-A	31	17	14	-3
OS-B	14	10	4	2
KL-HPL	22	7	15	-42
KL-A	15	8	7	1
KL-B	6	4	2	6
KL-C	2	4	-2	15
KL-D	-2	3	-5	15
FK-HPL	11	6	5	-45
FK-A	7	7	0	-14
FK-B	0	5	-5	20

TABLE 4-5 continued

LPU Type	$\frac{\Delta T_g^1}{(C)}$	$\frac{\Delta T_g^2}{(C)}$	$\frac{\Delta_c T_g^3}{(C)}$	$\frac{\Delta_c T_g^4}{(C)}$
<u>TDI Series</u>				
OS-B	85	61	24	10
OS-C	15	7	8	13
OS-D	12	1	11	24
KL-A	53	49	4	2
KL-B	45	34	11	13
KL-C	31	26	5	21
KL-D	31	19	12	24
KL-E	11	1	10	32
KL-F	12	1	11	34
FK-A	76	37	39	-5
FK-B	36	11	25	27
FK-C	6	1	5	30

- 1 Determined by DSC; Tg film - Tg polyol.
- 2 Calculated from equation 8 in text using k values from Figure 4-9.
- 3 Calculated from equation 9 in text.
- 4 Calculated from equation 10 in text. The Tg for HDI and TDI were determined from group contribution theory (refs 33-35).

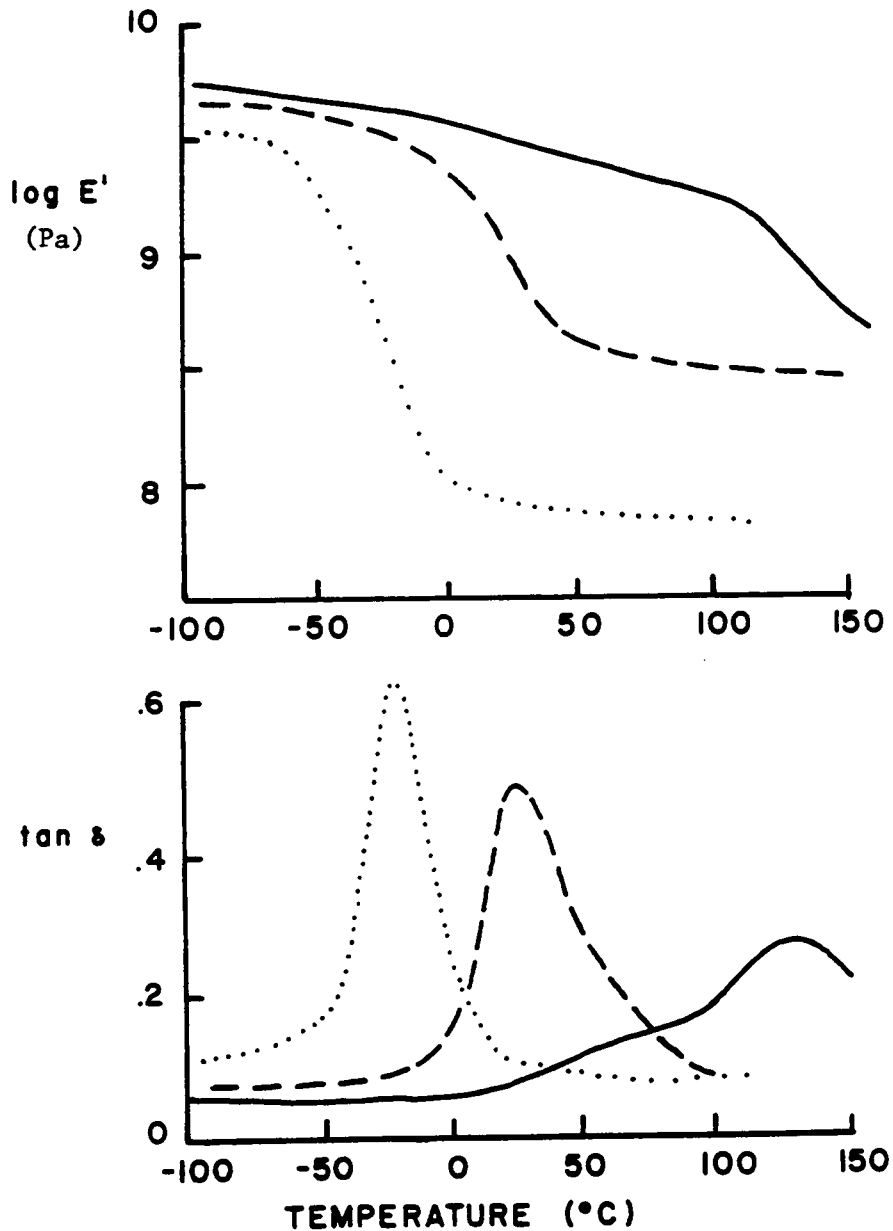


FIGURE 4-1. Dynamic mechanical properties of FK chain-extended hydroxypropyl lignins crosslinked with TDI: FK-A (—), FK-B (---), and FK-C (.....).

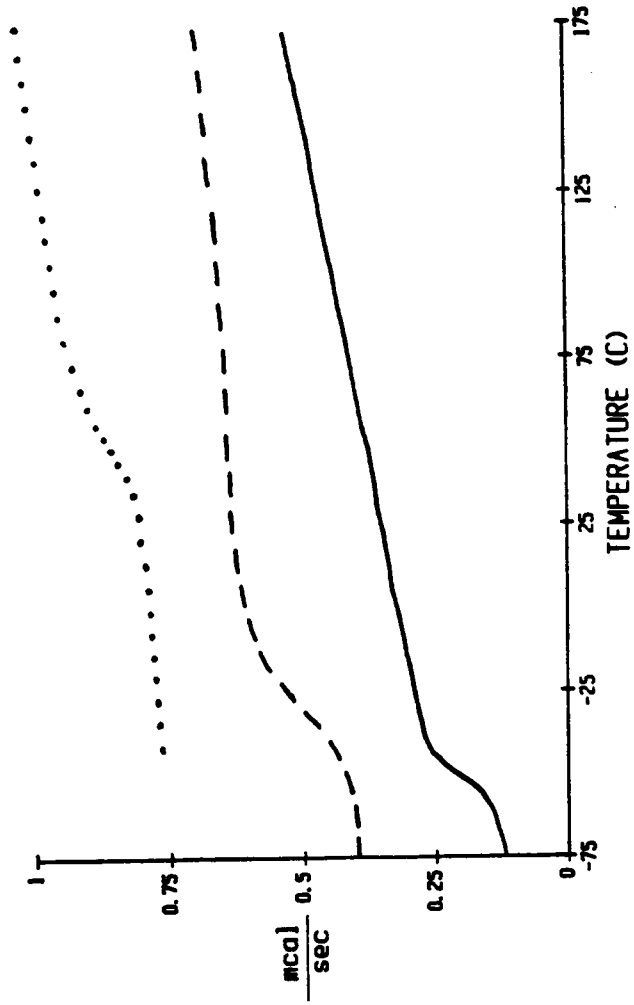


FIGURE 4-2. Differential scanning calorimetry thermograms of OS chain-extended hydroxypropyl lignin series crosslinked with TDI: OS-B (.....), OS-C (---), and OS-D (—).

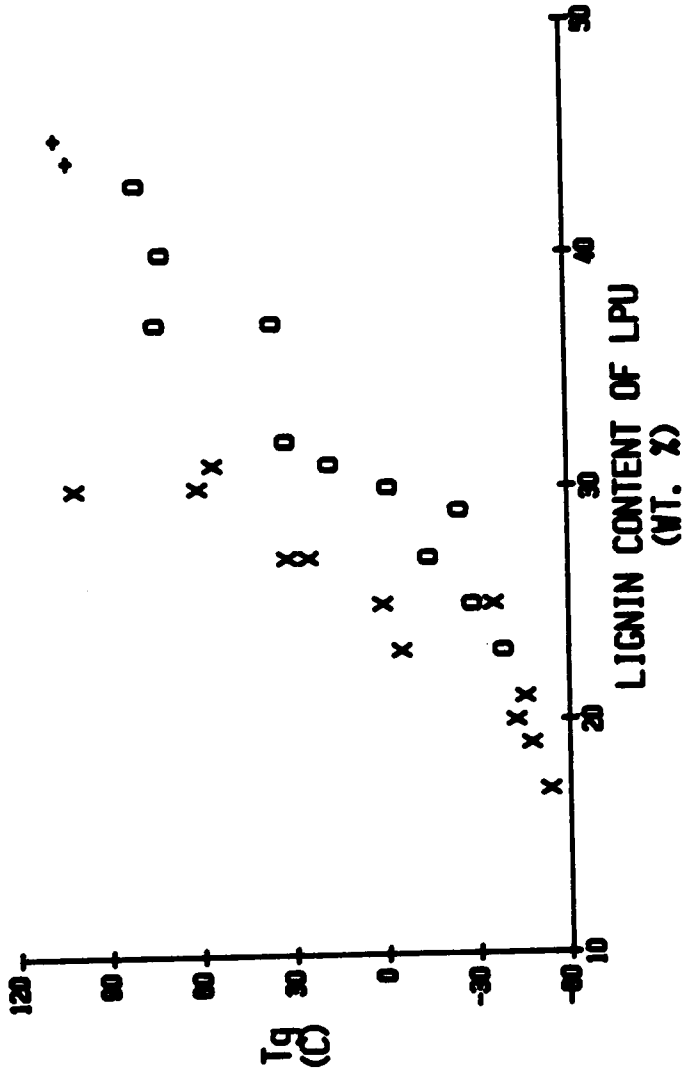


FIGURE 4-3. Effect of lignin content and diisocyanate type on the T_g of LPUs prepared from chain-extended hydroxypropyl lignins crosslinked with HDI (O) and TDI (X). Two points (+) were taken from reference 23 .

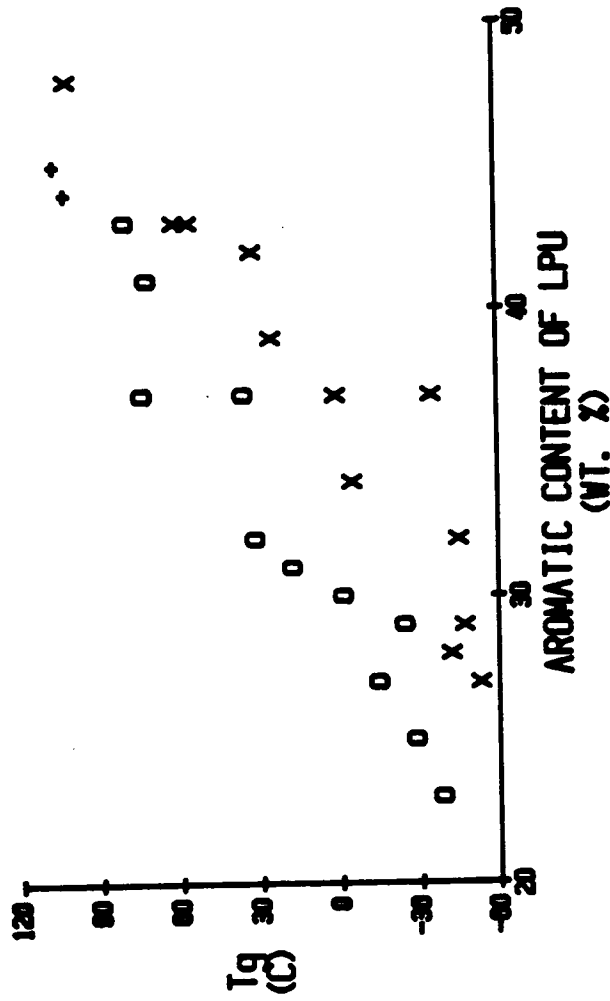


FIGURE 4-4. Glass transition temperatures of LPUs normalized for the aromatic content (wt. % of C₆H₆) of both the lignin and diisocyanate. The LPUs were crosslinked with HDI (O) and TDI (X). Two points (+) were taken from reference 23.

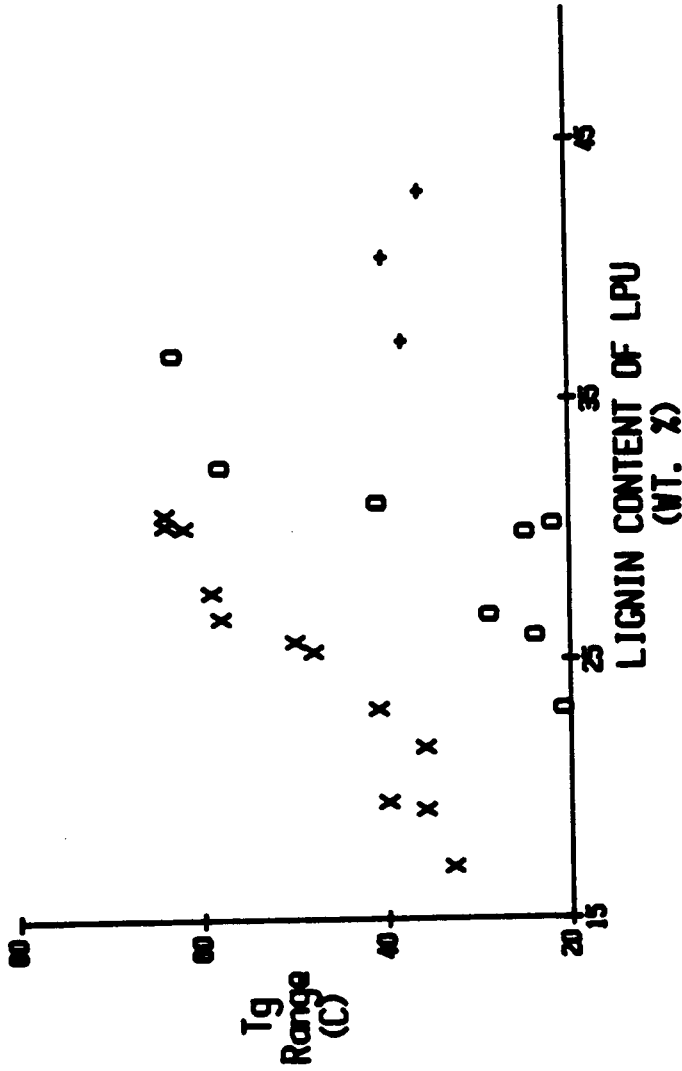


FIGURE 4-5. Effect of lignin content and diisocyanate type on the Tg range for LPUs crosslinked with HDI (O) and TDI (X). Networks formed from the original hydroxypropyl lignins and crosslinked with HDI are shown separately (+).

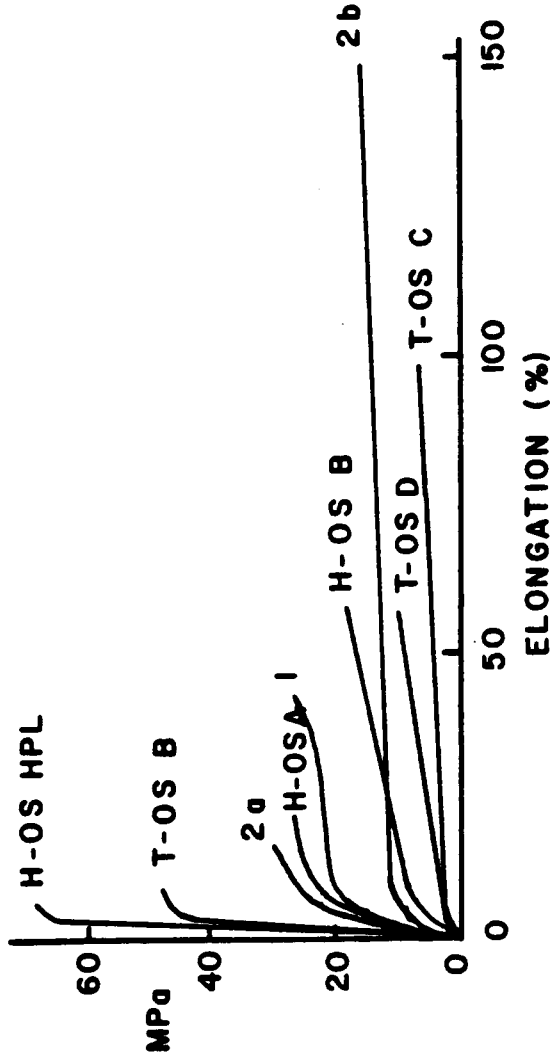


FIGURE 4-6. Load-elongation response of OS polyols crosslinked with HDI and TDI. The first letter represents the type of diisocyanate HDI (H) or TDI (T) and the second set of letters represent the polyol, ie. OS-A is a CEHPL organosolv lignin with a lignin content of 58% (reference 17). Response 1 is that of a HDI crosslinked LPU prepared from a mixture of a HPL and PEG (reference 15). Response 2a and 2b are polyurethanes prepared with a molecular weight between crosslinks (Mc) which is similar to the LPUs (reference 29).

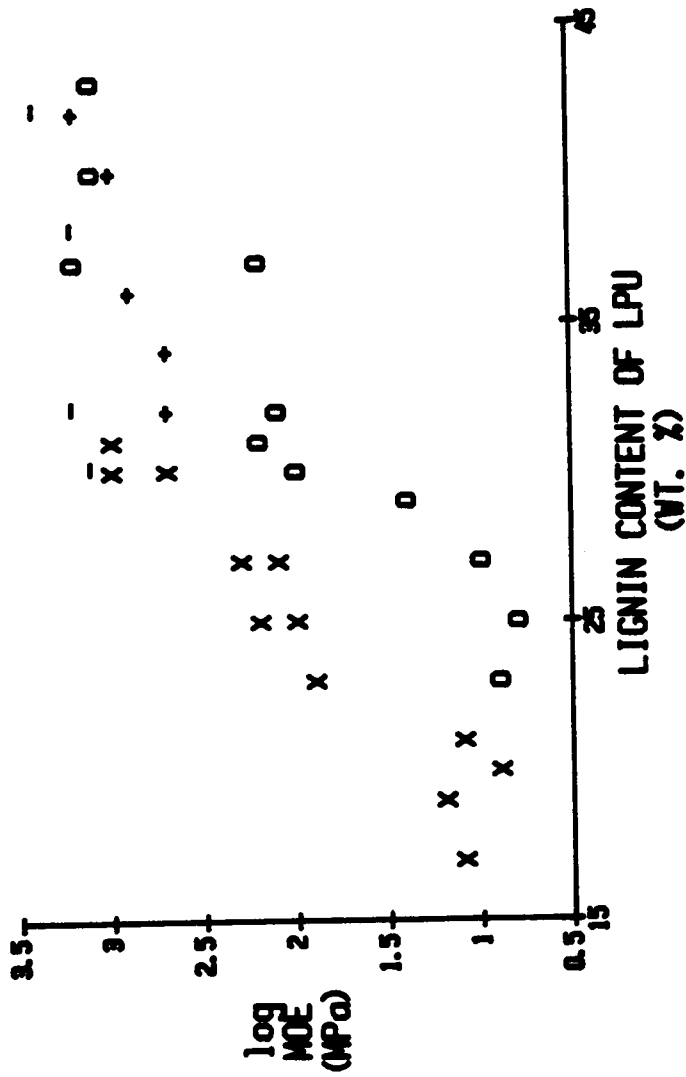


FIGURE 4-7. Effect of lignin content and diisocyanate type on the Youngs modulus (MOE) of LPUs crosslinked with HDI (O) and TDI (X). Also included are the MOE values for LPUs prepared from blends of HPLs and PEG and crosslinked with HDI (+) and TDI (-) (reference 15).

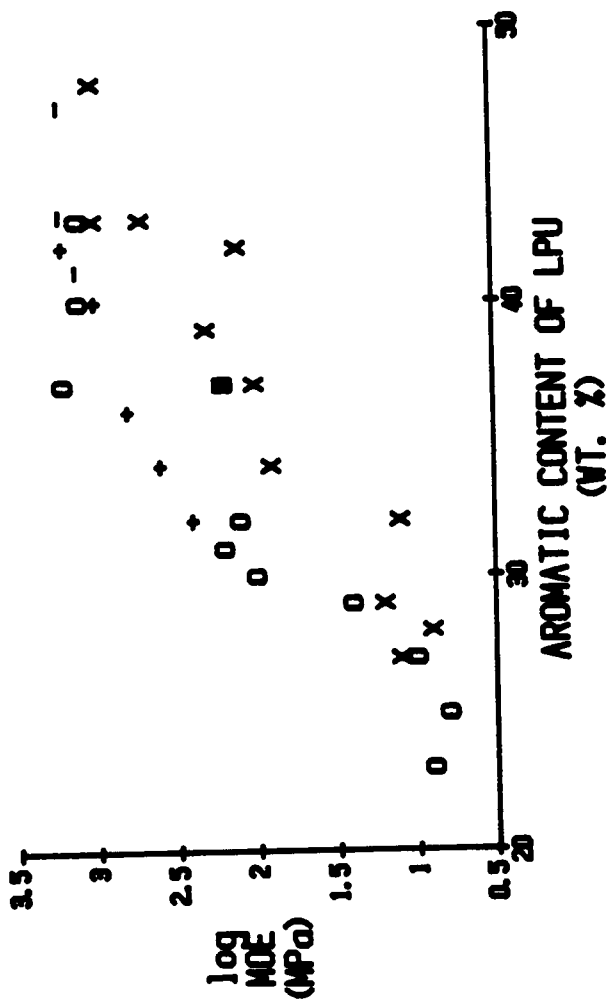


FIGURE 4-8. Young's modulus of LPUs, prepared from CEHPLs, normalized for the aromatic content (wt. % of C₆H₆) of both the lignin and diisocyanate. The LPUs were crosslinked with HDI (O) and TDI (X). Also included are the MOE values for LPUs prepared from blends of HPLs and PEG and crosslinked with HDI (+) and TDI (-) (reference 15).

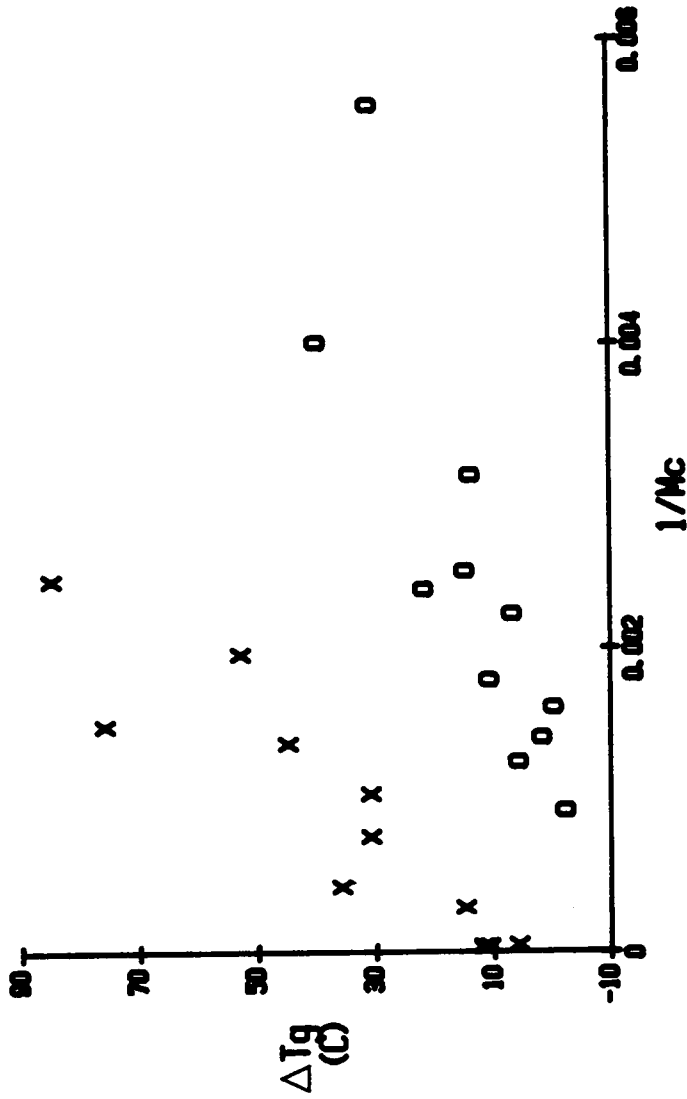


FIGURE 4-9. Relationship between the ΔT_g (Tg film - Tg polyol) and the molecular weight between crosslinks (Mc) for LPUs crosslinked with HDI (O) and TDI (X). The plots provide values for the model of Chan *et al.* (reference 36 and equation 9 in text).

CHAPTER 5

EFFECTS OF HYDROXYPROPYL LIGNIN MOLECULAR WEIGHT ON PREPOLYMER AND NETWORK PROPERTIES

SYNOPSIS

A series of five fractions with number average molecular weights (M_n) between 1,500 and 10,000 Daltons were isolated from a Kraft hydroxypropyl lignin (HPL). From $^1\text{H-NMR}$ and UV analysis the chemical properties of the HPLs were found to vary slightly with molecular weight. The hydroxyl content decreased while glass transition temperature (T_g) increased as the HPL molecular weight increased. The Fox-Flory equation could be used to model the M_n vs. T_g relationship.

The HPL fractions were used as polyols for the preparation of lignin-based polyurethane networks (LPUs). The T_g of the LPUs increased from 40 C to 120 C as the M_n of the polyol rose from 1,500 to 10,000. The molecular weight between crosslinks (M_c) of the networks was determined by swelling. An observed decrease in M_c with an increase in M_n was related to the functionality of the system. The strength properties of LPUs prepared from

fractionated HPLs were superior to those prepared from non-fractionated HPLs.

INTRODUCTION

A considerable amount of study has been devoted to characterizing lignin-based polyurethanes (1-7). The effects of molar substitution (MS) of the hydroxypropyl chain length (1), polyurethane network density (1-3), soft segment (4,5), lignin type (6) and diisocyanate type (1,7) have all been investigated. However, one important effect which has not been investigated directly is the molecular weight of the lignin polyol. This factor may be of great practical interest since lignins or lignin fractions from different sources will have different molecular weights and molecular weight distributions as well as different chemistry (8,9). The effects of differences in molecular weight have been indirectly noted in a study of polyurethanes prepared from lignins derived from various sources (6). Lignins from different sources are known to vary in their chemistry, but much less is known about variations in chemistry for molecular weight fractions of a single lignin.

A major limitation in studying the chemistry of molecular weight fractions of lignin is solubility. The poor solubility of lignin has complicated attempts at fractionating lignins (10,11). However, some success has been achieved with the fractionation of lignin derivatives (11-13). A series of lignosulfonates were fractionated and several chemical characteristics were determined (13). The molecular weights (determined by light scattering) of the fractions varied between 3,000 and 55,000 daltons. Over this range the phenolic hydroxyl content decreased by 40% while the UV absorptivity increased by 10% as the molecular weight increased. A thermal transition of the dry ligno-sulfonate fractions was reported to be between 260 and 295 C. These values are considerably above the values typically reported for lignin in wood.

Another study on changes in lignin chemistry with molecular weight also noted other differences (11). A crude extraction system provided five fractions which varied in their number average molecular weight (M_n) between 370 and 3,120 daltons. The UV absorbtivity decreased by 10% as the M_n increased. In agreement with other studies (13), the phenolic hydroxyl content decreased slightly with increased M_n .

In addition to variations in the chemistry of molecular weight fractions leading to changes in material properties, changes in functionality must be considered. Even if the hydroxyl content of lignin remained constant as the molecular weight increased, the average functionality of an individual molecule would increase. With a change in the functionality of the prepolymer, the process of forming a network also changes.

For highly cured networks, as the functionality of the system increases, generally the molecular weight between crosslinks (M_c) and the sol fraction decreases (15) assuming complete reaction. The probability of a molecule being incorporated into the network increases as the number of reactive sites on the molecule increases. Conversely, mono- or difunctional molecules may greatly limit the ability of a prepolymer to form a network. Monofunctional molecules act as chain-ends while difunctional molecules are chain-extenders. Neither of these molecules will act as junction points, which are required for the formation of a network. Thus, through changes in functionality the molecular weight of the lignin may influence the properties of the material.

The current work involves isolation and characterization of HPL fractions of varying molecular weights and the preparation of LPUs from the HPL fractions. It is anticipated that the properties of these networks will depend on the molecular weight of HPL fractions.

EXPERIMENTAL

Materials

Hydroxypropyl Lignins (HPLs): A pine Kraft lignin, INDULIN AT was obtained from Westvaco Corp., Charleston, SC. The lignin was reacted with propylene oxide in a stainless steel reactor as described in detail previously (17,18).

Diisocyanates: Practical grade hexamethylene diisocyanate (HDI) was purchased from Eastman Kodak Co., Rochester, NY.

Methods

Fractionation of HPLs: Fractional precipitation involved dissolution of 17 gm of a Kraft HPL in 1,250 ml of

acetone to give a 1% solution. After 24 hours (to insure complete dissolution) hexane, a non-solvent, was added. The solution was allowed to precipitate for two hours and then the supernatant was removed. The solvent from both fractions was evaporated under vacuum and the yield of HPL determined. The precipitate was then redissolved for 24 hours, in sufficient acetone to give a ca. 1% solution. Again, hexane was added as a non-solvent and the process was repeated. Five fractions were prepared using acetone/hexane ratios of 5, 2.5, 1.1, and 0.5. The final precipitate was used as the fifth fraction. All fractions were stored over P₂O₅.

HPL Characterization: The characterization techniques applied to the HPL fractions have been described in detail elsewhere (1).

Film preparation: The film preparation and analysis were described in detail elsewhere (1).

RESULTS AND DISCUSSION

Properties of Fractions

Application of classical fractionation techniques (19) to lignin has been limited by problems with both solubility and intermolecular association (10,11). Hydroxypropylation dramatically increases solubility and for both steric and electronic reasons should reduce association. Thus HPLs were considered a suitable candidate for solution fractionation. Five fractions were prepared at varying nonsolvent/solvent ratios. At a particular nonsolvent/solvent ratio, the soluble material was collected as the fraction. Thus for a hexane/acetone ratio (H/A) of 5, only the most soluble, low molecular weight material remained in solution. This material (Fraction 1) was collected while the precipitate was redissolved and the H/A ratio subsequently readjusted to 2.5. Again the soluble material was collected (Fraction 2). The process was repeated to produce the five fractions. The GPC chromatograms for the five fractions and the original non-fractionated HPL are shown in Figure 5-1.

Molecular Weight Properties: Yields and molecular weight characteristics of the five fractions and original

HPL (F-LPU 1 through 5 and O-LPU respectively) are shown in Table 5-1 (Section A). The original HPL possessed a broad molecular weight distribution (M_w/M_n), while all of the fractions showed a narrower distribution. It was apparent that as the amount of non-solvent, hexane, was decreased the molecular weight of the material increased. These results show that classical fractionation may be applied to HPLs to yield materials with different molecular weights. The number average degree of polymerization for these fractions varied between ca. 4 and 40 lignin C-9 units.

The yields of the fractions show that the three high molecular weight fractions contain more than the desired 20 percent of the original HPL. Five equal fractions were desirable to provide sufficient material for preparation of duplicate films. This distribution of yields could be made more uniform by reducing the H/A ratio for the first two fractions, and to a lesser extent the H/A ratio of the third and fourth fractions. This would result in more uniform yields but would raise the molecular weight of the first three fractions while lowering the molecular weight of the fourth fraction. These changes in the H/A ratio should produce a more uniform increase in the fraction's molecular weights.

Both the number average (M_n) and weight average (M_w) molecular weight increased in a consistent fashion as the H/A ratio decreased. As noted previously there is some controversy surrounding molecular weight determinations for lignins (10,20). This controversy centers around association phenomena (10) and reliable molecular weight standards for column calibration (20). It has been shown previously that acetylation and the use of DMF with LiBr reduces association (21). In addition, preparation of lignin derivatives, with a bulky group attached to the phenolic hydroxyl, should limit association for both steric and electronic reasons. However, appropriate molecular weight standards were still needed. Linear polystyrene standards were used in conjunction with lignin model compounds. A crystallizable hydroxypropylated trimeric lignin model (MW = 784) (22) provided an elution volume in good agreement with the line produced from the polystyrene standards. Thus calibration of the GPC columns for low and moderate molecular weight material was considered reliable.

The M_n values were determined by both GPC and VPO and the two techniques provided good agreement (ca. 10%). Thus the trend which showed both M_n and M_w increasing with decreasing H/A ratios was concluded to reflect real differences in molecular weight. The dispersity ratio

(M_w/M_n) for the fractions was substantially less than that of the original HPL. Considering the complex nature of this material, a dispersity ratio (DR) of 1.6 to 3.0 was a substantial improvement over the original material. The final precipitate will typically have a higher DR than the other fractions unless special effort is invested in removing the very high molecular weight material. While present as a small percentage of the total HPL, the very high molecular weight material will have substantial impact on M_w and thus increase the DR of the final fraction. This low DR has important implications for the utilization of these HPLs. With a reduction in the DR, the molecular weight distribution became more uniform. This leads to a more uniform distribution of reactive sites within each fraction. Thus, the fractionated HPLs may allow for the preparation of uniform materials with improved properties.

Thermal Properties of Fractions: It has been shown previously for both synthetic polymers and for lignosulfonates that a change in molecular weight results in a variation of a material's glass transition temperature (T_g) (23,24). As seen in Table 5-1 (Section B), the T_g of the HPL fractions increased as the molecular weight of the fraction rose. This relationship obeys the Fox-Flory relationship, equation 1:

$$T_g = T_{g\infty} - k/M_n \quad (\text{eq. 1})$$

where

T_g = the glass transition temperature of a specific fraction

M_n = the number average molecular weight of that fraction

$T_{g\infty}$ = the glass transition temperature of the material at infinite molecular weight

k = a constant, which is related to the degree of branching for the system (24).

The data for these fractions was fitted to the Fox-Flory relationship, and the results are shown in Figure 5-2. The fit for the five fractions was good with a $T_{g\infty}$ of 92 C and slope k of 1.5×10^5 . The data point for the original material did not fit onto the same line as the other points. This deviation could be due to the polydisperse nature of the unfractionated HPL.

Large differences in the thermal properties supported the molecular weight differences observed with GPC. The intercept of Eq. 1 or $T_{g\infty} = 92$ C for the very high

molecular weight HPL was higher than the 68 C predicted¹ from one of the simple copolymer equations (25).

The k value from Eq. 1 may be used to estimate the extent of branching of a system (24). However, k depends on chemical composition and the types and extent of secondary interactions and has not been measured for lignin systems. For a series of lignin derivatives k may serve as a useful measure of the branched macro-molecular architecture.

Chemical Composition of Fractions: Proton NMR and UV spectroscopy were used to characterize the chemical structure of the original HPL and the five fractions (Table 5-1, Section C). Integration of the ¹H-NMR signal of HPLs provides information on the relative abundance of different types of functional groups present in the molecule. Specifically, the ¹H-NMR spectra were divided into four regions with characteristic protons which have been previously assigned (21,26).

(¹ the T_g was predicted with eq. 3 using 180 C and -75 C as the T_g for lignin and PPO, respectively.)

The percent of the $^1\text{H-NMR}$ signal in the four regions was similar for the original HPL and the first four fractions. However, the high molecular weight fraction showed substantial differences. In particular, the high molecular weight fraction showed a reduction in the response from the aromatic and methyl protons and an increase in the range 6 & 7 acetoxy methyl protons. This signal was reproduced but is not understood at present. The final fraction may contain nonpolar impurities which lead to the large increase in the signal in the range of the acetoxy methyl protons. The reduction in the aromatic signal is reflected by the UV absorptivity at 280 nm. UV absorptivity of the HPLs, at 280 nm, is specific for lignin and correlated well with the relative abundance of the aromatic protons (range 2 & 3) (Figure 5-3). While the apparent differences in chemical structure with increasing molecular weight were not substantial, there was consistent agreement between the $^1\text{H-NMR}$ range 2 & 3 signal and the UV absorbance.

The percent hydroxyl of the fractions generally decreased as the molecular weight of the HPL increased. A decrease in total hydroxyl indicated that there would be fewer reactive sites for condensation with diisocyanates.

Polyurethane Networks

Effects of Molecular Weight on Dynamic Mechanical and Thermal Properties: Lignin-based polyurethane (LPU) films were prepared from the fractionated HPL at a constant NCO/OH ratio (1.6). The hydroxyl content was measured by titration rather than by $^1\text{H-NMR}$ as described earlier (21). Hydroxyl contents measured by titration were typically one-half those measured by $^1\text{H-NMR}$. Thus the diisocyanate content of these films was lower than for LPUs described earlier (1).

The DMTA spectra for these fractionated lignin polyurethane networks (F-LPUs) are shown in Figure 5-4. The molecular weight of the starting polyol influenced the observed T_g , measured by both DMTA and DSC, as well as the range over which the transition occurred. All of these results are shown in Table 5-2. These results may be rationalized by considering the network structure of the F-LPUs.

The dynamic mechanical and thermal properties of the F-LPUs may be influenced by several factors. Chemical composition has been shown to significantly influence the thermal properties of LPUs (6). However, differences in

chemical composition for the F-LPUs were minor relative to the large differences in the thermal properties. The other factor which may influence the thermal properties of LPUs was the molecular weight of the original HPL. The molecular weight of the original HPL may affect the thermal properties through two separate mechanisms. First as the molecular weight increased, the T_g of the HPL increased in a consistent fashion, which may be related to the number of end groups. The second factor may be related to the functionality of an individual molecule. For these HPLs, as the degree of polymerization increased, so did the number of reactive sites on a molecule. A change in polyol functionality may lead to a change in the network architecture. Interpretation of differences in the F-LPU behavior must consider both of these factors.

The effects of molecular weight may be visualized by considering the size of the molecule. In the LPU network both the HDI crosslinker (estimated from group contribution theory) and the propylene oxide soft-segment have low T_g s, -52 C and -75 C, respectively (28,29). These two components were connected in the curing reaction to produce a low T_g material around the aromatic lignin. Thus, as the temperature was increased, motion in the low T_g material would increase at a temperature well below that required

for motion of the lignin. Since the LPU was homogeneous the lignin molecule must participate in the observed T_g . Segmental motion of a large lignin molecule would be restricted by both size and branching.

Range of Energy Dissipative Mechanisms: The $\tan \delta$ peak width, measured at one-half peak height, and the T_g range may both be used to estimate the heterogeneity and complexity of the dispersions occurring as the temperature was increased (30). A broad $\tan \delta$ one-half peak width or a wide T_g range is typical of a chemically heterogeneous material such as lignin. PPO may be viewed as possessing simpler modes of molecular motions that would contribute to a narrow T_g . The increase in the $\tan \delta$ one-half peak width and T_g range with increased molecular weight (Table 5-2) may be related to the molecular weight distribution or the network architecture. A broad molecular weight distribution provided for a wide range of chemical features and variations in the number of reactive sites on a molecule. Both of these factors would be expected to increase the complexity of molecular events as the polymer passes through T_g , thus broadening the T_g .

Swelling of F-LPUs: Swelling experiments allow for characterization of the network architecture and entrapped

sol molecules for most crosslinked materials. If the Flory Huggins χ (X) parameter were known, the swelling experiments would also allow for determination of the molecular weight between crosslinks (M_c). The X parameter was estimated through calculation of an F-LPU solubility parameter from group contribution theory (1,28). A discussion of the calculation of the solubility parameter and M_c for LPUs may be found elsewhere (1,2). The results of the swelling experiments are shown in Table 5-3. Sol fraction and percent swelling both increased as the polyol molecular weight increased. The M_c determined from the swelling experiment and the calculated X decreased as the M_n increased. The M_c value of the O-LPU was high compared to the M_c value predicted for a hypothetical F-LPU with the same M_n . These results may be explained by considering the functionality of the polyol and how it changes with molecular weight.

To form a network the average functionality of the system must be greater than two (14). Thus a molecule which reacts at only one site will not significantly contribute to resisting an applied mechanical force. A molecule which was connected to the network at two points may act as a chain extender but not as a junction point. Only molecules which were connected into the network at

three or more independent sites may contributed as a junction or crosslink point. In the current study the crosslinker, HDI, was difunctional and thus the HPL polyol must provide the junction points for network formation. Considering the characteristics of the HPL it was obvious that the number of reactive sites per molecule increased as the molecular weight of an individual molecule increased. Thus for the paucidisperse high molecular weight fractions there would be relatively few molecules with only one or two reactive sites. With more molecules that may contribute to the network as junction points the M_c decreased. Conversely, the low molecular weight fractions would have a high concentration of mono- or difunctional molecules and networks formed from these materials, at constant NCO/OH ratio, would have a high M_c . Low molecular weight material in the unfractionated HPL would contribute to a higher M_c than expected from molecular weight alone. Thus it appeared that an increase in the M_n of the HPL produced an increase in the T_g and a decrease in the M_c of the resulting networks.

Application of a Network Model

Some networks may be conceptualized as having two components, a backbone and a crosslinking component (31).

The backbone of an LPU was represented by an idealized linear HPL-HDI copolymer. The crosslinking component may be visualized as additional HDI chains which could limit segmental motion of the idealized linear HPL-HDI copolymer. This concept has been used as the basis for modeling the difference between the T_g of a polyol and the T_g of a subsequent network (6,31), as shown in equation 2:

$$\Delta T_g = \Delta_c T_g + \Delta \rho T \quad (\text{eq. 2})$$

where

$$\Delta T_g = T_g \text{ of F-LPU} - T_g \text{ of F-HPL polyol}$$

$$\Delta_c T_g = \text{copolymer effect, i.e. } T_g \text{ of a comparable linear copolymer}$$

$$\Delta \rho T_g = \text{crosslinking effects}$$

For the F-LPU system ΔT_g was determined from experiment. The $\Delta_c T_g$ was also calculated from the Fox relationship (equation 3):

$$1/T_g = W_A/T_{gA} + W_B/T_{gB} \quad (\text{eq. 3})$$

where

T_g = the T_g of the copolymer ($^{\circ}\text{K}$)

T_{gA} and T_{gB} = the T_g of the respective homopolymers
($^{\circ}\text{K}$)

W_A and W_B = the weight fractions of the homopolymers

The calculated $\Delta_c T_g$ for the five fractions and an ideal high molecular weight fraction are shown as points in Figure 5-5. The T_g of an idealized HDI homopolymer is -52 C and was calculated from group contribution theory and thus the Fox relationship predicted that the T_g of an ideal HPL-HDI copolymer ($\Delta_c T_g$) would be between -52 C and the T_g of the HPL, and would depend on the weight fraction of the components (Eq. 3). The $\Delta_c T_g$ was calculated for each of the fractions and is shown in Table 5-4. The ΔT_g values, which were determined experimentally by the difference between the T_g of the film and the T_g of the polyol, are shown in Table 5-4. With the determination of both ΔT_g and $\Delta_c T_g$, the $\Delta \rho T_g$ values were calculated through equation 2 and are shown in Table 5-4.

The $\Delta \rho T_g$ values (Table 5-4) were positive and large. The differences in ΔT_g were related to the M_c of the F-LPUs. As the $1/M_c$ increased the ΔT_g increased (Figure

5-6). As M_c decreased, the chains were more hindered and the ΔT_g increased. Over this range of M_c , the differences were not substantial since all of these systems were highly crosslinked. However, compared to the linear copolymer, the $\Delta \rho T_g$ was substantial. Thus it appears that the crosslinking reactions, as indicated by $\Delta \rho T_g$, dominate the changes in the T_g of the network with crosslinking.

Mechanical Properties

?

Tensile samples were used to obtain the mechanical properties of the F-LPUs at room temperature. The Youngs modulus (MOE), ultimate strength and ultimate strain for the F-LPUs and the LPU prepared from the original nonfractionated HPL (O-LPU) are shown in Table 5-5. There was a significant increase in the MOE of the F-LPUs over that of the O-LPU. However, the change in the MOE with M_c was not consistent. The MOE of the F-LPUs reached a maximum for F-2 and then decreased as the M_c decreased. The ultimate strength increased while the ultimate strain did not vary consistently with decreasing M_c .

The trend of MOE versus M_c was surprising. The low MOE value for the F-1 network could be due to that network

being close to its T_g at ambient temperature. Thus, the fracture process might be different for the F-1 network compared to the other F-LPUs. The decrease in MOE with a decrease in M_c was opposite to the expected behavior. The observed loss of stiffness with M_c declining can not be completely explained at this time.

The increase in ultimate strength was strongly correlated with M_c . A similar trend had been reported earlier for LPUs (1) in which the strength of the network was seen to increase with a decrease in the hydroxypropyl chain length. However, in the LPUs studied previously, the change in network M_c was related to changes in chemical composition (specifically the lignin content of the network) while for the F-LPUs the change in strength appeared to be related to functionality and M_n . The variation of the F-LPUs strain may be related to the ability to form a uniform network. A relatively high ultimate strain for the F-1 network supported the attribution of a low MOE to a ductile-type failure. Mechanical properties of the F-LPUs varied with the network M_c . The ultimate strength of the networks increased as the M_c decreased.

CONCLUSIONS

A series of HPL polyols could be prepared by fractionation from dilute solution. The molecular weights of the fractions increased as expected from the fractionation procedure. The M_n of the fractions varied between 1,500 and 10,000 Daltons and the dispersity ratio was reduced to 1.6 - 3.3. The chemical composition of the fractions varied slightly with both the aromatic content and the percent hydroxyl, decreasing as the molecular weight increased. The T_g of the fractions varied inversely with molecular weight and the change followed the Fox-Flory relationship.

A series of polyurethane networks (F-LPUs) could be prepared from these HPL fractions. Both the $\tan \delta$ peak temperature and the T_g of the F-LPU increased as the molecular weight of the fraction increased. An increase in the T_g was not due to variation in the chemical composition of the HPLs but was related to the M_n of the fractions. The $\tan \delta$ at one-half peak width and the T_g range both increased with M_n which was indicative of a large number of different molecular motions contributing to the transition.

Swelling studies could be used to characterize the

network properties of the F-LPUs. Both the sol content and the percent swell decreased as the molecular weight of the polyol increased. This trend can be explained by considering the amount of mono- and difunctional molecules in the fractions. Small molecules act as chain ends or chain extenders, and do not contribute to the network as junction points. They would also be less likely to react with an isocyanate group and thus be isolated as part of the sol fraction.

Swelling experiments allowed the M_c of the F-LPUs to be determined. As the molecular weight of the fractions increased, the network M_c decreased. This was related to the average functionality of the polyol. As the functionality of the system increased and the percent of mono- and difunctional molecules decreased, the network M_c decreased.

The difference in T_g between prepolymer and film was attributed to two separable effects. These two effects were related to the T_g of the starting polyol and a crosslinking effect. The first effect ($\Delta_c T_g$) could be modeled with the Fox equation which predicted that an idealized linear HPL-HDI copolymer would have a T_g of between 11 C and 38 C less than the T_g of the original HPL

polyol. The second effect ($\Delta\rho T_g$) showed a large increase in the T_g of the HPL-HDI network due to crosslinking. The T_g increase ranged from 56 C to 70 C depending on the level of crosslinking.

Generally the mechanical properties of LPU's improved as the molecular weight of the HPL increased. At a comparable molecular weight, networks prepared from fractionated HPLs generally possessed better mechanical properties than networks prepared from the non-fractionated HPL.

REFERENCES: CHAPTER 5.

1. S. S. Kelley, Chapters 3 and 4 of this work (1986).
2. T. G. Rials and W. G. Glasser, Holzforschung, 38(4),191 (1984).
3. T. G. Rials and W. G. Glasser, Holzforschung, 38(5),263 (1984).
4. V. P. Saraf, W. G. Glasser, G. L. Wilkes, and J. E. McGrath, J. Appl. Polym. Sci., 30,2203 (1985).
5. V. P. Saraf, W. G. Glasser, and G. L. Wilkes, J. Appl. Polym. Sci., 30,3809 (1985).
6. T. G. Rials and W. G. Glasser, submitted to Holzforschung (1986).
7. V. P. Saraf and W. G. Glasser, J. Appl. Polym. Sci., 29,1831 (1984).
8. K. V. Sarkanen and H. L. Hergert in Chap. 2, Lignins: Occurrence, Formation, Structure and Reactions, K. V. Sarkanen and C. H. Ludwig, eds., Wiley-Interscience, New York, 1971.
9. W. G. Glasser, C. A. Barnett, and Y. Sono, J. Appl. Polym. Sci.: Appl. Polym. Sym., 37,441 (1983).
10. S. Sarkanen, D. C. Teller, J. Hall, and J. L. McCarthy, Macromol., 14,426 (1981)
11. W. Lange, O. Faix, and O. Beinhoff, Holzforschung, 37,63 (1983).
12. A. M. Bialski, J. L. Fong, N. G. Lewis, and C. E. Luthe, Can. J. Chem., in press (1986).
13. S. Yano, M. Rigdahl, P. Kolseth, and A. deRuvo, Svensk Papperstidn., 18,R170 (1984).
14. S. S. Kelley, T. G. Rials, and W.G. Glasser. accepted in J. Mater. Sci. (1986)

15. P. J. Flory, Principles of Polymer Chemistry, Cornell University Press, Ithaca, 1953.
16. P. J. Corish and M. J. Palmer, Advances in Polymer Blends and Reinforcement, Inst. Rubber Ind. Conf., Loughborough (1969).
17. L. C-F. Wu and W. G. Glasser, J. Appl. Polym. Sci., **29**,1111 (1984).
18. W. G. Glasser, L. C-F. Wu, and J-F. Selin, Wood and Adrcultural Residues: Research on Use for Feed, Fuels, and Chemicals, E. J. Soltes, ed., Academic Press, 1983, p. 149.
19. L. H. Tung, Fractionation of Synthetic Polymers, Marcel Dekker, 1977.
20. M. E. Himmel, K. K. Oh, D. W. Sopher, and H. L. Chung, J. Chromatogr., **267**,249 (1984).
21. W. G. Glasser, C. A. Barnett, T. G. Rials, and V. P. Saraf, J. Appl. Polym. Sci., **29**,1815 (1984).
22. J. A. Hyatt, submitted to Holzforschung (1986).
23. T. G. Fox and P. J. Flory, J. Appl. Phys., **21**,581 (1950).
24. H. G. Elias, Macromolecules: Structure and Properties. Vol. I, 2nd ed., Plenum Press, New York (1984).
25. T. G. Fox, Bull Am. Phys. Soc., **2**,1,123 (1956).
26. C. H. Ludwig, B. J. Nist, J. L. McCarthy, J. Amer. Chem. Soc., **86**,1196 (1964).
27. D. B. Johnson, W. E. Moore, and L. C. Zank, Tappi, **44**(11),793 (1961).
28. C. M. Hanson, J. Paint Technol., **39**,505, 104 (1967).
29. W. E. Wolstenholme, Polym. Sci. Eng., **(4)**, 142 (1968).

30. S. Lau, J. Pathak, and B. Wunderlich. Macromol, 15, 1278, (1982)
31. L. C. Chan, H. N. Nae, and J. K. Gillham, J. Appl. Polym. Sci., 29, 3307 (1984).

TABLE 5-1

MOLECULAR, THERMAL, AND CHEMICAL CHARACTERISTICS OF THE
ORIGINAL KRAFT HPL AND FIVE FRACTIONS OF VARYING MOLECULAR WEIGHT

	Original HPL	Fraction				
		<u>1</u>	<u>2</u>	<u>3</u>	<u>4</u>	<u>5</u>
<u>Section A</u>						
Acetone/Hexane	-	5.0	2.5	1.1	0.5	ppt
Weight Percent Soluble (%)	-	12	12	23	24	26
M _n x 10 ³ (VPO)	1.8	1.3	2.1	2.8	-	-
M _n x 10 ³ (GPC)	2.8	1.5	2.3	3.2	8.0	10.0
M _w x 10 ³ (GPC)	25.7	3.0	4.8	5.9	19.4	33.1
DR	9.3	2.0	1.6	1.9	2.4	3.3
S _n x 10 ³	8.0	1.5	2.1	2.9	9.6	15.2
<u>Section B</u>						
T _g (C)	50	-5	24	40	66	86
T _g Range (C)	36	22	28	34	40	39

TABLE 5-1 continued

Section C	Original HPL	Fraction				
		1	2	3	4	5
¹ H-NMR Range (% Total Signal)						
2-3	12	10	13	12	10	7
4-5	40	36	35	41	38	39
6-7	24	26	28	24	28	44
8	24	28	24	23	26	22
UV absorptivity (lit mol ⁻¹ cm ⁻¹)	22.1	20.2	22.6	21.6	20.7	19.4
Total OH (Wt. % by titration)	6.5	6.3	7.1	6.4	6.0	4.7

TABLE 5-2

THERMAL PROPERTIES OF LPUS PREPARED WITH THE ORIGINAL
AND FRACTIONATED HPLs.

Fraction	M _n	DMTA		T _g Range (C)
		Tan δ Peak (C)	1/2 Peak Width (C)	
Original	2,800	90	32	36
1	1,500	48	18	18
2	2,300	70	17	20
3	3,200	94	21	28
4	8,000	108	33	32
5	10,000	126	36	36

TABLE 5-3

NETWORK PROPERTIES OF LPU_s PREPARED WITH THE ORIGINAL
AND FRACTIONATED HPL_s.

<u>Fraction</u>	<u>M_n</u>	<u>Sol Content</u> <u>(%)</u>	<u>Swell</u> <u>(%)</u>	<u>Mc¹</u>
Original	2,800	10.6	286	2,000
1	1,500	17.1	363	2,500
2	2,300	11.5	249	1,400
3	3,200	8.0	173	800
4	8,000	5.9	145	700
5	10,000	3.7	132	400

¹ Calculated from equation 1 in Chapter 4. The chi value was calculated from group contribution theory.

TABLE 5-4

DETERMINATION OF COPOLYMER EFFECT, c_{Tg} , AND CROSSLINKING EFFECT, T_g ,
 IN THE T_g OF LPU PREPARED FROM THE ORIGINAL AND FRACTIONATED HPLs

Fraction	$\frac{\Delta T_{g1}}{(C)}$	$\frac{\Delta c_{Tg2}}{(C)}$	$\frac{\Delta \rho_{Tg3}}{(C)}$
Original	33	27	60
1	45	-11	56
2	40	-20	60
3	41	-22	63
4	36	-30	66
5	34	-35	69
Theoretical ⁴	32	-38	70

¹from experiment, T_g film - T_g polyol

²from Fox equation, Figure 5

³by difference, equation 2 in text

⁴from Fox-Flory plots, equation 1 in text

TABLE 5-5

MECHANICAL PROPERTIES OF LPUs PREPARED FROM THE ORIGINAL
AND FRACTIONATED HPLs

Fraction	<u>Mc</u>	Youngs Modulus (MPa)	Ultimate Strength (MPa)	Ultimate Strain (%)
Original	2,000	1,050	48.7	5.7
1	2,500	1,520	43.5	4.2
2	1,400	2,030	44.5	1.5
3	800	1,550	49.3	1.9
4	700	1,200	56.7	2.6
5 ¹	400	-	-	-

156

¹ Samples were too fragile to be reliably tested.

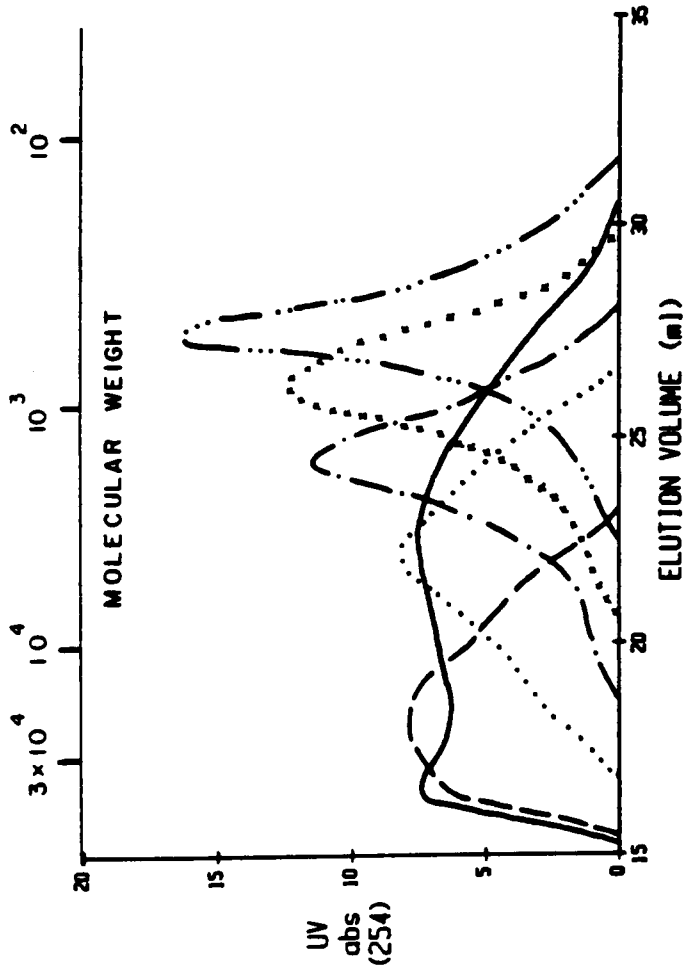


FIGURE 5-1. High pressure gel-permeation chromatograms of the original (—) and fractionated HPLs: fraction 1 (—...), fraction 2 (x x), fraction 3 (—·—·), fraction 4 (·····), and fraction 5 (— — —).

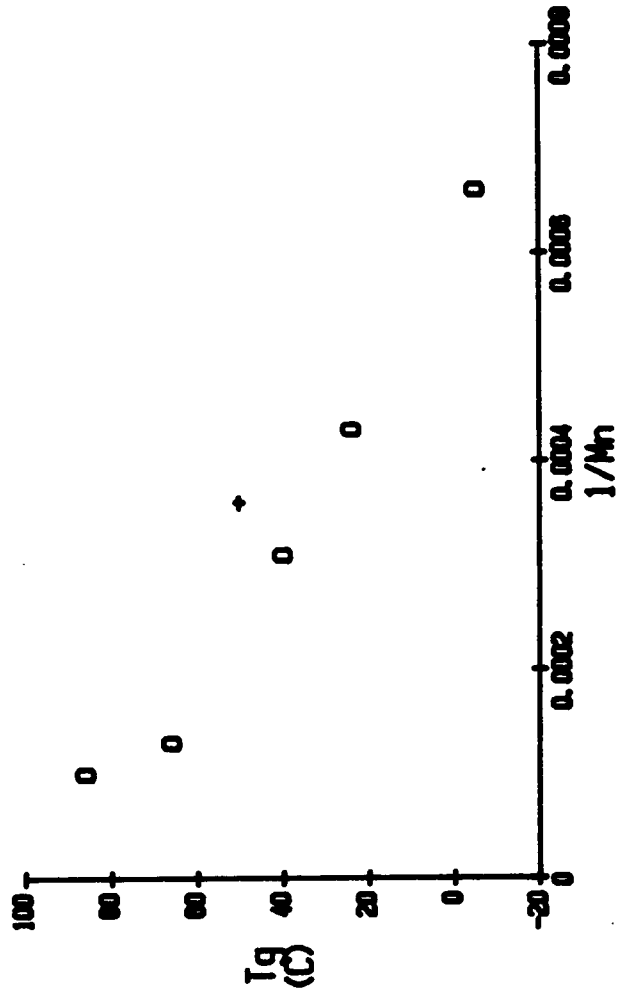


FIGURE 5-2. Plot of the Fox-Flory relationship (equation 1 in text) for the (O) fractionated and (+) original HPLs.

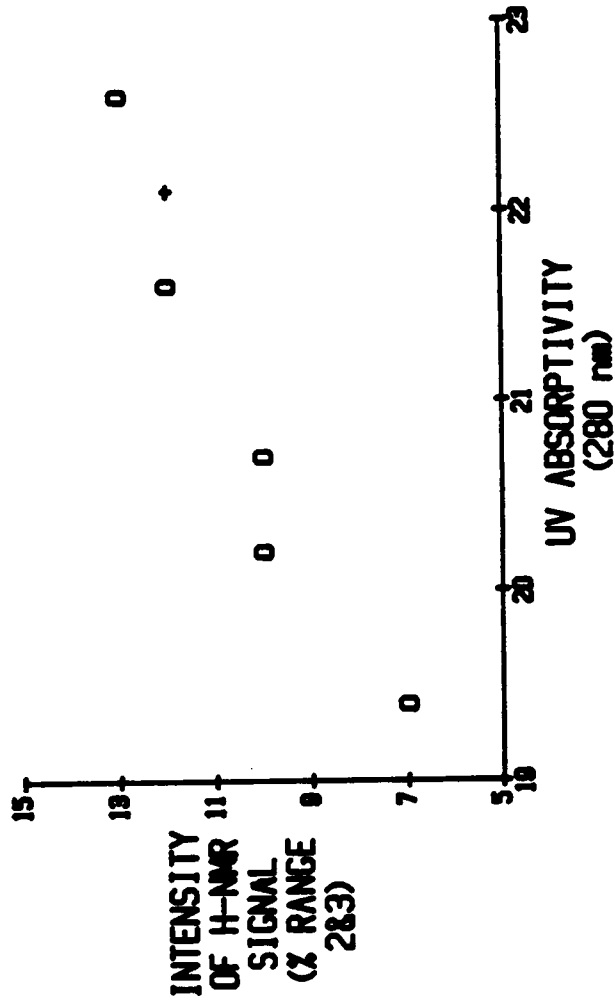


Figure 5-3 Relationship between intensity of aromatic $^1\text{H-NMR}$ signal (Range 2&3) and UV absorbivity (280 nm) for the original (+) and fractionated (O) HPLs.

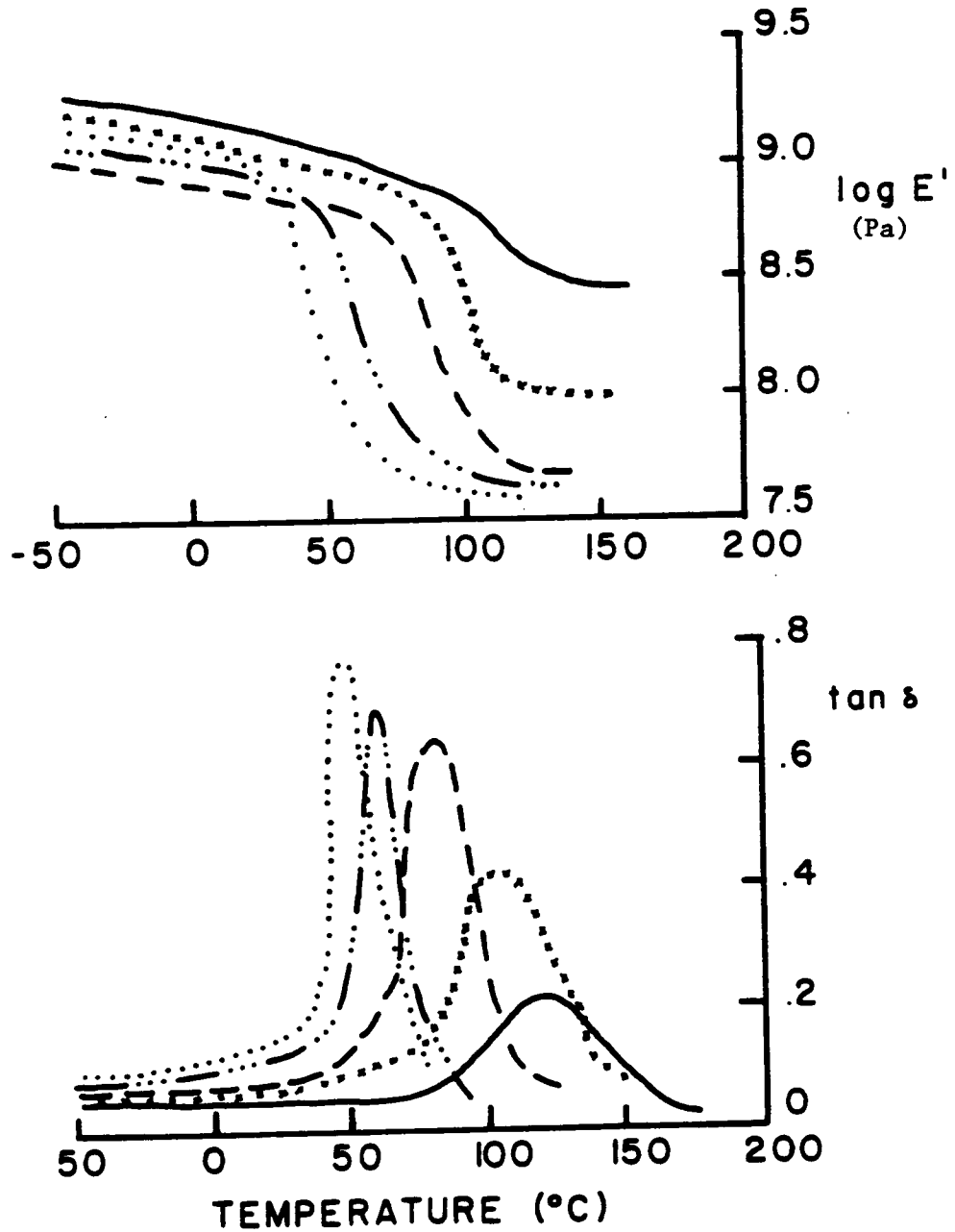


FIGURE 5-4. $\tan \delta$ and $\log E'$ response for LPUs prepared from the fractionated HPLs: fraction 5 (—), fraction 4 (x x), fraction 3 (— —), fraction 2 (— · ·), and fraction 1 (· · · ·).

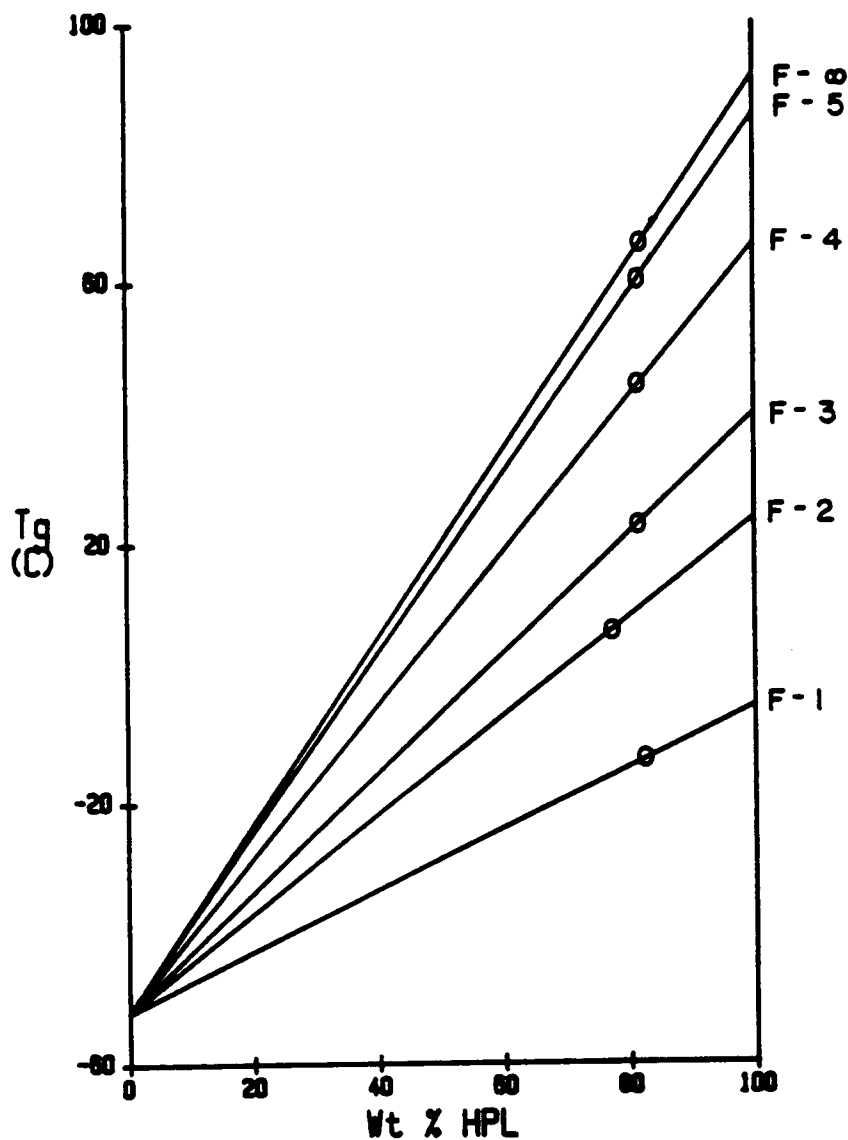


FIGURE 5-5. Fox equation (equation 3 in text) used to determine $\Delta_c T_g$ (O) for the equation of Chan et al.. The T_g s of the fractionated HPLs were determined from DSC while the T_g of polymeric HDI and a very high molecular weight HPL were determined from group contribution theory (reference 28) and the Fox-Flory relationship (equation 1), respectively.

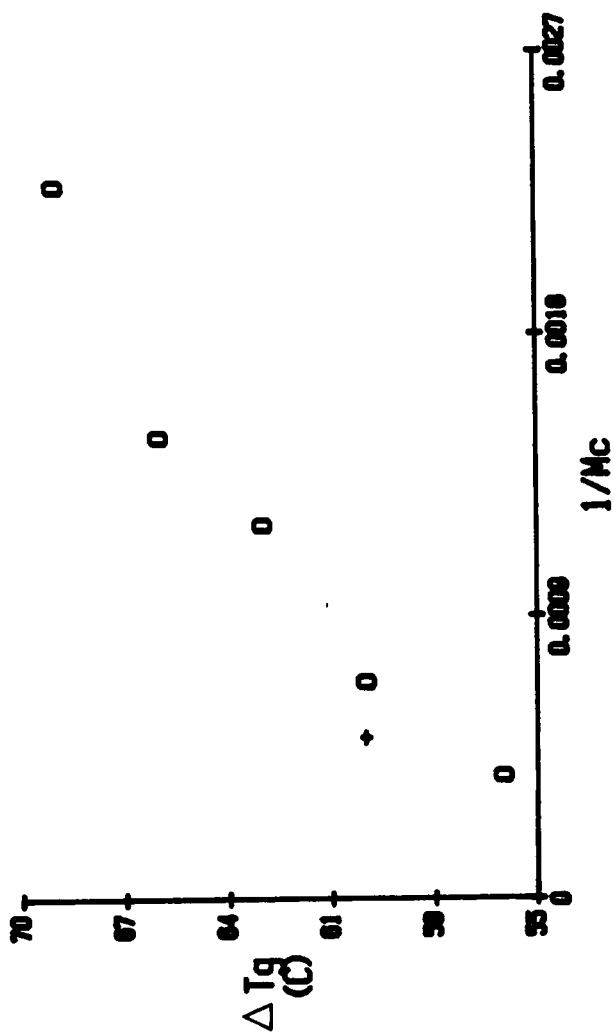


FIGURE 5-6. Effect of the molecular weight between crosslinks (M_c) on ΔT_g of LPUs prepared from fractionated HPLs (O) and the original HPL (X), from equation 9 in Chapter 4.

CHAPTER 6

POLYMER-POLYMER COMPOSITES FROM LIGNIN-BASED POLYURETHANES AND POLYMETHYL METHACRYLATE

SYNOPSIS

Several types of lignin-polyurethane/polymethyl methacrylate (LPU/PMMA) composites were prepared. The composition and the presence of crosslinking were found to influence the thermal and mechanical properties of the composites. All composites were judged to possess two phase structures. The mechanical properties of the interpenetrating polymer networks (IPNs) were heavily dependent on composition and the presence of crosslinks in the LPU. The modulus behavior of the different IPNs could be explained by models which accounted for either dual phase continuity or phase inversion.

INTRODUCTION

Interpenetrating polymer networks (IPNs) constitute a group of materials possessing unique properties which are related to their method of synthesis. At room temperature IPNs typically consist of a flexible elastomer and one or more rigid, high modulus components. By controlling the method of preparation, a synergistic effect may be observed in the new material's properties. These materials have been the subject of several recent reviews (1-3).

Commonly, the nomenclature used for IPNs defines which of the components is crosslinked (1). A full IPN, or simply IPN, is a system where both components, flexible and rigid, are crosslinked. A simultaneous IPN is one where low molecular weight components are mixed and then cured such that both networks form together. A sequential IPN is prepared by polymerizing one component and then swelling this cured component with the second monomer which is then reacted.

Semi-IPNs are materials which contain only one crosslinked component (1). Thus a semi-1-IPN designates a material in which the first component is crosslinked while the second component is linear. Conversely, in a

semi-2-IPN, the first component is linear and the second component is crosslinked. Each of these variations can affect the IPN morphology and, thus, the thermal and mechanical properties (1-3).

One of the most commonly studied IPNs is comprised of a flexible polyurethane as component one and a rigid acrylate as component two (4-8). These systems are typically IPNs or semi-1-IPNs. The material properties of these IPNs have been found to depend on composition, molecular weight between crosslinks (M_c), and acrylate type and composition. Each of these variables can affect the extent of phase separation and, hence, properties.

The factor which affects an IPN's properties to the greatest extent is composition (4-9). As more of a high T_g , high modulus component is included in the IPN, the T_g and/or modulus generally increases. If the differences in the properties of the IPN's two components are large, then the composite is very sensitive to composition.

After composition the most critical variable is the construction of the IPN, semi or full (7,9,10). In either an IPN or semi-1-IPN, crosslinking of the first formed polymer is thought to limit phase separation of the second

polymer. If the first-formed polymer is linear (i.e., semi-2-IPN or blend) the morphology has been found to be irregular and coarse, which can lead to poor mechanical properties. A number of workers (1,9,10) have made several comparisons between blends, semi-IPNs and IPNs prepared from several different polymers. These studies have generally shown a decrease in mechanical properties as the morphology of the system becomes more heterogeneous.

Variation in the network density of the second component of a semi-2-IPN does not have a dramatic impact on properties (11). This could be attributed to phase separation of the first component during cure, which might not be influenced by the unreacted second component.

There are a number of models which have been developed to describe the mechanical behavior of IPNs. Three representative models are the simple logarithmic rule of mixtures (1), the Davies equation (12) and the Budiansky equation (13), equations 1, 2 and 3, respectively:

$$\log E = \phi_1 \log E_1 + \phi_2 \log E_2 \quad (\text{eq. 1})$$

$$E^n = \phi_1 E_1^n + \phi_2 E_2^n \quad (\text{eq. 2})$$

$$\phi_2 = \frac{G_1 - G}{G(G_1 - G_2)} (3/5 G + 2/5 G_2) \quad (\text{eq. 3})$$

where

E_i and G_i are, respectively, the Youngs and shear moduli of the different components, and ϕ_i is the volume fraction of the i^{th} component.

A fit of the IPN experimental data to equation 1 indicates simple additivity of properties with no significant interaction between the two components. Equation 2, with the exponent $n = 1/5$ implies dual phase continuity, or good mixings between the two components (4,13). A decrease in the exponent is an indication of poor mixing. The S-shaped curve which results from equation 3 suggests the presence of phase inversion (4), which has been observed experimentally. Thus a fit of the modulus data to one of these equations may indicate the presence of a distinct morphology.

Recent work with both transmission electron microscopy (14) and small-angle neutron scattering (15) has indicated that "mixing" in IPNs may not take place on a truly molecular level. These studies, on different IPNs, showed

that the dual phase morphology which has been proposed may be more appropriately viewed as an interconnected colloidal structure (15) . Thus, micro-phase separation may occur for some IPNs, even though the mechanical properties of the material indicate both components are making a contribution.

Some research has focused on IPNs where one component was derived from a natural source (17-19). Castor and plant-extracted oils have been used to prepare polyurethanes or polyester elastomers which were then used as the first component in both sequential and simultaneous IPNs. The thermal and mechanical properties were found to vary with composition and method of preparation. As with all IPNs prepared from petroleum-based materials, the thermal and mechanical properties of IPNs prepared from naturally occurring materials varied with the morphology. It is important to note that the properties of the IPNs could be varied in a predictable and controllable manner.

With past success in preparing lignin-based polyurethanes (20,21), and work by others showing the potential of IPNs with a naturally-derived component (17-19), it was desirable to investigate the properties of lignin-based polyurethanes/polymethyl methacrylate

(LPU/PMMA) IPNs. It was anticipated that the LPU/ PMMA IPNs should behave in a fashion similar to other IPNs. Thus, the material properties of the LPU/PMMA IPNs should respond in a predictable manner to changes in composition and network density.

EXPERIMENTAL

Materials

With the exception of the hydroxypropyl lignin polyols (21), all of the IPN components were purchased from commercial sources (Table 6-1).

Prepolymer Preparation-Polymethyl Methacrylate (PMMA): Inhibitor was removed from the methyl methacrylate (MMA) by a wash with 0.1 N. aqueous sodium hydroxide, followed by three rinses with distilled water (5). The MMA was stored over molecular sieves. The ethylene dimethacrylate was used as purchased.

A PMMA oligomeric mixture was prepared in a 250 ml round-bottomed flask equipped with a nitrogen purge, stirrer, reflux condenser and thermometer. The flask was charged with 40 gm of MMA and 0.15 gm of BPO which was

stirred until it dissolved. The reaction was heated to 60 C. under nitrogen for 90 minutes and then quenched in an ice bath. The mixture was stored in a freezer and used within two weeks. The crosslinkable MMA prepolymer was prepared following the same procedure except 39 gm of MMA and 1 gm of ethylene dimethacrylate were used with 0.15 gm of BPO.

Chain-Extended Hydroxypropyl Lignins (CEHPL): The preparation of CEHPLs is described in detail elsewhere (21). Schematically, the CEHPL copolymer can be viewed as an aromatic center with multiple radiating propylene oxide arms. The arms are terminated with a secondary hydroxyl group. The average length of the arms (MS) can be determined by $^1\text{H-NMR}$. The composition of the CEHPLs and the properties of polyurethane networks prepared from them are also detailed elsewhere (21).

Preparation of Polymer-Polymer Composites: The composite composition was calculated on a weight basis. The CEHPL was weighed into a flask and the PMMA oligomer mixture was added. This mixture was stirred until it was completely mixed. The HDI was added with stirring to give an NCO/OH ratio of 1.8 (21). Finally, 3 wt. % based on the NCO component, of (T-9) catalyst was added with rapid

stirring. The mixture was degassed and poured into Teflon molds which were then sealed.

The mixture was held at room temperature for two hours, 55 C for 16 hours, and 105 C for 4 hours. The covers were removed and the IPNs were post-cured at 135 C for two hours. This preparation allowed for the formation of the polyurethane followed by curing of the MMA (5).

The lignin polyurethane (LPU) controls were prepared as described above, but stabilized MMA was used without BPO initiator. The residual MMA was removed at 135 C under vacuum. The crosslinked LPU was prepared with an NCO/OH ratio of 1.8 while the branched LPU had an NCO/OH ratio of 0.66. Pure PMMA samples were prepared using the curing conditions described above. The stoichiometric M_c for the X-PMMA was $1,670 \text{ g M}^{-1}$.

Methods

The thermal and mechanical properties of the IPNs were characterized by Dynamic Mechanical Thermal Analysis (DMTA), Differential Scanning Calorimetry (DSC), and stress/strain testing. These techniques have been previously described in detail elsewhere (21).

RESULTS AND DISCUSSION

An abbreviated nomenclature will be used to identify the type of composite, the composition and presence (or absence) of crosslinking. Thus the different IPNs are designated: simultaneous full-IPNs (IPNs), simultaneous semi-1-IPNs (S-1s), simultaneous semi-2-IPNs (S-2s), and the simultaneous linear blends (Bs). Composition is designated by the lignin-based polyurethane (LPU) content of the IPN. Thus a material with 75% LPU is labeled as .75. The composition and nomenclature of the composites which were studied are shown in Table 6-2.

Variations in Composite Type and Composition

Dynamic Mechanical and Thermal Behavior

The DMTA results for the different composites are presented below: 1) the $\log E'$ and $\tan \delta$ responses for the IPNs are shown in Figure 6-1, 2) the $\log E'$ and $\tan \delta$ responses for the S-1 series are shown in Figures 6-2 and 6-3, respectively, 3) the $\log E'$ and $\tan \delta$ responses for the S-2 series are shown in Figures 6-4 and 6-5, respectively, and 4) the $\log E'$ and $\tan \delta$ responses for

the Bs are shown in Figure 6-6. All of these materials showed some similarities but also some subtle differences.

Common to all of the composites were changes in the magnitude of the $\tan \delta$ peak temperature response with changes in composition. Essentially, as the acrylate content of the materials increased, the magnitude of the high temperature peak increased while the intensity of the low temperature peak decreased. For most of the composites, two separate $\tan \delta$ peaks could be identified, although the peak temperature varied for several of the compositions as will be discussed below.

The $\log E'$ response for the composites also showed several constant trends as the acrylate content varied. As the acrylate content increased, the room temperature $\log E'$ response increased. An increase in the acrylate content also reduced the abruptness of the low temperature $\log E'$ decline.

All of these materials were also analyzed by DSC. This allowed for an independent observation of the Tgs and in some cases resolution of a transition temperature that was not accurately observed by DMTA. Both the DMTA and DSC transition temperatures are shown in Table 6-3. Differences

in the T_g observed by DMTA and DSC are due to heating rate and frequency effects. The T_g s presented in Table 6-3 also highlight some of the subtle differences between the composites.

Shifts in T_g : Analysis of the DMTA $\tan\delta$ behavior focused on the temperature, shape and magnitude of the peaks. The DSC analysis was used to corroborate the changes in the T_g observed with DMTA. Observation of two separate T_g s indicated that the two components (LPU and PMMA) were phase separated. However, the presence of some interaction was indicated by the change in the peak temperature and shape. Significant interaction between a polymer and a second component will cause a shift in the \tan peak temperature (18). If there was no interaction between two polymers, the $\tan\delta$ peak temperatures or T_g s should have been independent of the amount of the second polymer. It was apparent from both techniques (DMTA and DSC) that for all the composites, at all weight fractions, the T_g s of both the LPU and PMMA components were shifted towards one another. This was an indication of at least a limited interaction between the two components.

The shift of the T_g s was typically 10 - 15 C for the IPNs and S-1s while for the S-2s and Bs the shift was 10 -

20 C. With a few exceptions, the shift in the T_g was not strongly dependent on the composition (wt. fraction) or the method of preparation. The most notable exceptions were for the IPN(.5), S-1(.6), and S-1(.5), each of which showed one of the two peaks had broadened and the peak temperature had shifted substantially (see Figures 6-1 and 6-3). For the IPN(.5) and S-1(.5) an extraneous broad peak was seen at a low temperature (ca. 20 C), while for the S-1(.6) the extraneous peak was seen at high temperature (ca. 80 C). The extraneous peaks were only observed in the systems which contained crosslinked LPU. Broadening of $\tan \delta$ or $\log E''$ peaks has been observed previously with conventional polyurethane/PMMA IPNs (22). The behavior was attributed to small fluctuations in composition on a very local scale. Thus each region would undergo a transition temperature which was dependent on the behavior of the nearest neighbors. A second interpretation for $\tan \delta$ peak broadening (9,22) was advanced based on interphase behavior. This idea postulates the presence of an interphase that gives rise to a transition, on a local scale, intermediate between the transition of the two original components.

A convergence of all of the transition peak temperatures implies interaction between the two components

of the composites. Partial or complete miscibility between polymers has been noted for mixtures where each component possesses similar solubility parameters (usually due to a similar chemical composition) or in mixtures with strong secondary interactions (24,25). For the LPU/PMMA system there was potential for strong secondary interactions between the aromatic electrons present in the lignin component of the LPU and the electrons in the PMMA ester side group. This interaction could lead to some mixing of the two IPN components independent of the method of preparation.

Secondary interactions between PMMA and aromatic systems have been previously noted (25,26). In particular, interactions between the ester electrons in PMMA and the aromatic system in polycarbonate (PC) were thought to contribute to limited miscibility between those two polymers (25). The extent of interaction was promoted by the orientation of the aromatic ring which lies in a plane parallel to the polymer backbone. The same circumstances were present in the LPU where the lignin aromatic rings are able to lie in parallel planes.

In another related work (26), partial miscibility was seen for hydroxypropyl lignin (HPL)-PMMA blends. Here the

extent of interaction depended on the characteristics of the solvent from which the blends were cast. Interactions between the HPL and PMMA were noted for compositions up to 40 percent HPL.

Thus, it seemed likely that the nonbonded interactions between the LPU and PMMA had an effect on the dynamic mechanical and thermal properties of the IPNs. It was surprising that the magnitude of the interaction (judged by T_g shifts) was not correlated to composition. Shifts in the T_g also appeared to be relatively independent of the composite type. The slightly larger shifts in the LPU T_g s seen in the S-2 and B materials were attributed to large differences in the T_g s of the original components rather than to differences in the composite type. The observation of an anomalous peak in three composites (IPN(.5), S-1(.6) and S-1(.5)) may be related to further differences in morphology or the presence of an interphase (22,23).

Activation Energies of S-1s: A second indication of interaction between the two components of the IPN may be found in the T_g activation energies (E_a). The E_a values for the transitions in the S-1 series, where they could be reliably determined are shown in Table 6-4. From the data

in Table 6-4 it appeared that the E_a values of the PMMA transition decline as the LPU content of the IPN increased.

If there were no interactions between the LPU and PMMA, the E_a of the PMMA should not depend on the LPU content. The observed substantial decrease in the PMMA E_a could not be related, in a simple manner, to an increase in the free volume of the system since the T_g of the material remains relatively constant over this same composition range. Thus, it appeared that there was some interaction between the components on a molecular level that was responsible for a change in the E_a with a change in composition. However, the gradual change in E_a with composition was reasonable for systems which interact. But the gradual change in E_a with composition conflicts with the relatively constant T_g observed over the same range. This apparent discrepancy has not been resolved at this time.

Log E' Behavior: The log E' response of a composite in which both components (LPU and PMMA) are continuous should not decrease substantially above the LPU T_g and below PMMA T_g . Materials comprised of PMMA domains in an LPU matrix would be expected to exhibit a large decrease in the log E' response above the LPU T_g because discrete glassy PMMA domains would not be able to make a substantial

contribution to the material's mechanical properties. However, if the PMMA formed a continuous supermolecular structure the log E' would remain relatively high, even above the LPU T_g.

The log E' response for the different IPNs varied consistently. In particular the log E' response for the IPNs and S-1s differed from that of the S-2s and blends. The log E' response declined sharply at low temperature (ca. -25 C) for all the composites with an LPU content of 75%. For the IPN(.5), S-1(.6) and S-1(.5), the log E' did not sharply decline at ca. 20 C, the temperature which corresponded to the tan δ peak for the LPU. A complete decline in the log E' response was not observed until the temperature rose above the PMMA T_g. This may be indicative of the presence of a continuous PMMA phase. However, the log E' response of S-2(.6), S-2(.5), and B(.5) showed a large decrease in the log E' at the LPU T_g. The decline in the log E' response was essentially complete immediately above the LPU T_g. It should be noted that the PMMA domains may have been present to act as filler particles in the rubbery LPU, thereby making a small contribution to the dynamic mechanical properties above the LPU T_g.

The log E' response plateaued at temperatures above the

LPU T_g for both the IPN and S-1 and not for the S-2 or B. Both of these behaviors, the presence of a plateau for the IPN(.75) and S-1(.75) and the absence of a distinct low temperature decrease in the IPN(.5), S-1(.6) and S-1(.5) indicate differences in morphology between the IPN and S-1 group and the S-2 and B group.

One of the basic tenets behind the concept of IPNs is that a high level of crosslinking of one polymer will limit phase separation of the second component as it is polymerized. By limiting phase separation the material will possess a more homogeneous morphology which may lead to synergistic behavior (1,27). In some cases, differences in a material's morphology should be reflected to a greater extent by the log E' response rather than the tan behavior. The IPNs and S-1s, with their limited phase separation, may form a more continuous supermolecular network throughout the composite than comparable linear blends. However the branched LPU of the S-2s and Bs might allow for substantial phase separation, and thus form the more common PMMA domain imbedded in an LPU matrix or vice versa, depending on composition. The two types of materials would be expected to have very different log E' behavior above the LPU T_g .

As mentioned before, the major difference between these

log E' responses of these two groups was the presence or absence of crosslinking for the LPU. An Mc value for the LPU was experimentally found to be 770 gm/mol. This value is indicative of a highly crosslinked network which would not allow for a substantial amount of phase separation.

Thus the log E' data supported the concept of a supermolecular PMMA structure which was continuous throughout the IPNs and S-1s, while the log E' behavior of the S-2s and Bs indicated the presence of a rubbery matrix.

Mechanical Properties

Effects of Crosslinking: The MOE, ultimate strength and ultimate strain, for the different LPU-PMMA composites are shown in Table 6-5. The blends were too brittle to allow for sample preparation and testing. The composition of the material affected the mechanical properties of all the LPU-PMMA composites. In general, the MOE and ultimate strength declined while the ultimate strain increased as the LPU content increased. Differences between the MOE of the IPN, S-1 and S-2 at 25 percent and the IPN, S-1 and S-2 at 40 percent were not significant. However, as the LPU content increased to above 50 percent, there were significant differences between the IPN and S-1 group and

the S-2. The IPN and S-1 group, with the crosslinked LPU, provided a higher MOE than the S-2 group with a branched LPU component.

Differences between the various IPNs were also supported by ultimate strength data. The S-2 series, which at high LPU contents may be comprised of a rubbery matrix, produced lower strength values than either the IPNs or S-1s. Even at LPU contents up to 75%, the IPNs and S-1s showed good strength properties while the S-2 were quite weak. This was an indication that for the IPNs with low PMMA contents the high strength PMMA made a greater contribution to the mechanical properties in the IPNs and S-1s than in the S-2s.

The differences in the ultimate mechanical properties were similar to the $\log E'$ response, which reflected variation in the morphology of the IPN and S-1 compared to the S-2. Several models have been developed that predict a material's mechanical properties for different molecular morphologies (1,12,13). For this work the material response used in the models was the Young's modulus (MOE) instead of the $\log E'$. The MOE values were felt to more accurately reflect the material's characteristics and could be easily replicated.

The MOE values predicted from equations 1 - 3 are also shown in Figure 6-5. The MOE values for the IPNs decreased as the amount of high modulus PMMA decreased. Both the IPN and S-1 MOEs followed a similar gradual decline, while the MOE values for the S-2 series showed a sharp drop between 40 and 50 percent PMMA. The trends in the MOE values with the IPNs and S1s behaving in a similar manner and the S-2s behaving differently parallels the log E' response.

Figure 6-5 also shows the predicted MOE based on three different models. Equation 1 (12) was simply the logarithmic rule of mixtures which predicted a MOE value which was the sum of the parts. This model would be appropriate for the behavior of a random copolymer. Equation 2 was the model developed by Davies (12) which predicted a positive interaction between the two components. This model was thought to be appropriate for materials which possess dual phase continuity (4). The Budiansky equation (Eq. 3) (13) was used to model materials which undergo phase inversion.

Through the use of these models, possible differences in the morphology of the LPU/PMMA IPNs may be discussed. The MOE values for both the IPNs and S-1s, within

experimental error, followed the behavior predicted by the Davies equation, while the Budiansky equation provided a good fit for the MOE values of the S-2s. The fit of the experimental data to the models corresponds to predicted differences in morphology based on different methods of synthesis.

Both the IPN and S-1 were prepared with the tightly crosslinked LPU formed first. This could limit phase separation of the PMMA and provide for a morphology with dual phase continuity. The S-2 was prepared with a branched rather than a crosslinked LPU component. Thus, at room temperature the first formed component, the rubbery LPU, retained molecular mobility which could allow for phase separation during the polymerization of the PMMA. These differences were seen qualitatively in the log E' and ultimate strength response of the IPNs. The dual phase continuity of the IPNs and S-1s allowed the stronger PMMA to support the rubbery LPU, while in the S-2s the continuous LPU matrix was not substantially reinforced by PMMA domains.

CONCLUSIONS

LPU/PMMA composites may be prepared by several different reaction sequences. The polymerization sequence and presence or absence of crosslinking allowed for the preparation of IPNs, semi-1-IPNs, semi-2-IPNs and blends over a range of compositions. The dynamic mechanical, thermal and mechanical properties of these materials were found to vary with composition.

Dynamic mechanical and thermal analysis showed a separate T_g for both the LPU and PMMA. These T_g s were shifted towards one another, away from the T_g of the pure components. This modification in the T_g , which did not appear to be directly related to the material's composition, indicated partial interaction between the two components. Previous work with similar systems has noted the possibility of secondary interactions between the aromatic system and $n-\pi$ electrons in the PMMA side chain. A substantial broadening of the $\tan \delta$ response indicated some mixing for systems where the LPU was crosslinked (IPN and S-1) and comprised 50 - 60% of the material. The $\log E'$ response also appeared to depend on the presence of crosslinks in the LPU. These differences in the $\log E'$ response were substantiated by tensile tests.

Both the MOE and ultimate strength increased while the ultimate strain decreased as the PMMA content increased. The mechanical properties were also affected by the presence or absence of crosslinking in either component. In particular, the MOE values for both the IPNs and S-1s were greater than expected from a simple logarithmic rule of mixtures. The MOE values for both the IPNs and S-1s followed the behavior predicted by the model developed by Davies. This model is thought to be appropriate for materials which possess dual phase continuity. The MOE values for the S-2s follow behavior predicted by a model developed by Budiansky. This model is appropriate for material which undergoes phase inversion. Thus it was concluded that the presence of crosslinking in the IPN and S-1 allowed each component to form continuous structures throughout the material.

REFERENCES: CHAPTER 6.

1. L. H. Sperling, Interpenetrating Polymer Networks and Related Materials, Plenum, New York, 1981.
2. H. L. Frisch, K. C. Frisch, and D. Klemperer, Pure Appl. Chem., **53**,1557 (1981).
3. Y. S. Lipatov and L. M. Sergeeva, Interpenetrating Polymeric Networks, Naukova Dumka, Kiev, 1979.
4. G. Allen, M. J. Bowden, S. M. Todd, D. J. Blundell, G. M. Jeffs, and W. E. A. Davies, Polymer, **15**,28 (1974).
5. E. F. Cassidy, H. X. Xiao, K. C. Frisch, and H. L. Frisch, J. Polym. Sci.: Polymer Chem. Ed., **22**,2667 (1984).
6. L. Hermant and G. C. Meyer, Eur. Polym. J., **20**(1),85 (1984).
7. D. J. Hourston and Y. Zia, J. Appl. Polym. Sci., **29**,2951 (1984).
8. J. H. Lee and S. C. Kim, Polym J., **16**(6),453 (1984).
9. Y. S. Lipatov, T. S. Chramova, L. M. Sergeeva, and L. V. Karabonova, J. Polym. Sci.: Polym. Chem. Ed., **15**,427 (1977).
10. S. C. Kim, D. Klemperer, K. C. Frisch, and H. L. Frisch, Macromol., **9**,263 (1976).
11. D. J. Hourston and J. A. McCluskey, J. Appl. Polym. Sci. **31**,645 (1986).
12. W. E. A. Davies, J. Phys. D: Appl. Phys., **4**,318 (1971).
13. B. J. Budiansky, Mech. Phys. Solids, **13**,223 (1965).
14. J. M. Widmaier and L. H. Sperling, Macromol., **15**.625 (1982).

15. L. H. Sperling, A. Klein, A. M. Fernandez, and M. A. Linne, Am. Chem. Soc., Div. Polym. Chem. Polym. Prepr., **24**,386. (1983).
16. L. H. Sperling and J. A. Manson, J. Am. Oil Chem. Soc., **60**(11),1887 (1983).
17. M. A. Linne, L. H. Sperling, A. M. Fernandez, S. Qureshi, and J. A. Manson, in Rubber Modified Thermoset Resins, C. K. Riew and J. K. Gillham, eds., ACS Advances in Chemistry Series, No. 208, American Chemical Society, Washington, D.C., p. 37 (1984).
18. V. Huelck, D. A. Thomas, and L. H. Sperling, Macromol., **5**,340 (1972).
19. M. Patel, R. Patel, and B. Suthar, Die Macromolke. Chem., **187**(3),525 (1986).
20. W. G. Glasser, C. A. Barnett, T. G. Rials, and V. P. Saraf, J. Appl. Polym. Sci., **29**,1815 (1984).
21. S. S. Kelley, Chapters 3, 4, and 5 of this work. (1987)
22. Y. S. Lipatov, L. M. Sergeeva, L. V. Karabonova, A. Y. Nesterov and T. D. Ignatova, Vysokomol. Soved., **A18**(5),1025 (1976).
23. O. Blabisi, L. M. Robeson, and M. T. Shaw, Polymer-Polymer Miscibility, Academic Press, New York, 1979.
24. T. K. Kwei, J. Poly. Sci.: Polym. Let., **22**,307 (1984).
25. Z. G. Gardlund, in Polymer Blends and Composites in Multiphase Systems, C. D. Hon, ed., ACS Advances in Chemistry Series No. 206, American Chemical Society, Washington, D.C., p. 129 (1984).
26. S. L. F. Ciemniecki, M. S. thesis, Virginia Tech. (1986).
27. G. P. Belonoskaya, J. D. Chernova, L. A. Korotneva, L. S. Andrianova, B. A. Dolgoplosk, S. K. Zakharov, Y. N. Lazanov, K. K. Kalninsh, L. M. Kaljuzhnaya, and M. F. Lebedeva, Eur. Polym. J., **12**,817 (1976).

28. L. C. Chan, H. N. Nae, and J. K. Gillham, J. Appl. Polym. Sci., 29,3307 (1984).
25. V. P. Saraf and W. G. Glasser, J. Appl. Polym. Sci., 29,1831 (1984).

TABLE 6-1

SOURCES OF VARIOUS CHEMICALS USED IN PREPARATION OF LPU/PMMA COMPOSITES

<u>Material</u>	<u>Description</u>	<u>Supplier</u>
MMA	Methyl methacrylate	Aldrich Chemical Co.
EDMA	Ethylene Dimethacrylate	Polysciences, Inc.
HDI	Hexamethylene Diisocyanate	Eastman Kodak Co.
T-12	Dibutyltin Dilaurate	Pfalz and Bauer
BPO	Benzyl Peroxide	Aldrich Chemical Co.
CEHPL	Chain-extended Hydroxypropyl Lignin	See text

TABLE 6-2

NOMENCLATURE AND COMPOSITION OF LPU/PMMA COMPOSITES

<u>Composite Type</u>	<u>Code</u>	<u>MS of¹ CEHPL</u>	<u>Weight Frac.² LPU (%)</u>	<u>Lignin³ Content (%)</u>
Simultaneous IPNs: Lignin polyurethane crosslinked, poly- methyl methacrylate crosslinked	IPN(1.0)	4.5	100	30
	IPN(.75)	4.5	75	22.5
	IPN(.5)	4.5	50	15
	IPN(.25)	4.5	25	7.5
	IPN(0)	-	0	0
Semi-1-IPN: Lignin polyurethane crosslinked, poly- methyl methacrylate linear	S-1(1.0)	4.5	100	30
	S-1(.75)	4.5	75	22.5
	S-1(.6)	4.5	60	18
	S-1(.5)	4.5	50	15
	S-1(.4)	4.5	40	12
	S-1(.25)	4.5	25	7.5
	S-1(0)	-	0	0
	S-1(0)	-	0	0
Semi-2-IPN: Lignin polyurethane branched, poly- methyl methacrylate crosslinked	S-2(1.0)	4.5	100	30
	S-2(.75)	4.5	75	22.5
	S-2(.6)	4.5	60	18
	S-2(.5)	4.5	50	15
	S-2(.4)	4.5	40	12
	S-2(.25)	4.5	25	7.5
	S-2(0)	-	0	0
	S-2(0)	-	0	0

TABLE 6-2 continued

<u>Composite Type</u>	<u>Code</u>	MS of ¹ <u>CEHPL</u>	Weight Frac. ² <u>LPU (%)</u>	Lignin ³ <u>Content (%)</u>
Blend: Lignin	B-(1.0)	4.5	100	30
polyurethane	B-(.75)	4.5	75	22.5
branched, polymethyl	B-(.5)	4.5	50	15
methacrylate linear	B-(.25)	4.5	25	7.5
	B-(0)	-	0	0

¹Molar substitution of propylene oxide on lignin
²Weight fraction of LPU in composites
³Lignin content of composite

TABLE 6-3
 DYNAMIC MECHANICAL AND THERMAL PROPERTIES OF IPNs, S-1s, and S-2s.

Composite Type	LPU/PMMA	DMTA		DSC	
		Tan δ	Peak Temp. (C)	LPU	PMMA
IPN(1.0)	1.0	-37	-	-41	-
IPN(.75)	.75	-18	NR	-30	NR
IPN(.5)	.5	22	108	19	100
IPN(.25)	.25	-23	110	-26	104
IPN(0)	0.0	-	126	-	118
S-1(1.0)	1.0	-37	-	-41	-
S-1(.75)	.75	-22	112	-34	NR
S-1(.6)	.6	-24	88	-30	84
S-1(.5)	.5	21	109	10	100
S-1(.4)	.4	NR ¹	105	-20	101
S-1(.25)	.25	NR	110	-18	104
S-1(0)	0.0	-	116	-	108
S-2(1.0)	1.0	-	-	-59	-
S-2(.75)	.75	-31	NR	-39	NR
S-2(.6)	.6	-28	NR	-34	NR
S-2(.5)	.5	-26	96	-32	91
S-2(.4)	.4	NR	110	-25	101
S-2(.25)	.25	NR	108	NR	100
S-2(0)	0.0	-	126	-	118

TABLE 6-3 continued

Composite Type	LPU/PMMA	DMTA		DSC	
		Tan δ LPU	Peak Temp. (C) PMMA	Tg (C) LPU	PMMA
B(1.0)	1.0	-	-	-59	-
B(.75)	.75	-34	NR	-47	NR
B(.5)	.5	-28	91	-40	86
B(.25)	.25	NR	102	NR	99
B(0)	0.0	-	116	-	108

1 Transition could not be resolved.

TABLE 6-4

EFFECT OF S-1 COMPOSITION ON THE ACTIVATION ENERGY (E_a)
OF THE GLASS TRANSITION (T_g)

Composite Type	LPU (%) ¹	$T_g(C)$	$\frac{LPU}{E_a}$ (kJ/mol)	$T_g(C)$	$\frac{PMMA}{E_a}$ (kJ/mol)
S-1(1.0)	1.0	-37	196	-	-
S-1(.75)	0.75	-22	218	112	183
S-1(.6)	0.60	-24	NR ²	88	203
S-1(.5)	0.50	21	NR	109	224
S-1(.4)	0.40	NR	-	105	253
S-1(.25)	0.25	NR	-	110	276
S-1(0)	0.0	-	-	116	308

¹ Weight content of LPU in composite.

² Not Resolved.

TABLE 6-5
EFFECT OF COMPOSITION ON THE MECHANICAL PROPERTIES OF
IPNs, S-1s, AND S-2s¹.

<u>Composite Type</u>	<u>LPU/PMMA</u>	<u>Youngs Modulus (MPa)</u>	<u>Ultimate Strength (MPa)</u>	<u>Ultimate Strain (%)</u>
IPN(1.0)	1.0	8	3.8	34.9
IPN(.75)	.75	80	11.3	33.9
IPN(.5)	.5	500	16.6	28.4
IPN(.25)	.25	1,740	33.5	6.2
IPN(0)	0.0	3,200	35.0	2.4
S-1(1.0)	1.0	8	3.8	34.9
S-1(.75)	.75	80	10.5	29.9
S-1(.6)	.6	150	14.9	30.0
S-1(.5)	.5	490	23.5	22.8
S-1(.4)	.4	600	29.4	21.1
S-1(.25)	.25	1,630	38.0	17.7
S-1(0)	0.0	2,840	36.2	4.2

TABLE 6-5 continued
 EFFECT OF COMPOSITION ON THE MECHANICAL PROPERTIES OF
 IPNs, S-1s, AND S-2s¹.

<u>Composite Type</u>	<u>LPU/PMMA</u>	<u>Youngs Modulus (MPa)</u>	<u>Ultimate Strength (MPa)</u>	<u>Ultimate Strain (%)</u>
S-2(1.0)	1.0	-	-	-
S-2(.75)	.75	5	1.2	31.2
S-2(.6)	.6	17	4.8	24.0
S-2(.5)	.5	80	8.3	25.1
S-2(.4)	.4	550	24.1	20.3
S-2(.25)	.25	1,840	37.0	16.8
S-2(0)	0.0	3,200	35.0	2.4

¹ The Blends were too brittle to allow for testing.

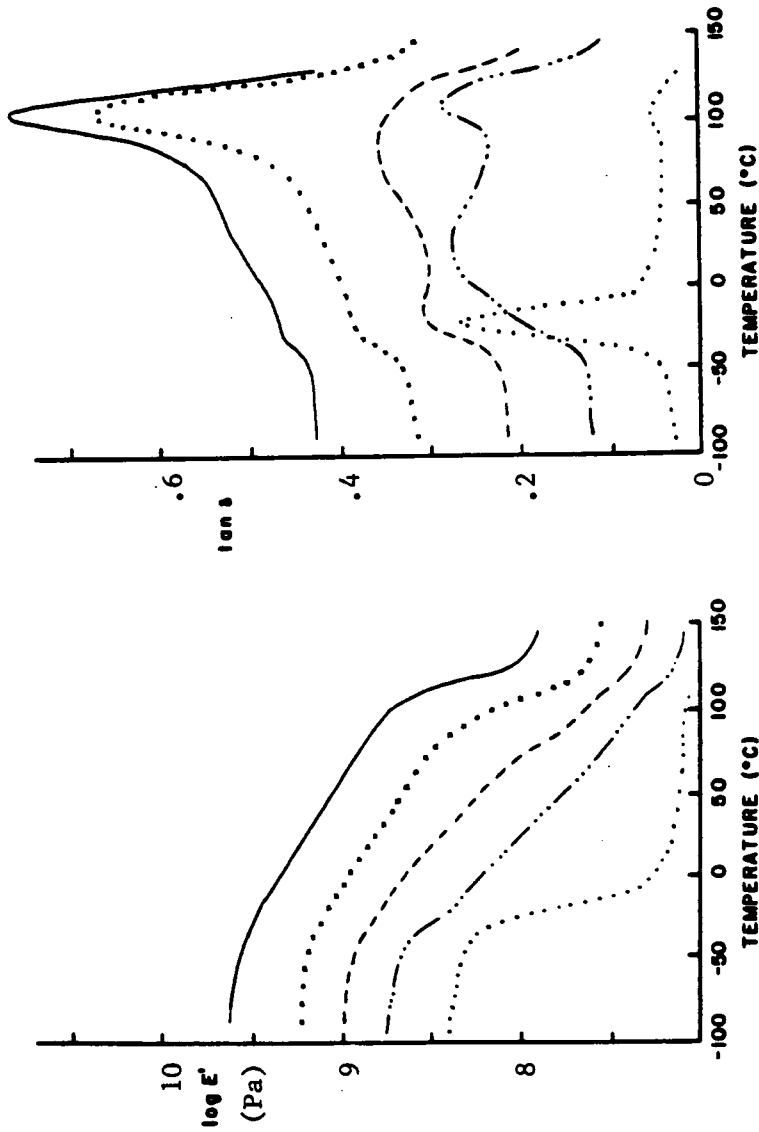


FIGURE 6-1. Dynamic mechanical properties of S-1s with varying LPU/PMMA compositions: (.....) S-1(.75), (---) S-1(.6), (—) S-1(.5), (X X) S-1(.4), and (—) S-1(.25). The T_g of the LPU was -37°C and the T_g of the PMMA was 116°C .

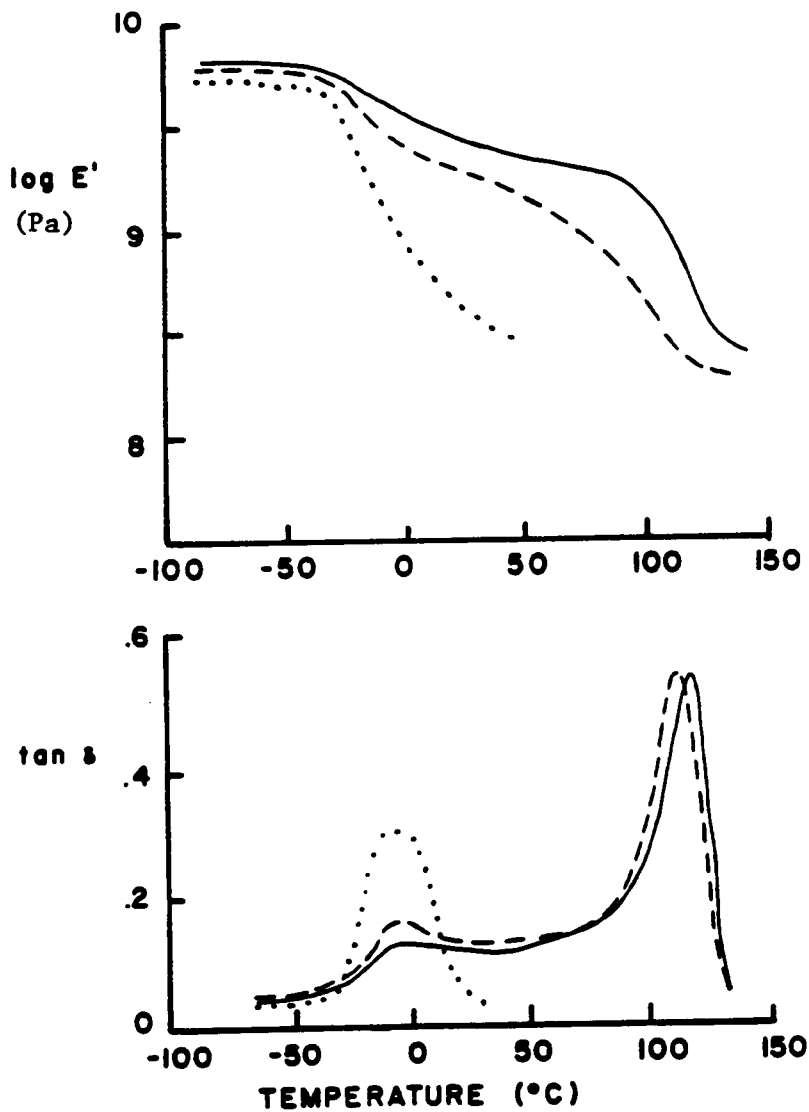


FIGURE 6-2. Dynamic mechanical properties of IPNs with varying LPU/PMMA compositions: (.....) IPN(.75), (— —) IPN(.5), and (——) IPN(.25). The T_g of the LPU was -37 C and the T_g of the PMMA was 126 C.

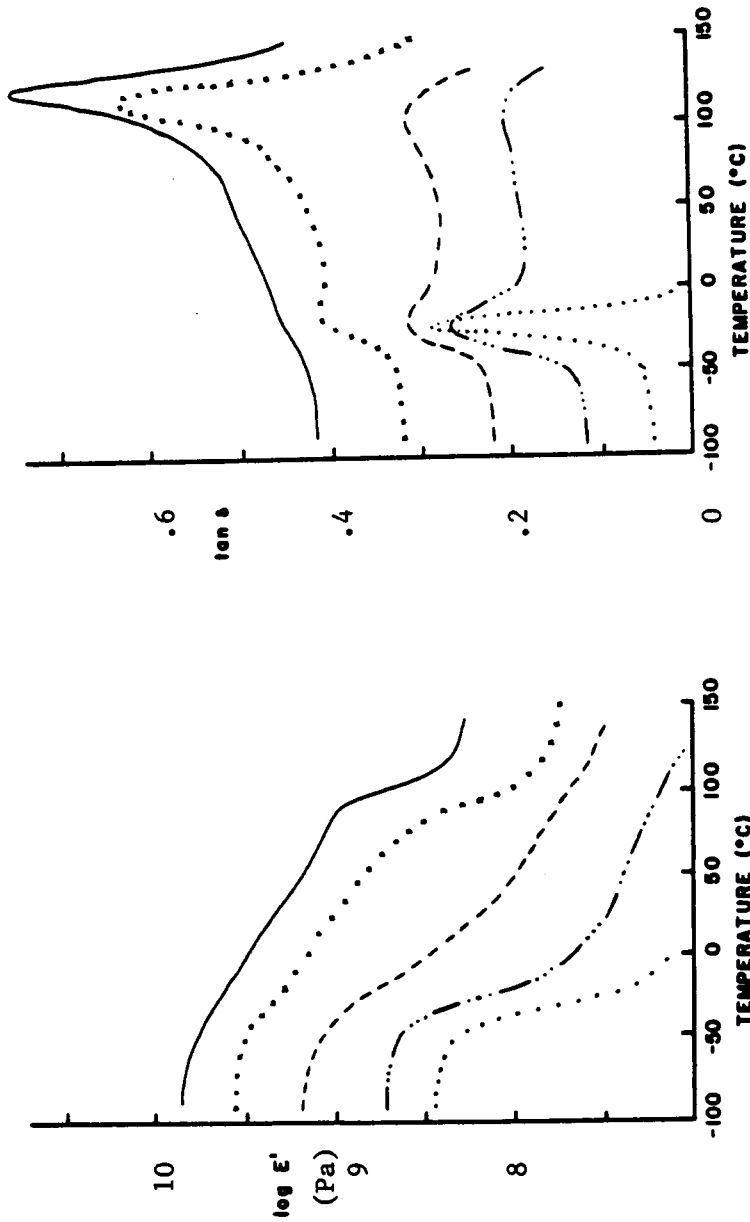


FIGURE 6-3. Dynamic mechanical properties of S-2s with varying LPU/PMMA compositions: (.....) S-2(.75), (—) S-2(.6), (---) S-2(.5), (X X) S-2(.4), and (— · —) S-2(.25). The T_g of the LPU was ca. -52 C and the T_g of the PMMA was 126 C.

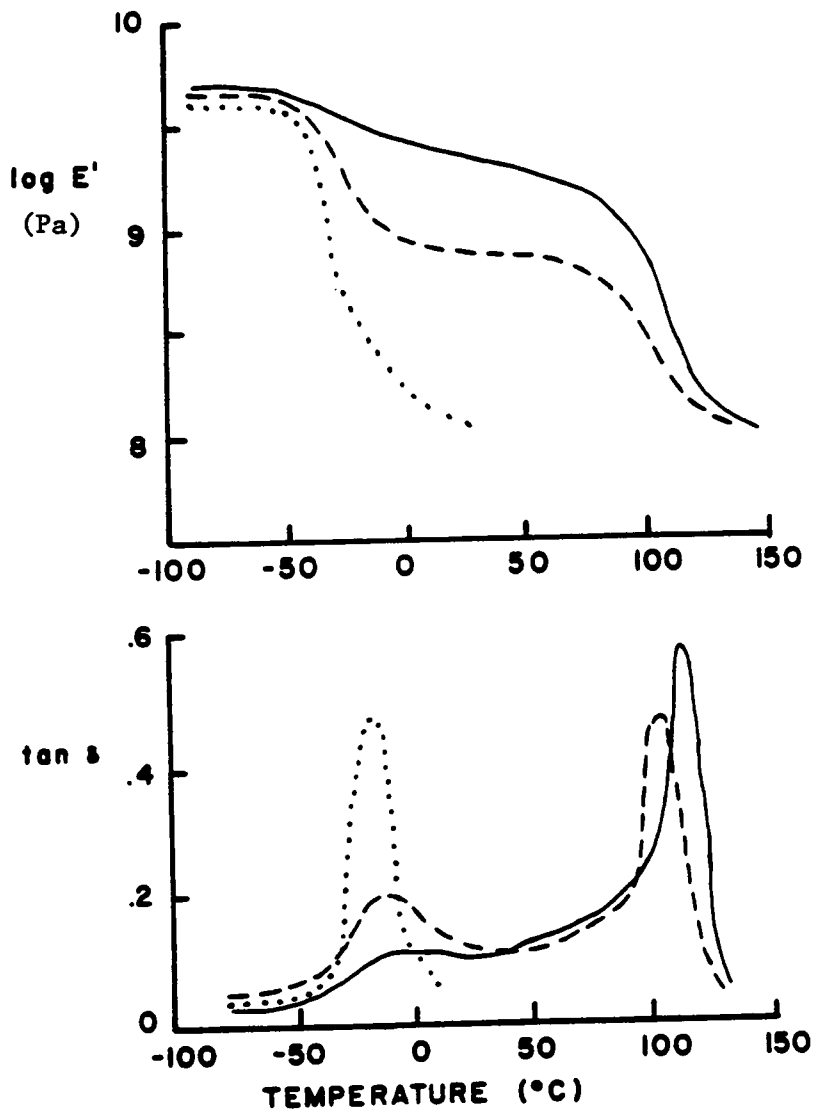


FIGURE 6-4. Dynamic mechanical properties of Blends with varying LPU/PMMA compositions: (· · · ·) B(.75), (— —) B(.5), and (——) B(.25). The T_g of the LPU was ca. -52 C and the T_g of the PMMA was 116 C.

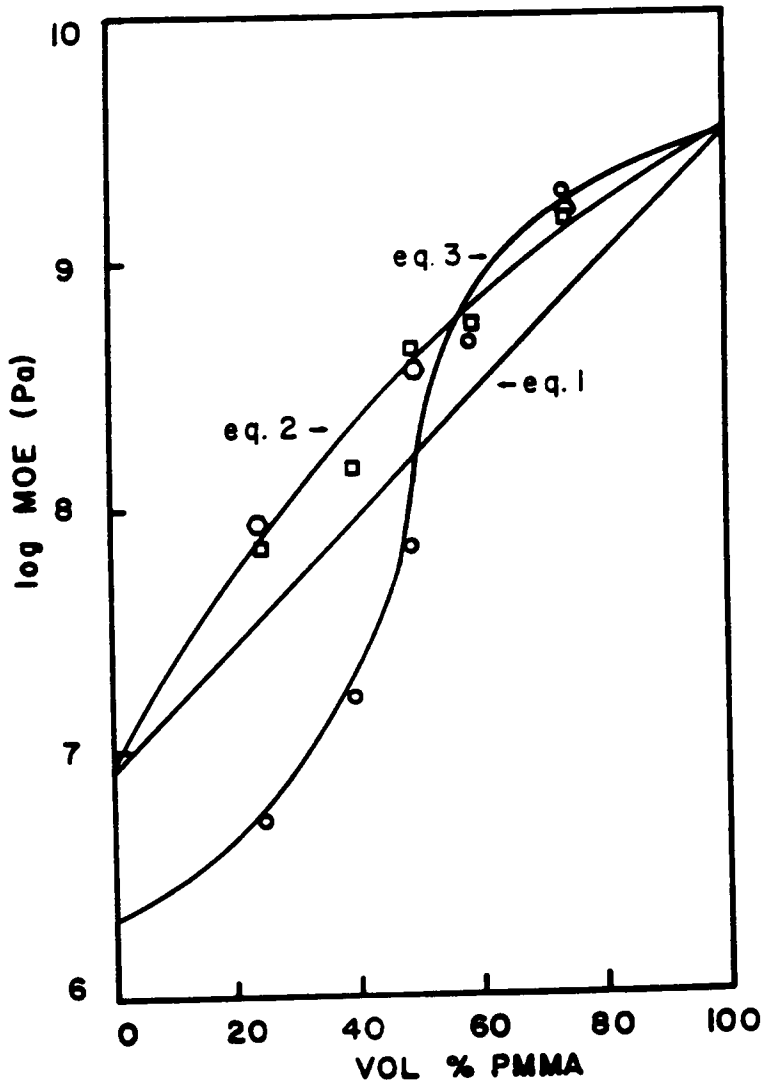


FIGURE 6-5. Effect of composition and IPN type of the Young's modulus (MOE): (○) IPNs, (□) S-1s, and (○) S-2s. The lines represent equations 1-3 in the text. These equations are the logarithmic rule of mixtures (eq. 1, ref.12) the equation of Davies with $n=1/5$ (eq. 2, ref.12) and the equation of Budiansky (eq.3, ref.13).

CHAPTER 7

EFFECT OF LIGNIN CONTENT ON THE PROPERTIES OF INTERPENETRATING POLYMER NETWORKS

SYNOPSIS

A series of lignin-based polyurethane/polymethylmethacrylate (LPU/PMMA) interpenetrating polymer networks (IPNs) were prepared. While the LPU/PMMA ratio remained constant (1:1), the properties of the LPU were controlled by varying the composition of the lignin polyol. The lignin polyol may be viewed as a lignin star with radial hydroxypropyl arms. The composition of the lignin polyol was varied by varying the length of the hydroxypropyl arms. An increase in the lignin content of the polyol resulted in a decrease in the molecular weight between crosslinks (M_c) and an increase in secondary interactions between the LPU and PMMA. These two effects resulted in single phase materials when the lignin content of the composite rose above 25 weight percent. As the lignin content increased, the strength properties of the IPNs increased. The dynamic mechanical, thermal, and ultimate mechanical properties of the entire series of IPNs could be explained by the presence of dual phase continuity.

INTRODUCTION

Polymerization of two or more polymers in the presence of one another allows for the preparation of interpenetrating polymer networks (1-7). Typically one of the polymeric components is an elastomer, though both may be rigid materials. Under favorable circumstances the preparation of an IPN allows for a synergistic interaction between the polymer components (1-3).

A number of factors have been found to influence the properties of IPNs. These factors include the type and concentration of the components, the presence or absence of crosslinking, and the homogeneity of the IPN. The effects of composition and crosslinking have been investigated for LPU/PMMA IPNs (8). Both the chemical nature of the components and the extent of crosslinking can influence the apparent homogeneity of the system. Typically, the most homogeneous IPNs provide the best mechanical properties.

The homogeneity of semi-1 and IPNs may also be influenced by the molecular weight between crosslinks (M_c) of the first-formed component (1,9). As M_c of component one decreased, the mobility of the chains, usually an

elastomer, decreased, which can limit the amount of phase separation or the size of domains. In one study (9), two transitions were observed when the polyurethane was lightly crosslinked. This was taken as an indication of a two phase system. As the crosslink density increased, a single $\tan \delta$ peak was observed in the dynamic mechanical response, an indication of a homogeneous system. The $\tan \delta$ one-half peak width also increased as the crosslink density increased, which was taken as an indication of increased mixing. This trend was also confirmed qualitatively with transmission electron microscopy. The M_c of the second-formed component was not found to have a substantial effect on the IPN properties (10).

The extent of mixing of IPNs can also be varied by changes in the composition of one of the two components (5,7,10). Several studies have investigated the properties of three-component IPNs. The solubility parameter of the rigid component was varied by modifying the composition. Depending on the method of preparation, the miscibility of these materials, as measured by dynamic mechanical analysis, could be enhanced or reduced. One particular system (7) showed three broad peaks in the $\tan \delta$ curve, each of which could be assigned to one of the three components present. In the present study, the composition of the

lignin-based copolymer has been varied to allow for changes in the solubility parameter of the elastomer.

Secondary interactions may influence the miscibility of polymer blends (11,13). It is also reasonable that secondary interactions could influence the miscibility of IPNs. Studies (14,15) have investigated the effects of ionic interactions or hydrogen bonding on the properties of IPNs. Various polar groups or specific interactions were introduced into the IPN to improve miscibility.

Previous studies have also suggested the presence of secondary interactions between the carbonyl side group in PMMA and aromatic electrons of a second polymer (16,17). This apparent interaction was reflected in a change of the glass transition temperature (T_g) of the components with changes in composition.

Previous work has shown that lignin-based polyurethanes (LPUs) could be used as one component of an IPN (8). The properties of the IPNs varied in a consistent manner with composition and the type of IPN. In this study the effects of the LPU composition and the M_c of the LPU were investigated. Specifically, at a constant LPU/PMMA composition, the effects of lignin content on the dynamic

mechanical, thermal, and mechanical properties of IPNs were investigated.

EXPERIMENTAL

Materials

The sources and preparation of the IPN components were discussed in detail previously (8). The various lignin polyols have been characterized in detail (17). In the current study, the IPNs were prepared so that both components LPU and PMMA were crosslinked. The composition of the various IPNs are listed in Table 7-1.

Methods

The dynamic mechanical, thermal, and ultimate mechanical properties of the IPNs were determined using standard techniques described elsewhere (18).

RESULTS AND DISCUSSION

Dynamic Mechanical and Thermal Properties

Changes in the composition of one component of an IPN have previously been shown to influence the material properties (5,8,11). The chain-extended hydroxypropyl lignin (CEHPL) polyol may be viewed as a highly aromatic center with radiating polypropylene oxide arms. The arms contain a terminal hydroxyl group which was reacted with hexamethylene diisocyanate (HDI) to form the LPU. The average number of hydroxypropyl chains in a radiating arm was termed the molar substitution (MS). Variations in the MS has a significant effect on the properties of the resulting LPU (18), which may in turn influence the properties of the IPN. A decrease in MS raised T_g , increased modulus and reduced M_c of LPUs (18). A decrease in MS also corresponds to an increase in the lignin content and thus an increase in the aromatic content of the LPU. This increase in the LPU aromatic content may affect the extent of interaction between the two components of the IPN (18).

Effects of LPU Composition: A series of IPNs, with 50% LPU, was prepared with lignin contents between 13 and

28%. (The number following the IPN designation refers to the lignin content in the LPU.) The dynamic mechanical responses for the two extremes and two intermediate materials are shown in Figure 7-1. Two $\tan \delta$ peaks were noted previously for IPN-15 (8) and were seen for IPN-13. As the lignin content increased (IPN-13 through IPN-28), the two $\tan \delta$ peaks merged into a single broad peak centered about 76 C. The merger of the two peaks indicated the presence of a single phase material. The $\log E'$ (Figure 7-1) also reflected the changes seen in the $\tan \delta$ behavior. As the lignin content of the LPUs increased, the $\log E'$ response progressed from two separate declines on heating, to a gradual broad decrease, to a single sharp decrease. The $\tan \delta$ peak temperatures and the DSC T_g values are shown in Table 7-2.

Both the $\tan \delta$ peak temperatures and the T_g values merged as the lignin content of the IPNs increased. This trend is shown in Figure 7-2 for the $\tan \delta$ peak temperatures. The increase in the T_g of LPU with increasing lignin or aromatic content has been observed in several polyurethane systems (18,19). The rigid aromatic group provides for more stiffness in the polymer, increasing the material's T_g . However, the observed increase in the LPU T_g may also be due to secondary

interactions between the LPU and high T_g PMMA. Secondary interactions between aromatic polymers and PMMA have been attributed to electronic effects between the aromatic electrons of the LPU and $n-\pi$ electrons in the PMMA side chain (16). Both the increased lignin content and the potential interaction would be expected to raise the T_g of the LPU. To separate these effects, one may note changes in the PMMA T_g which should be due solely to secondary interactions.

In the absence of any interaction between the LPU and PMMA, the PMMA $\tan \delta$ peak temperature should not deviate from 116 C. However, as seen in Figure 7-2, the PMMA $\tan \delta$ peak temperature steadily declined from 116 C. The steady decline in the PMMA T_g may be attributed to increased interaction between the PMMA and the low T_g LPU. The increase in the T_g of IPN-28 compared to that of IPN-25 was due to an increase in the T_g of the LPU. With the presence of a single T_g , an increase in the T_g of the LPU from IPN-25 to IPN-28 resulted in an increase in the T_g of the IPN.

It appeared that the extent of interaction between the low T_g LPU and high T_g PMMA increased as the aromatic content of the LPU increased, thus reducing the T_g of the

PMMA. While a similar change in the T_g of PMMA has been observed in other systems with an aromatic component (16), this reduction could also be due to a decrease in the molecular weight of the PMMA. One might speculate that as the M_c of LPU decreased, LPU mobility was limited which in turn could limit the mobility of the reacting PMMA chain ends. However, it should be noted that the polymerization of the PMMA was carried out at elevated temperatures, thus all of the LPUs were in the rubbery state while the PMMA was polymerized.

Thus, it appeared in these IPNs the convergence of the LPU's T_g was due to a combination of two effects. First, the LPU T_g increased due to an increase in the lignin content of the network. Secondly the T_g of the LPU increased while the T_g of the PMMA decreased due to interactions between the LPU and the PMMA.

Effect of M_c : The extent of secondary interactions may also be affected by the M_c of the LPU (9,20). This conclusion was based on the T_g of PMMA of IPN-28 compared to that of IPN(.75) shown in a previous study (8). Both of these materials contained a comparable quantity of lignin (28% for IPN-28 vs. 30% for IPN(.75)). But the IPN(.75) still exhibited two T_g s while the IPN-28 as a system showed

a single intermediate T_g . The M_c of the LPU in IPN-28 was much lower, leading one to conclude that M_c affected the extent of interaction. A low M_c could increase the extent of interaction by limiting phase separation between the two components of the IPN. Based on the change in the T_g of both components it appeared that aromaticity and M_c both played a role in allowing secondary interactions to influence material properties.

Mechanical Properties:

With the observation of extensive interaction between the various LPUs and PMMA, the mechanical properties of the IPNs were of considerable interest. Previous studies have shown a substantial improvement in mechanical properties with increased IPN homogeneity or decreased M_c of the low modulus component (20). The use of different CEHPLs allowed for a decreased M_c . Migration of the component's T_g s into a single broad peak indicated the presence of a homogeneous system. The Young's modulus (MOE), ultimate strength and ultimate strain for the IPNs from different LPUs are shown in Figure 7-3. Both the MOE and ultimate strength increased and the ultimate strain decreased as the lignin content of the LPU increased.

It should be noted that the mechanical properties of IPN-25 and IPN-28, which showed a single T_g , continue the trend set by the other IPNs which showed two distinct transitions. Thus for this series of IPNs, the mechanical properties were strongly correlated with the lignin content. The presence of one or two T_g s did not interrupt the correlation between mechanical properties and lignin content. This consistent trend may be rationalized from the previous conclusion of dual phase continuity of the LPU/PMMA IPNs (8).

With the observation of a single T_g for IPN-25 and IPN-28, the materials were considered to be homogeneous. If the other IPNs, with two T_g s, formed discrete LPU or PMMA domains, then the mechanical properties of these materials would be substantially different from the two homogeneous materials. But the mechanical properties of all of the IPNs exhibited a continuous change in properties which was dependent on the lignin composition of the LPU. This behavior may be rationalized if both components were continuous throughout the composite.

CONCLUSIONS

IPNs can be prepared from LPUs with different lignin contents and different hydroxypropyl chain lengths. The lignin content of the polyols was increased by decreasing the MS of the radiating propylene oxide arms. Dynamic mechanical and thermal properties of these IPNs was related to the lignin content of the LPU. As the lignin content of the IPNs increased, the LPU T_g increased and the PMMA T_g decreased. Finally at LPU lignin contents above 25%, the two separate T_g s merged to provide a single broad transition. Again this behavior can be rationalized through the presence of secondary interactions between the lignin in the LPU and the PMMA and restrictions on phase separation by the highly crosslinked LPU.

The mechanical properties of these IPNs also depended on the LPU lignin content. The MOE and ultimate strength increased and the ultimate strain decreased as the lignin content of the IPN increased. The trends in the mechanical properties of the IPNs did not seem to depend on the presence of two or one transitions in the material. This observation supports the previous conclusion of dual phase continuity in IPNs.

REFERENCES: CHAPTER 7.

1. L. H. Sperling, Interpenetrating Polymer Networks and Related Materials, Plenum, New York, 1981.
2. H. L. Frisch, K. C. Frisch, and D. Klempner, Pure Appl. Chem., **53**,1557 (1981).
3. Y. S. Lipatov and L. M. Sergeeva, Interpenetrating Polymeric Networks, Naukova Dumka, Kiev, 1979.
4. G. Allen, M. J. Bowden, S. M. Todd, D. J. Blundell, G. M. Jeffs, and W. E. A. Davies, Polymer, **15**,28 (1974).
5. E. F. Cassidy, H. X. Xiao, K. C. Frisch, and H. L. Frisch, J. Polym. Sci.: Polymer Chem. Ed., **22**,2667 (1984)
6. L. Hermant and G. C. Meyer, Eur. Polym. J., **20**(1),85 (1984).
7. D. J. Hourston and Y. Zia, J. Appl. Polym. Sci., **29**,2951 (1984).
8. S. S. Kelley, Chapter 6 of this work (1987).
9. D. J. Hourston and J. A. McCluskey, J. Appl. Polym. Sci., **30**,2157 (1985).
10. D. J. Hourston and J. A. McCluskey, J. Appl. Polym. Sci., **31**,645 (1986).
11. R. B. Fox, J. L. Bitner, J. A. Hinkley, and W. Carter, Polym. Eng. Sci., **25**(3),157 (1985).
12. O. Blabisi, L. M. Robeson, and M. T. Shaw, Polymer-Polymer Miscibility, Academic Press, New York, 1979.
13. T. K. Kwei, J. Poly. Sci.: Polym. Let., **22**307 (1984).
14. S. Nishi and T. Kotaka, Macromol., **18**(8),1519 (1985).

15. E. F. Cassidy, H. X. Xiao, K. C. Frisch, and H. L. Frisch, J. Polym. Sci.: Polym. Chem. Ed., 22,1851 (1984).
16. Z. G. Gardlund, in Polymer Blends and Composites in Multiphase Systems, C. D. Hon, ed., ACS Advances in Chemistry Series No. 206, American Chemical Society, Washington, D.C., p. 129 (1984).
17. S. L. F. Ciemniecki, M. S. Thesis. Virginia Tech. (1986).
18. S. S. Kelley, Chapters 3 and 4 in this work (1987).
19. V. P. Saraf, W. G. Glasser, G. L. Wilkes, and J. E. McGrath, J. Appl. Polym. Sci., 30,2207 (1985).
20. J. H. Lee and S. C. Kim, Polym J., 16(6),453 (1984).

TABLE 7-1

COMPOSITION OF LPU/PMMA IPNs PREPARED FROM LIGNIN POLYOLS OF VARYING HYDROXYPROPYL CHAIN LENGTHS.

<u>Composite Type</u>	<u>Code</u>	MS of ¹ <u>CEHPL</u>	Weight Frac. ² <u>LPU (%)</u>	Lignin ³ <u>Content (%)</u>
Simultaneous IPN: both components crosslinked	IPN-13	6.3	50	13
	IPN-15	4.5	50	15
	IPN-17	5.3	50	17
	IPN-19	4.0	50	19
	IPN-21	2.5	50	21
	IPN-25	2.1	50	25
	IPN-28	1.7	50	28

1 Average molar substitution of propylene oxide on lignin; see Chapter 3.

2 Weight fraction of LPU in composites

3 Lignin content of composite

TABLE 7-2

EFFECT OF LIGNIN CONTENT ON THE THERMAL PROPERTIES
OF IPNs PREPARED WITH DIFFERENT CEHPLs

Composite Type	Lignin Content of LPU (%)	Aromatic Content of of LPU (%)	DMTA		DSC	
			Tan δ LPU	Peak Temp. (C) PMMA	T _g (C) LPU	T _g (C) PMMA
IPN-13	13	5.3	-22	108	-29	106
IPN-15	15	6.4	-20	102	-26	92
IPN-17	17	7.2	-15	98	-20	89
IPN-19	19	8.1	15	83	8	78
IPN-21	21	8.9	42	72	35	65
IPN-25	25	10.6		48 ¹		44 ¹
IPN-28	28	11.9		76 ¹		70 ¹

¹ Single transition observed

TABLE 7-3
EFFECT OF LIGNIN CONTENT ON THE MECHANICAL PROPERTIES
OF IPNs PREPARED WITH DIFFERENT CEHPLs

<u>Composite Type</u>	<u>Lignin Content of IPU (%)</u>	<u>Youngs Modulus (MPa)</u>	<u>Ultimate Strength (MPa)</u>	<u>Ultimate Strain (%)</u>
IPN-13	13	300	16.6	29
IPN-15	15	500	16.6	28
IPN-17	17	620	18.4	23
IPN-19	19	860	21.6	23
IPN-21	21	1,110	24.5	13
IPN-25	25	1,580	24.2	5
IPN-28	28	1,690	28.7	3

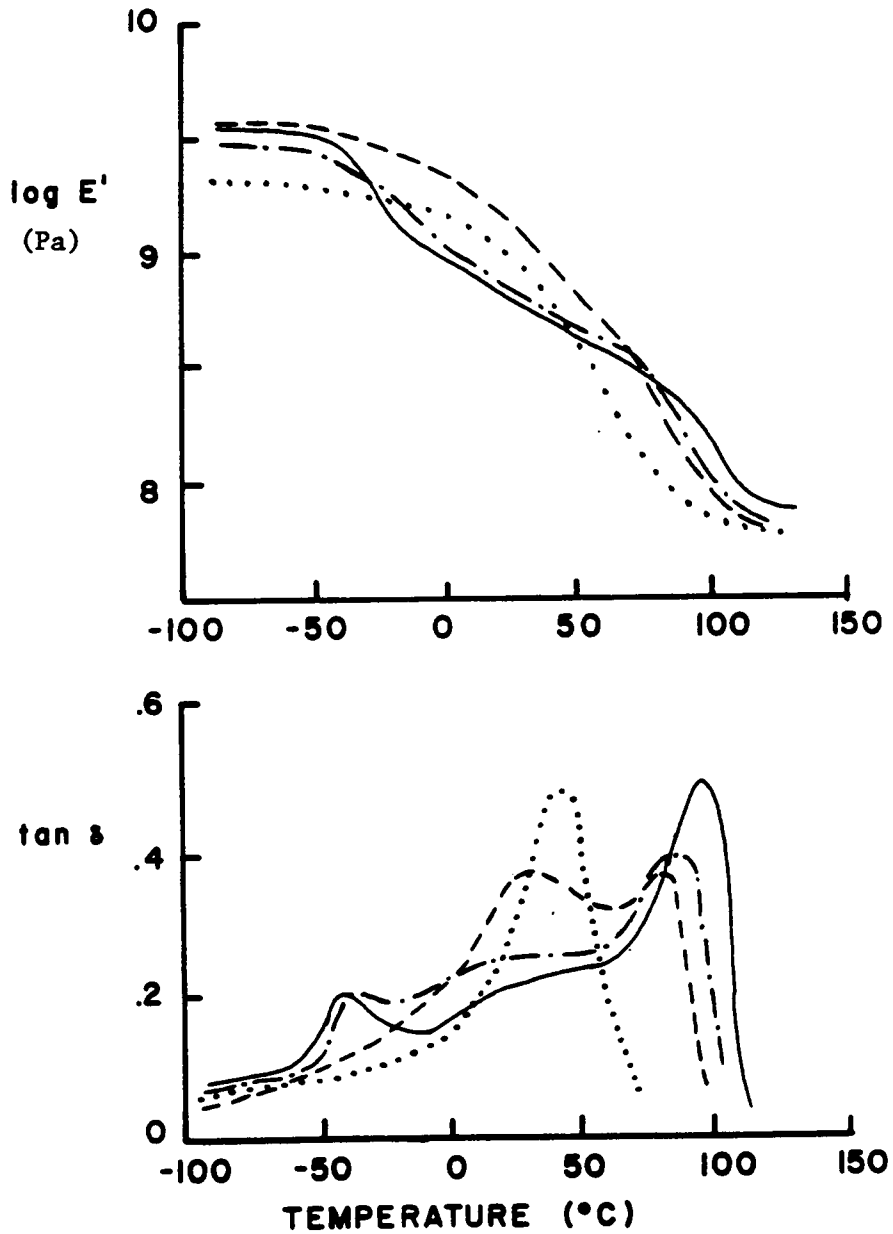


FIGURE 7-1. Effect of lignin content on the dynamic mechanical properties of IPNs: IPN-28 (· · · ·), IPN-21 (— —), IPN-17 (— · —), and IPN-13 (——).

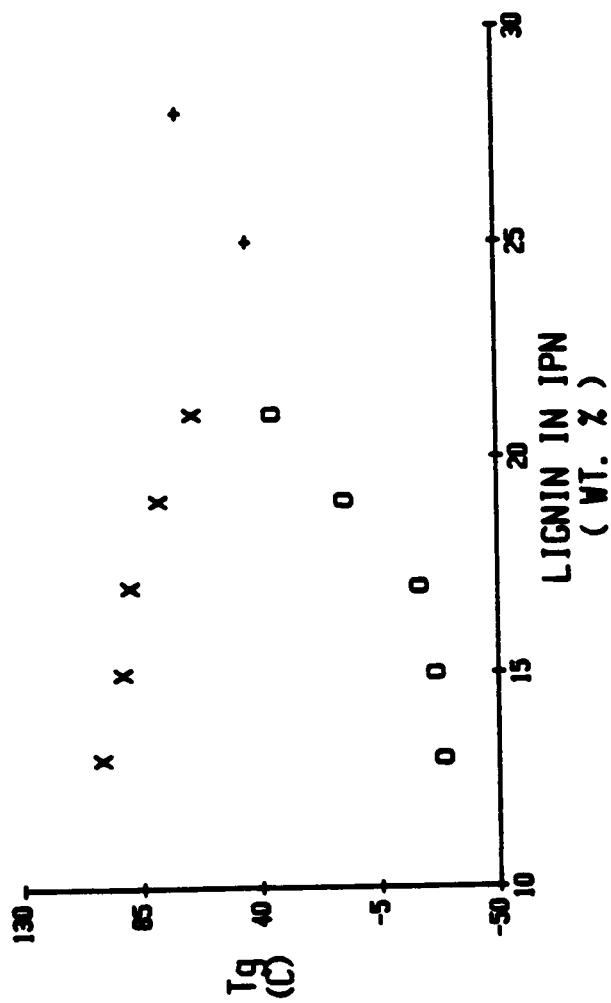


FIGURE 7-2. Effect of lignin content on the T_g of IPN: T_g of the PMMA (X), T_g of the LPU (O), and T_g of IPN-25 and IPN-28 where only one T_g was observed (+).

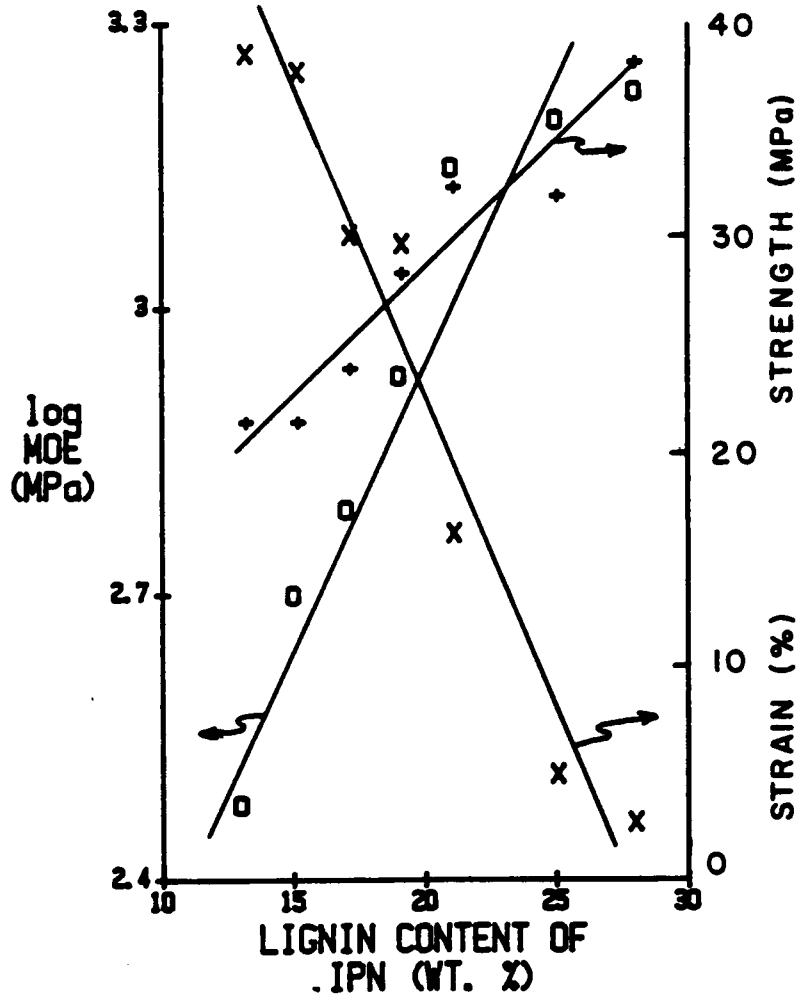


FIGURE 7-3. Effect of lignin content on the mechanical properties of IPNs: Young's modulus, (MPa) (O), ultimate strength, (MPa) (X) and ultimate strain, (%) (+).

CHAPTER 8

CONCLUSIONS

These results show that chain-extended hydroxypropyl lignin copolymers can be prepared and characterized. These copolymers can be covalently incorporated into polyurethane networks. The properties of these networks depend on the lignin content, diisocyanate type and crosslink density.

Specifically, chain extended hydroxypropyl lignins (CEHPLs) have been prepared and isolated from the reaction mixtures. The extent of molar substitution (MS) varied between one and seven propylene oxide units. The MS was determined by two $^1\text{H-NMR}$ techniques which provided fair agreement. Total hydroxyl contents could be determined by either titration or $^1\text{H-NMR}$ analysis although titration was considered to be a more reliable method for total OH determination. Both the lignin $^1\text{H-NMR}$ aromatic signal and the UV absorptivity decreased as the lignin content of the CEHPL copolymer decreased. The increase in molecular weight of the CEHPL was greater than predicted, an observation which could be attributed to either changes in the hydrodynamic volume of the reactions or condensation reactions between lignin molecules. Thermal analysis showed

a predictable decrease in the T_g as the lignin content of the CEHPL decreased. The change in T_g with a change in the copolymer composition followed the behavior predicted by the Gordon-Taylor relationship. None of the observed CEHPL copolymer properties appeared to be related to the origin of the original lignin.

The CEHPL copolymer could be incorporated into lignin-based polyurethane networks (LPUs). These LPUs contained between 17 and 43% lignin depending on the formulation. Dynamic mechanical and thermal analysis showed a single T_g which varied between -50 C and 120 C. The Youngs modulus (MOE) of these same LPUs varied between 10 and 1400 MPa. Both the T_g and the MOE were strongly correlated with the lignin content of the LPU and the type of diisocyanate, hexamethylene or toluene diisocyanate, used for crosslinking. Differences between the networks crosslinked with two diisocyanates could be observed when the T_g and MOE were normalized for the aromatic content of the materials. Swelling experiments were used to substantiate the possible differences in the crosslink density. The molecular weight between crosslinks (M_c) was found to increase dramatically as the MS of the CEHPLs increased. The highly chain extended polyols also contained a high sol content. Both the large M_c and high

sol content indicated the formation of an incomplete network, possibly due to cyclization reactions. The change in the T_g with the formation of a network could not be explained by a copolymer effect and a crosslinking effect as suggested by Chan et al. While the change in T_g was strongly correlated to M_c , changes in composition led to difficulties in the determination of the copolymer effect. As with the CEHPL characteristics, the LPU properties appeared to be independent of the source of the lignin.

Classical non-solvent/solvent fractionation of hydroxypropyl lignins (HPLs) could be performed to isolate fractions with varying molecular weight. The paucidisperse HPL fractions ranged in molecular weight (M_n) between 1.5 and 10.0×10^3 daltons. The thermal properties of the fractions behaved according to the Fox-Flory relationship. The aromatic content and hydroxyl content of the HPLs decreased slightly as the molecular weight increased. The fractionated HPLs were incorporated into polyurethane (F-LPU) networks. The T_g of the F-LPU increased while the M_c decreased as the HPL molecular weight increased. These observations could be related to the average functionality of the polyols. Network formation was limited by the presence of molecules which did not contribute as network junction points (mono- and difunctional molecules). The

strength properties of the F-LPUs were superior to those of an LPU prepared from a non-fractionated HPL. In contrast to the results from the previous section, the change in T_g with the formation of the network could be explained by the model of Chan *et al.*

Finally, the LPUs were used as one component in the preparation of a series of LPU/polymethyl methacrylate (PMMA) composites. Several of these composites were prepared to form interpenetrating polymer networks (IPNs). Dynamic mechanical and thermal analysis showed all of the materials to be phase separated but indicated the presence of some secondary interactions between the two components. The extent of interaction did not appear to depend on the IPN type. The mechanical properties of the IPNs, especially MOE, did vary with the material's composition and the method of preparation. Specifically the presence of crosslinking in the LPU led to MOE values which behaved as if the IPNs possessed dual phase continuity. The absence of crosslinking in the LPU appeared to allow for phase inversion as the IPN composition changed.

A second series of IPNs was prepared to investigate the effects of the lignin content of the LPU on material properties. As the lignin content increased, the extent of

secondary interactions between the two components increased until a single T_g was observed. Secondary interactions between the aromatic electrons and $n-\pi$ electrons on PMMA have been observed in other systems. The extent of secondary interactions also appeared to depend on the M_c of the LPU, with more highly crosslinked systems exhibiting more interactions. The mechanical properties of the IPNs depended on the lignin content and not the presence of one or two phases.

This series of studies has demonstrated that lignin copolymers may be prepared and characterized. These copolymers may be utilized in a number of systems in a controllable and predictable manner. And while lignin is a complex material, the characterization of a few specific properties allows for the reliable utilization of lignin copolymers from a wide variety of materials.

**The vita has been removed from
the scanned document**